RIVISTA DEL NUOVO CIMENTO VOL. 11, N. 12 1988

# Application of the Green's Functions Method to the Study of the Optical Properties of Semiconductors.

G. STRINATI

*Dipartimento di Fisica dell'Università «La Sapienza» - 00185 Roma, Italia* (*)

(ricevuto l'1 Dicembre 1986)

## 1. – Introduction.

The relevance of many-body effects, over and above the independent-particle approximation, on the optical properties of semiconductors has been increasingly recognized over the years. Specifically, the collective effect of screening has long been known to be essential to account for the reduction of the electron-hole attraction in an exciton and for the polarization accompanying a single-particle excitation. Only more recently however, it has been possible to give quantitative account of these phenomena by combining Green's function techniques of quantum field theory with the description of band structures in

---

(*) Present address: Scuola Normale Superiore, 56100 Pisa, Italy.

terms of localized (molecularlike) orbitals [1-3]. The theory of elementary excitations in crystalline semiconductors with electronic states that are to some extent localized, which has emerged from these efforts, can be considered rather well established by this time.

Objective of this paper is to give a pedagogical review of the theoretical framework underlying the calculations of many-particle properties in semiconductors which are based on the concepts of single- and two-particle excitations. Biased by the beliefs that, quite generally, only through detailed knowledge of the theory one can correctly formulate the problems and that, for the specific physical phenomena of interest, the Green's functions method provides the very language to describe them, we shall put special emphasis on the working procedures that are important for appreciating the subtleties of the method, but are not commonly described in the literature. For these reasons, results of numerical calculations will be only sketchly presented and references will be given to the original papers for additional details. In particular, when relating theoretical results with experimental quantities, the direct link between the two-particle Green's function and the correlation functions of linear response theory will extensively be exploited. It is, in fact, the focus on the correlation functions that renders the Green's functions method quite efficient and practical by avoiding the calculation of redundant information.

To keep the presentation as compact as possible, we shall avoid the formulation of Green's functions theory in terms of conventional diagrammatic techniques [4], but we shall rather adopt the alternative formulation in terms of functional derivatives techniques that reduces the many-body problem directly to the solution of a coupled set of nonlinear integral equations [5]. In this way, the screening mechanism which is so important in a semiconductor will be introduced from the outset in the formal theory by replacing the ordinary Coulomb interaction between electrons by a modified (time-dependent) interaction that takes into account the polarization of the medium represented by the remaining electrons.

We confine ourselves in this paper to the zero-temperature limit which is appropriate to describe the optical properties of a semiconductor, although extention to finite temperatures is feasible [6]. The system we consider are $N$-interacting electrons moving in the static potential of the ions. The spatial symmetry of this potential will be left as much as possible unspecified but we will restrict eventually to insulting systems with crystalline (space group) symmetry, while actual calculations will be presented for cubic covalent semiconductors. No coupling with phonons as well as no magnetic and relativistic effects will be considered throughout.

This paper is organized in two parts. The first part (sect. **2-7** and appendices A-E) introduces the theoretical tools and the associated calculation methods and approximation procedures which connect the study of the optical properties of semiconductors to the Green's functions method. The second part (sect. **8-11** and appendices F-H) deals more specifically with the computation of quantities (such as the optical absorption coefficient) characterizing single- and two-particle excitations in (covalent) semiconductors.

## 2. – Generalized Green's functions.

We consider a (nonrelativistic) $N$-electron system which interacts with a static potential $V(\boldsymbol{r})$. The corresponding second-quantized Hamiltonian has the form

$$\hat{H} = \int \mathrm{d}\boldsymbol{x}\, \hat{\Psi}^\dagger(\boldsymbol{x})\, h(\boldsymbol{r})\, \hat{\Psi}(\boldsymbol{x}) + \frac{1}{2}\int \mathrm{d}\boldsymbol{x}\, \mathrm{d}\boldsymbol{x}'\, \hat{\Psi}^\dagger(\boldsymbol{x})\, \hat{\Psi}^\dagger(\boldsymbol{x}')\, v(\boldsymbol{r}, \boldsymbol{r}')\, \hat{\Psi}(\boldsymbol{x}')\, \hat{\Psi}(\boldsymbol{x}) . \tag{2.1}$$

In eq. (2.1) $\boldsymbol{x}$ signifies the set of space ($\boldsymbol{r}$) and spin ($\xi$) variables, the $\hat{\Psi}(\boldsymbol{x})$ are field operators, $h(\boldsymbol{r})$ is the one-electron Hamiltonian

$$h(\boldsymbol{r}) = -\frac{\hbar^2}{2m}\nabla^2 + V(\boldsymbol{r}) \tag{2.2}$$

and

$$v(\boldsymbol{r}, \boldsymbol{r}') = \frac{e^2}{|\boldsymbol{r} - \boldsymbol{r}'|} \tag{2.3}$$

is the Coulomb interaction [7].

We consider also an external (scalar) potential $U(\boldsymbol{x}, \boldsymbol{x}'; t)$ which is local in time but nonlocal in space and which couples bi-linearly to the field operators. The interaction Hamiltonian is thus taken of the form

$$\hat{H}'(t) = \int \mathrm{d}\boldsymbol{x}\, \mathrm{d}\boldsymbol{x}'\, \hat{\Psi}^\dagger(\boldsymbol{x})\, U(\boldsymbol{x}, \boldsymbol{x}'; t)\, \hat{\Psi}(\boldsymbol{x}') , \tag{2.4}$$

which is guaranteed to be Hermitian by requiring $U(\boldsymbol{x}, \boldsymbol{x}'; t)$ to be Hermitian in the $\boldsymbol{x}$ variables at any $t$. This potential is further assumed to vanish as $|t| \to \infty$.

The introduction of the interaction (2.4) may be considered as a purely formal tool to generate in a compact form the equations of motion for the Green's functions together with a number of useful relations. It will be understood, in fact, that the external potential will be allowed to vanish at the end of the calculation. Nevertheless, the formalism we shall develop could be used as well to follow the time development of the Green's functions of the system under the action of a physical external (local) potential of the form

$$U(\boldsymbol{x}, \boldsymbol{x}'; t) = U(\boldsymbol{x}, t)\, \delta(\boldsymbol{x}, \boldsymbol{x}') . \tag{2.5}$$

More general forms of coupling to scalar and vector (electromagnetic) potentials will be considered in sect. **5** and in appendix C.

The interaction Hamiltonian (2.4) enables us to introduce an *interaction picture* by defining the time dependence of the field operators with respect to the unperturbed Hamiltonian (2.1):

$$\hat{\Psi}(1) \equiv \hat{\Psi}(\boldsymbol{x}_1,\ t_1) = \exp[i\hat{H}t_1/\hbar]\,\hat{\Psi}(\boldsymbol{x}_1)\,\exp[-i\hat{H}t_1/\hbar]. \tag{2.6}$$

Similarly, we write

$$\begin{aligned}\hat{H}'_{\mathrm{I}}(t) &= \exp[i\hat{H}t/\hbar]\,\hat{H}'(t)\,\exp[-i\hat{H}t/\hbar] = \\ &= \int \mathrm{d}\boldsymbol{x}\,\mathrm{d}\boldsymbol{x}'\,\hat{\Psi}^{\dagger}(\boldsymbol{x},\ t^{+})\,U(\boldsymbol{x},\ \boldsymbol{x}';\ t)\,\hat{\Psi}(\boldsymbol{x}',\ t),\end{aligned} \tag{2.7}$$

where for later convenience $t^{+}$ stands for $t+\delta$ ($\delta \to 0^{+}$), and we introduce the (formal) operator

$$\hat{S} = \exp\left\{-\frac{i}{\hbar}\int_{-\infty}^{+\infty}\mathrm{d}t\,\hat{H}'_{\mathrm{I}}(t)\right\}. \tag{2.8}$$

The *generalized* single- and two-particle Green's functions are then defined to be

$$G_1(1,\ 2) = -\frac{i}{\hbar}\,\frac{\langle N|T[\hat{S}\hat{\Psi}(1)\,\hat{\Psi}^{\dagger}(2)]|N\rangle}{\langle N|T[\hat{S}]|N\rangle} \tag{2.9}$$

and

$$G_2(1,\ 2;\ 1',\ 2') = \left(-\frac{i}{\hbar}\right)^2\frac{\langle N|T[\hat{S}\hat{\Psi}(1)\,\hat{\Psi}(2)\,\hat{\Psi}^{\dagger}(2')\,\hat{\Psi}^{\dagger}(1')]|N\rangle}{\langle N|T[\hat{S}]|N\rangle}, \tag{2.10}$$

respectively, where $|N\rangle$ denotes the ground state of the unperturbed $N$-electron system and $T$ is Wick's time-ordering operator which includes a minus sign for any permutation of (fermion) field operators. Equations (2.9) and (2.10) reduce to the definitions of the ordinary single- and two-particle Green's functions [4] when the external potential $U$ is allowed to vanish. Notice also that all the $U$-dependence in the generalized Green's functions is contained in the operators $\hat{S}$.

## 3. – Equations of motion for the generalized single-particle Green's function.

The presence of the time-ordering operator in eqs. (2.9) and (2.10) requires us to consider, besides the $S$-matrix $T[\hat{S}]$, the time evolution operator in the interaction picture $T[\hat{S}(t_a,\ t_b)]$, where

$$\hat{S}(t_a,\ t_b) = \exp\left\{-\frac{i}{\hbar}\int_{t_a}^{t_b}\mathrm{d}t\,\hat{H}'_{\mathrm{I}}(t)\right\} \tag{3.1}$$

(with the understanding that the operator (3.1) makes sense only within a time-ordered product). This operator satisfies the following relevant properties:

$$\text{(3.2)} \qquad \text{i)} \quad T[\hat{S}(t_a, t_c)] = T[\hat{S}(t_a, t_b)]\, T[\hat{S}(t_b, t_c)]$$

(group property);

$$\text{(3.3)} \qquad \text{ii)} \quad T[\hat{S}(t_a, t_b)\, \hat{\Psi}(1)\, \hat{\Psi}(2)] = T[\hat{S}(t_a, t_1)]\, \hat{\Psi}(1)\, T[\hat{S}(t_1, t_2)]\, \hat{\Psi}(2)\, T[\hat{S}(t_2, t_b)]\,,$$

for $t_a > t_1 > t_2 > t_b$;

$$\text{iii)} \begin{cases} \dfrac{\partial}{\partial t_a} T[\hat{S}(t_a, t_b)] = -\dfrac{i}{\hbar} \hat{H}'_{\mathrm{I}}(t_a)\, T[\hat{S}(t_a, t_b)]\,, & \text{(3.4}a\text{)} \\[2ex] \dfrac{\partial}{\partial t_b} T[\hat{S}(t_a, t_b)] = \dfrac{i}{\hbar} T[\hat{S}(t_a, t_b)]\, \hat{H}'_{\mathrm{I}}(t_b)\,. & \text{(3.4}b\text{)} \end{cases}$$

The equation of motion for $G_1(1, 2)$ and its adjoint are then obtained by taking the derivative of $G_1(1, 2)$, alternatively, with respect to $t_1$ and $t_2$. After the time dependence of the various factors entering the definition (2.9) is made explicit, in addition to eqs. (3.1)-(3.4) we require the equations of motion of the field operators

$$\text{(3.5}a\text{)} \qquad \frac{\partial}{\partial t_1} \hat{\Psi}(1) = -\frac{i}{\hbar} \left[ h(1) + \int \mathrm{d}3\, v(1, 3)\, \hat{\Psi}^{+}(3)\, \hat{\Psi}(3) \right] \hat{\Psi}(1)\,,$$

$$\text{(3.5}b\text{)} \qquad \frac{\partial}{\partial t_2} \hat{\Psi}^{+}(2) = \frac{i}{\hbar} \left[ h(2)\, \hat{\Psi}^{+}(2) + \hat{\Psi}^{+}(2) \int \mathrm{d}3\, v(2, 3)\, \hat{\Psi}^{+}(3)\, \hat{\Psi}(3) \right],$$

as well as the identity

$$\text{(3.6)} \qquad \frac{\partial}{\partial t_1} \theta(t_1 - t_2) = -\frac{\partial}{\partial t_2} \theta(t_1 - t_2) = \delta(t_1 - t_2)\,,$$

where $\theta$ is the unit step function. In eqs. (3.5) we have introduced the notation $v(1, 2) = v(\boldsymbol{r}_1, \boldsymbol{r}_2)\, \delta(t_1 - t_2)$ and $h(1) = h(\boldsymbol{r}_1)$, while the integrals extend over space, spin, and time variables which are collectively denoted by 1, ... .

Manipulations lead then to the following equations:

$$\text{(3.7}a\text{)} \qquad \left[ i\hbar \frac{\partial}{\partial t_1} - h(1) \right] G_1(1, 2) - \int \mathrm{d}3\, U(1, 3)\, G_1(3, 2) + \\ + i\hbar \int \mathrm{d}3\, v(1, 3)\, G_2(1, 3^{+}; 2, 3^{++}) = \delta(1, 2)\,,$$

$$\text{(3.7}b\text{)} \qquad \left[ -i\hbar \frac{\partial}{\partial t_2} - h(2) \right] G_1(1, 2) - \int \mathrm{d}3\, G_1(1, 3)\, U(3, 2) + \\ + i\hbar \int \mathrm{d}3\, v(2, 3)\, G_2(1, 3^{--}; 2, 3^{-}) = \delta(1, 2)\,,$$

where $3^\pm$ implies that the time variable $t_3$ is augmented (diminished) by a positive infinitesimal, and we have introduced the notation

$$U(1,\,2) = U(\boldsymbol{x}_1,\,\boldsymbol{x}_2;\,t_1)\,\delta(t_1 - t_2)\,. \tag{3.8}$$

A characteristic feature of eqs. (3.7) is that, besides the single-particle Green's function, they involve also the two-particle Green's function. A whole hierarchy of equations involving higher-order Green's functions can thus be generated in this way [8]. It is customary to replace this hierarchy of equations by a coupled nonlinear set of integro-differential equations connecting the single-particle Green's function to the self-energy operator ($\Sigma$), the (irreducible scalar) vertex function ($\tilde{\Gamma}$), and other derived quantities like the (irreducible) polarizability ($\tilde{\chi}$), the dynamically screened interaction ($W$), etc. To this end, we begin by eliminating formally the two-particle Green's function from eqs. (3.7) by utilizing the following functional derivative identity:

$$G_2(1,\,3;\,2,\,3^+) = G_1(1,\,2)\,G_1(3,\,3^+) - \frac{\delta G_1(1,\,2)}{\delta U(3)}\,, \tag{3.9}$$

which holds in this form for generalized Green's functions defined in the presence of the local potential $U(1)$ (cf. eq. (2.5)). Potentials of the more general form (3.8) will instead be needed to generate the equation of motion for the two-particle Green's function. Equation (3.9) is derived in appendix A where the calculus with functional derivatives is also briefly reviewed.

Inserting the identity (3.9) into the equations of motion (3.7) yields two functional differential equations:

$$\left[i\hbar\frac{\partial}{\partial t_1} - h(1) - U(1) + i\hbar\int \mathrm{d}3\,v(1,\,3)\,G_1(3,\,3^+)\right]G_1(1,\,2) - \\ - i\hbar\int \mathrm{d}3\,v(1^+,\,3)\,\frac{\delta G_1(1,\,2)}{\delta U(3)} = \delta(1,\,2) \tag{3.10a}$$

and

$$\left[-i\hbar\frac{\partial}{\partial t_2} - h(2) - U(2) + i\hbar\int \mathrm{d}3\,v(2,\,3)\,G_1(3^-,\,3)\right]G_1(1,\,2) - \\ - i\hbar\int \mathrm{d}3\,v(2^-,\,3)\,\frac{\delta G_1(1,\,2)}{\delta U(3)} = \delta(1,\,2)\,. \tag{3.10b}$$

Equations (3.10) are not yet in a form suitable for taking the limit as $U \to 0$, since this process would require explicit knowledge of the functional dependence of $G_1$ on $U$ itself. To avoid any reference to the external potential, it is convenient to rewrite eqs. (3.10) in terms of the *self-energy operator* which is defined by the two alternative expressions

$$\Sigma(1,2)=\Sigma_{\mathrm{H}}(1,2)+i\hbar\int \mathrm{d}34\, v(1^+,3)\,\frac{\delta G_1(1,4)}{\delta U(3)}\,G_1^{-1}(4,2)\,, \tag{3.11a}$$

$$\overline{\Sigma}(1,2)=\Sigma_{\mathrm{H}}(1,2)+i\hbar\int \mathrm{d}34\, G_1^{-1}(1,4)\,\frac{\delta G_1(4,2)}{\delta U(3)}\,v(3,2^-)\,. \tag{3.11b}$$

Here $\Sigma_{\mathrm{H}}$ stands for the Hartree contribution to the self-energy

$$\Sigma_{\mathrm{H}}(1,2)=\delta(1,2)\left[-i\hbar\int \mathrm{d}3\, v(1,3)\,G_1(3,3^+)\right], \tag{3.12}$$

while the rest is sometimes referred to as the *mass operator* and indicated by $M(\overline{M})$. The inverse $G_1^{-1}$ of the generalized single-particle Green's function (2.9) is defined by

$$\int \mathrm{d}3\, G_1^{-1}(1,3)\,G_1(3,2)=\int \mathrm{d}3\, G_1(1,3)\,G_1^{-1}(3,2)=\delta(1,2)\,. \tag{3.13}$$

Demanding the left and right inverse of $G_1$ to be equal requires the two expressions (3.11) to coincide. This property can be verified for the *exact* self-energy through a diagrammatic expansion; its relevance will appear when it will be imposed as a constraint on the choice of the *approximate* form of the self-energy (sect. **6**).

Equations (3.10) can now be cast in the form

$$\left[i\hbar\frac{\partial}{\partial t_1}-h(1)-U(1)\right]G_1(1,2)-\int \mathrm{d}3\,\Sigma(1,3)\,G_1(3,2)=\delta(1,2) \tag{3.14a}$$

or, alternatively,

$$\left[-i\hbar\frac{\partial}{\partial t_2}-h(2)-U(2)\right]G_1(1,2)-\int \mathrm{d}3\, G_1(1,3)\,\overline{\Sigma}(3,2)=\delta(1,2)\,. \tag{3.14b}$$

Equations (3.14) express *Dyson's equation* in differential form (cf. appendix B) and give to $\Sigma$ the physical meaning of a nonlocal and energy-dependent effective single-particle potential, as it will be discussed in sect. **9**. Hereafter we shall limit to consider only one of the two equations (3.14), since the other is implied by the condition $\Sigma=\overline{\Sigma}$.

We proceed now to eliminate any explicit reference to the external potential in the self-energy operator (3.11). To this end, we introduce the following auxiliary quantities.

i) The *total* (*classical*) *potential* $V$ is defined as

$$V(1)\equiv U(1)-i\hbar\int \mathrm{d}3\, v(1,3)\,G_1(3,3^+)\,. \tag{3.15}$$

Regarding alternatively $G_1$ as a functional of $V$ instead of $U$ and using the «chain rule» (A.8) as well as eq. (A.7) yield

$$M(1,\,2) = -i\hbar\int \mathrm{d}345\,v(1^+,\,3)\,G_1(1,\,4)\,\frac{\delta G_1^{-1}(4,\,2)}{\delta V(5)}\,\frac{\delta V(5)}{\delta U(3)}\,. \tag{3.16}$$

ii) Equation (3.16) suggests to introduce a *scalar* (*irreducible*) *vertex function* $\tilde{\Gamma}$ defined as

$$\tilde{\Gamma}(1,\,2;\,3) \equiv -\frac{\delta G_1^{-1}(1,\,2)}{\delta V(3)} = \delta(1,\,3)\,\delta(2,\,3) + \frac{\delta M(1,\,2)}{\delta V(3)}\,, \tag{3.17}$$

where the right side has been obtained by combining eqs. (B.4), (3.11), and (3.15). Since the mass operator $M$ depends on the external potential $U$ (or alternatively on $V$) only through its dependence on the generalized single-particle Green's function (cf. eqs. (3.11)), we can again use the «chain rule» for functional differentiation together with eq. (A.7) to obtain an integral equation for $\tilde{\Gamma}$:

$$\begin{aligned}\tilde{\Gamma}(1,\,2;\,3) &= \delta(1,\,3)\,\delta(2,\,3) + \int \mathrm{d}45\,\frac{\delta M(1,\,2)}{\delta G_1(4,\,5)}\,\frac{\delta G_1(4,\,5)}{\delta V(3)} = \\ &= \delta(1,\,3)\,\delta(2,\,3) + \int \mathrm{d}4567\,\frac{\delta M(1,\,2)}{\delta G_1(4,\,5)}\,G_1(4,\,6)\,G_1(7,\,5)\,\tilde{\Gamma}(6,\,7;\,3)\,.\end{aligned} \tag{3.18}$$

This can be considered as the equation defining $\tilde{\Gamma}$, whereby the limit $U \to 0$ can explicitly be taken.

iii) Equation (3.16) suggests to introduce also an *inverse* (*longitudinal*) *dielectric matrix* $\epsilon^{-1}$ defined as

$$\epsilon^{-1}(1,\,2) \equiv \frac{\delta V(1)}{\delta U(2)}\,. \tag{3.19}$$

From the definition (3.15) and from the identity

$$-i\hbar G_1(1,\,1^+) = \frac{\langle N|T[\hat{S}\hat{\rho}(1)]|N\rangle}{\langle N|T[\hat{S}]|N\rangle} \equiv \langle\hat{\rho}(1)\rangle\,, \tag{3.20}$$

where $\hat{\rho}(1) = \hat{\Psi}^\dagger(1)\,\hat{\Psi}(1)$ is the density operator, we can express

$$\epsilon^{-1}(1,\,2) = \delta(1,\,2) + \int \mathrm{d}3\,v(1,\,3)\,\frac{\delta\langle\hat{\rho}(3)\rangle}{\delta U(2)}\,. \tag{3.21}$$

The functional derivative of the average density with respect to the external potential in eq. (3.21) is a measure of the *polarizability* of the system. Its connection with the corresponding quantity of linear response theory (cf. sect. 5) is most readily drawn by utilizing the identity (3.9):

$$\tag{3.22} \chi(1,2) \equiv \frac{\delta\langle\hat{\rho}(1)\rangle}{\delta U(2)} = i\hbar[G_2(1,2;1^+,2^+) - G_1(1,1^+)G_1(2,2^+)] = -\frac{i}{\hbar}\frac{\langle N|T[\hat{S}\hat{\rho}'(1)\hat{\rho}'(2)]|N\rangle}{\langle N|T[\hat{S}]|N\rangle},$$

where we have introduced the density deviation operator

$$\tag{3.23} \hat{\rho}'(1) = \hat{\rho}(1) - \langle\hat{\rho}(1)\rangle .$$

From the last line of eq. (3.22) $\chi$ is seen to be symmetric under the interchange of its arguments. Moreover, it is convenient to single out from $\chi$ the part which is irreducible with respect to the bare Coulomb potential $v$ by regarding the average density as a functional of the total potential $V$:

$$\tag{3.24} \begin{aligned} \chi(1,2) &= \int d3\,\frac{\delta\langle\hat{\rho}(1)\rangle}{\delta V(3)}\,\frac{\delta V(3)}{\delta U(2)} = \int d3\,\frac{\delta\langle\hat{\rho}(1)\rangle}{\delta V(3)}\,\epsilon^{-1}(3,2) = \\ &= \int d3\,\frac{\delta\langle\hat{\rho}(1)\rangle}{\delta V(3)}\left[\delta(3,2) + \int d4\,v(3,4)\frac{\delta\langle\hat{\rho}(4)\rangle}{\delta U(2)}\right] = \\ &= \tilde{\chi}(1,2) + \int d34\,\tilde{\chi}(1,3)\,v(3,4)\,\chi(4,2), \end{aligned}$$

where we have defined the *irreducible polarizability* $\tilde{\chi}$ to be

$$\tag{3.25} \tilde{\chi}(1,2) \equiv \frac{\delta\langle\hat{\rho}(1)\rangle}{\delta V(2)} .$$

Equation (3.24) can be regarded as an integral equation to be solved for $\chi$ once the kernel $\tilde{\chi}$ is specified. Knowledge of $\tilde{\chi}$, in turn, can be related to that of the vertex function (3.17) through the identity (A.7)

$$\tag{3.26} \begin{aligned} \tilde{\chi}(1,2) &= -i\hbar\,\frac{\delta G_1(1,1^+)}{\delta V(2)} = i\hbar\int d34\,G_1(1,3)\,\frac{\delta G_1^{-1}(3,4)}{\delta V(2)}\,G_1(4,1^+) = \\ &= -i\hbar\int d34\,G_1(1,3)\,G_1(4,1)\,\tilde{\Gamma}(3,4;2) . \end{aligned}$$

Notice that $\tilde{\chi}$ also is symmetric under interchange of its arguments, and that we can express the *(longitudinal) dielectric matrix* $\epsilon$ in terms of $\tilde{\chi}$ as follows:

$$\tag{3.27} \begin{aligned} \epsilon(1,2) &\equiv \frac{\delta U(1)}{\delta V(2)} = \frac{\delta}{\delta V(2)}\left[V(1) - \int d3\,v(1,3)\,\langle\hat{\rho}(3)\rangle\right] = \\ &= \delta(1,2) - \int d3\,v(1,3)\,\tilde{\chi}(3,2), \end{aligned}$$

where

$$\int \mathrm{d}3\,\epsilon^{-1}(1,3)\,\epsilon(3,2) = \int \mathrm{d}3\,\epsilon(1,3)\,\epsilon^{-1}(3,2) = \delta(1,2)\,. \tag{3.28}$$

Equation (3.28) follows from eq. (A.3) and the «chain rule» (A.8).

iv) It is further convenient to introduce the *dynamically screened interaction* $W$ defined as

$$W(1,2) \equiv \int \mathrm{d}3\,\epsilon^{-1}(1,3)\,v(3,2)\,. \tag{3.29}$$

We can express alternatively

$$\begin{aligned} W(1,2) &= v(1,2) + \int \mathrm{d}34\,v(1,3)\,\tilde{\chi}(3,4)\,W(4,2) = \\ &= v(1,2) + \int \mathrm{d}34\,v(1,3)\,\chi(3,4)\,v(4,2)\,, \end{aligned} \tag{3.30}$$

where the first line can be interpreted as an integral equation defining $W$, while the last line represents its formal solution. From the last line it also follows that $W(2,1) = W(1,2)$.

With the definitions (3.17), (3.19), and (3.29) the mass operator (3.16) can be cast in its final form

$$M(1,2) = i\hbar \int \mathrm{d}34\,W(1^+,3)\,G_1(1,4)\,\tilde{\Gamma}(4,2;3)\,. \tag{3.31}$$

Equations (3.14), (3.18), (3.26), (3.30), and (3.31) constitute the set of coupled equations which link $M$, $\tilde{\Gamma}$, $\tilde{\chi}$, and $W$. They are represented graphically in fig. 1 together with the expression for $\overline{M}$ (cf. equation (3.11*b*))

$$\overline{M}(1,2) = i\hbar \int \mathrm{d}34\,\tilde{\Gamma}(1,4;3)\,G_1(4,2)\,W(3,2^-)\,. \tag{3.32}$$

Notice that the limit $U \to 0$ can be readily taken in these equations.

All quantities considered thus far are still *exact*. Approximations can be generated either by expressing the set of coupled equations as (infinite) series in terms of $G_1^{(0)}$ and $v$, thereby reproducing the Feynman-Dyson perturbation theory [4], or by truncating the set of coupled equations by making specific *ansatz* on the functional form of the mass operator $M$ in terms of the self-consistent $G_1$ and $W$ [5, 6, 8]. Different approximations will be relevant to different physical situations, and for any given approximation it will be important to check whether it satisfies rather general conservation criteria such as the conservation of the number of particles, the total energy, etc. A prescription to generate such *conserving approximations* will be discussed in sect. **6**.

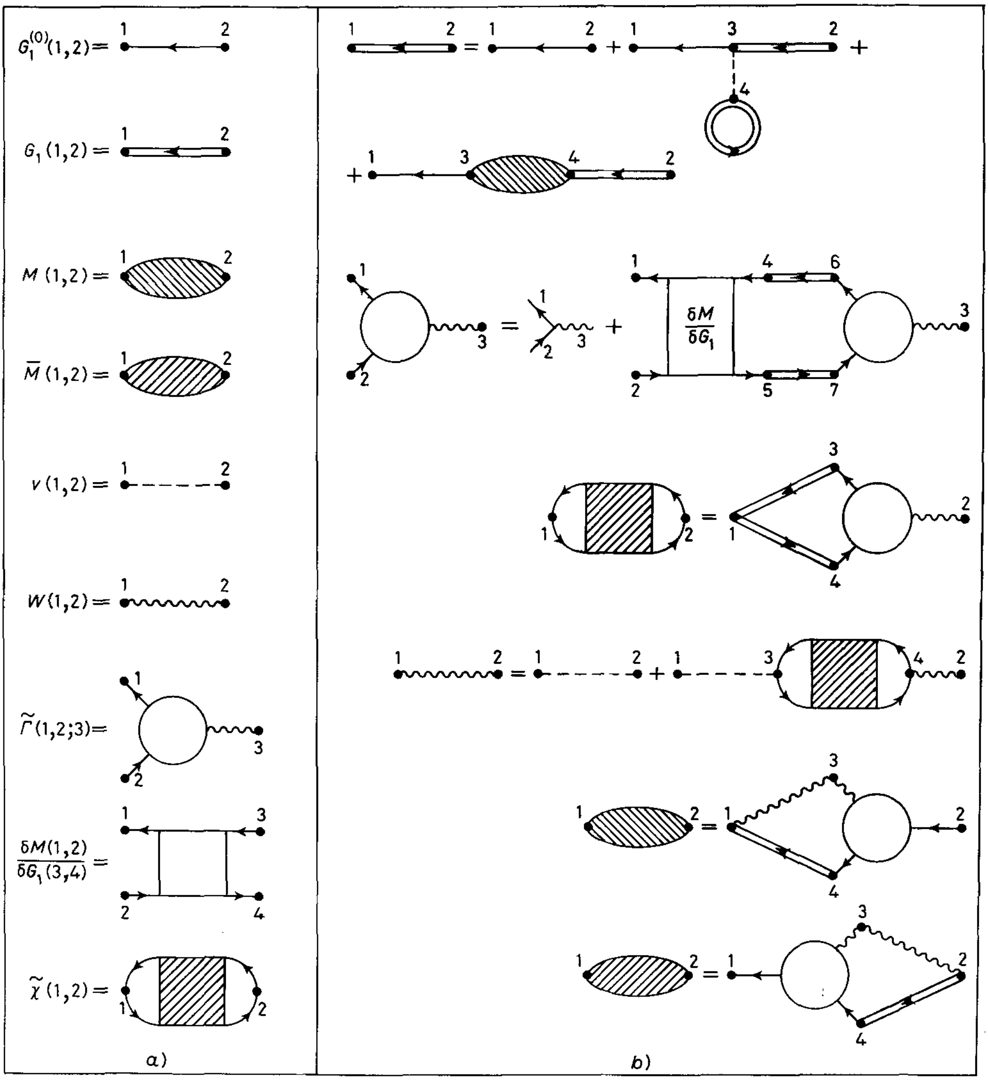

Fig. 1. – *a*) Graphical symbols corresponding to the relevant quantities needed to represent *b*) the coupled set of equations for $M$, $\tilde{\Gamma}$, $\tilde{\chi}$, and $W$.

## 4. – Bethe-Salpeter equation for the two-particle Green's function.

The equation of motion for the two-particle Green's function, which is the analog of the Dyson's equation (B.6) for the single-particle Green's function, can be most readily obtained by introducing the *two-particle correlation function* defined as

$$L(1, \boldsymbol{x}'t; 2, \boldsymbol{x}t^+) \equiv -G_2(1, \boldsymbol{x}'t; 2, \boldsymbol{x}t^+) + G_1(1, 2)G_1(\boldsymbol{x}'t, \boldsymbol{x}t^+) . \tag{4.1}$$

In fact, for generalized Green's functions evolving in the presence of an external potential of the type (3.8), $L$ can be expressed by means of the identity (A.12), namely,

$$L(1,\, \boldsymbol{x}'t;\, 2,\, \boldsymbol{x}t^+) = \frac{\delta G_1(1,\, 2)}{\delta U(\boldsymbol{x},\, \boldsymbol{x}';\, t)}\,. \tag{4.2}$$

A combination of eq. (4.2) with eqs. (A.7), (A.8), and (B.4) then yields

$$\begin{aligned} L(1,\, \boldsymbol{x}'t;\, 2,\, \boldsymbol{x}t^+) &= -\int \mathrm{d}34\, G_1(1,\, 3)\, \frac{\delta G_1^{-1}(3,\, 4)}{\delta U(\boldsymbol{x},\, \boldsymbol{x}';\, t)}\, G_1(4,\, 2) = \\ &= \int \mathrm{d}34\, G_1(1,\, 3) \left[ \delta(t_3 - t_4)\, \delta(t_4 - t)\, \delta(\boldsymbol{x}_3,\, \boldsymbol{x})\, \delta(\boldsymbol{x}_4,\, \boldsymbol{x}') + \frac{\delta\Sigma(3,\, 4)}{\delta U(\boldsymbol{x},\, \boldsymbol{x}';\, t)} \right] G_1(4,\, 2) = \\ &= G_1(1,\, \boldsymbol{x}t)\, G_1(\boldsymbol{x}'t,\, 2) + \int \mathrm{d}3456\, G_1(1,\, 3)\, G_1(4,\, 2)\, 3\, \frac{\delta\Sigma(3,\, 4)}{\delta G_1(6,\, 5)}\, L(6,\, \boldsymbol{x}'t;\, 5,\, \boldsymbol{x}t^+)\,. \end{aligned} \tag{4.3}$$

This is an integral equation for $L$, whereby $\boldsymbol{x}$, $\boldsymbol{x}'$, and $t$ play the role of external variables and the kernel

$$\Xi(3,\, 5;\, 4,\, 6) = \frac{\delta\Sigma(3,\, 4)}{\delta G_1(6,\, 5)} \tag{4.4}$$

represents an *effective two-particle interaction*. Notice that the limit as $U \to 0$ can be explicitly taken in eq. (4.3). Notice also the following properties.

i) The topology of its diagrammatic structure (cf. fig. 2*a*)) implies that eq. (4.3) can be generalized to hold for arbitrary values of the external time variables $t$ and $t'$ and not just in the limit $t' = t^-$. We can then write compactly

$$\begin{aligned} L(1,\, 2;\, 1',\, 2') &= G_1(1,\, 2')\, G_1(2,\, 1') + \\ &\quad + \int \mathrm{d}3456\, G_1(1,\, 3)\, G_1(4,\, 1')\, \Xi(3,\, 5;\, 4,\, 6)\, L(6,\, 2;\, 5,\, 2')\,. \end{aligned} \tag{4.5}$$

Equation (4.5) is known as the Bethe-Selpeter equation for $L$ [8].

ii) It is convenient to single out from the outset the Coulomb term in the effective interaction $\Xi$ by breaking up the self-energy $\Sigma$ as the sum of the Hartree term (3.12) and the mass operator $M$ (cf. eqs. (3.11)), to obtain

$$\Xi(3,\, 5;\, 4,\, 6) = -i\hbar\delta(3,\, 4)\, \delta(5,\, 6)\, v(3,\, 6) + \frac{\delta M(3,\, 4)}{\delta G_1(6,\, 5)}\,. \tag{4.6}$$

This splitting will enable us to identify the irreducible (or proper) part of $L$ as well as other correlation functions (appendix C).

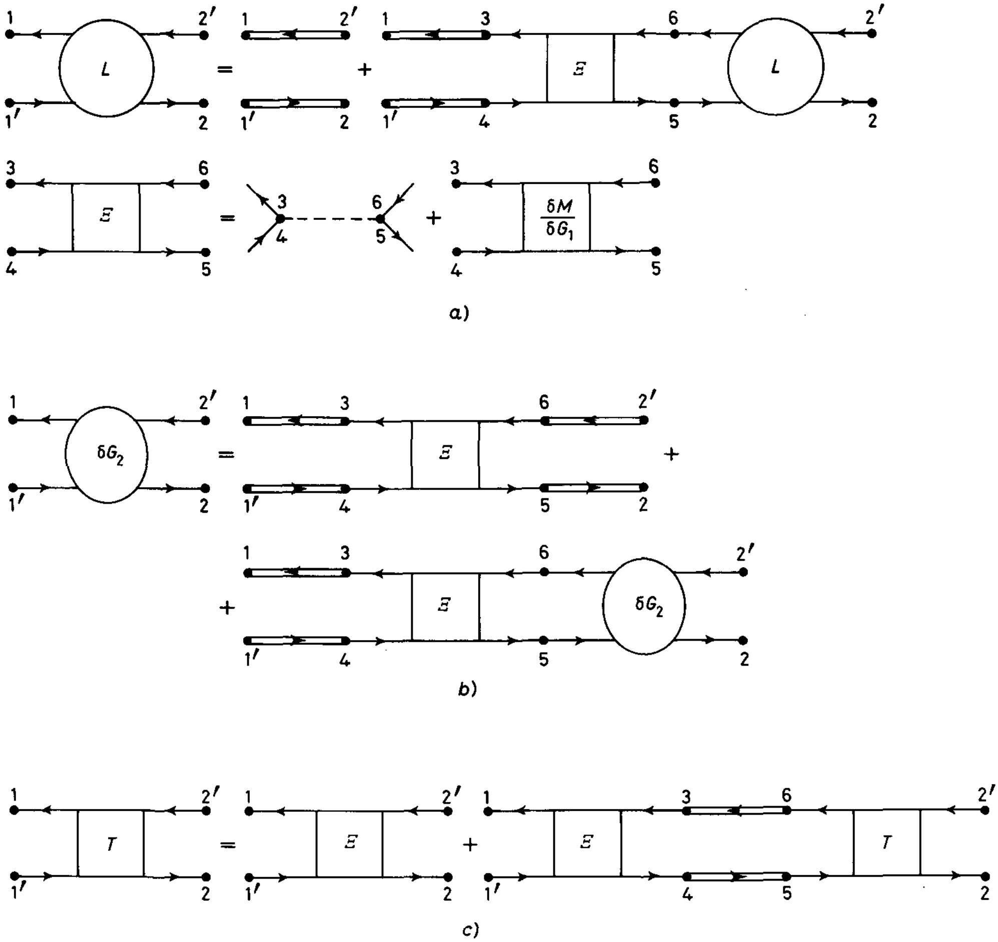

Fig. 2. – Bethe-Salpeter equation for *a*) the two-particle correlation function $L$, *b*) the bound part of the two-particle Green's function $\delta G_2$, and *c*) the many-particle $T$-matrix.

iii) A connection between the integral equations (4.5) for $L$ and (3.18) for $\tilde{\Gamma}$ can be drawn from the identity

$$(4.7)\qquad L(1,\,3;\,2,\,3^+) = \int \mathrm{d}45\, G_1(1,\,4)\, G_1(5,\,2)\, \Gamma(4,\,5;\,3)\,,$$

where we have introduced the *scalar* (*reducible*) *vertex function* $\Gamma$ defined as

$$(4.8)\qquad \Gamma(1,\,2;\,3) \equiv \int \mathrm{d}4\, \tilde{\Gamma}(1,\,2;\,4)\, \epsilon^{-1}(4,\,3) =$$

$$= -\int \mathrm{d}4\, \frac{\delta G_1^{-1}(1,\,2)}{\delta V(4)}\, \frac{\delta V(4)}{\delta U(3)} = -\frac{\delta G_1^{-1}(1,\,2)}{\delta U(3)}\,.$$

The last line of eq. (4.8) has been obtained from the definitions (3.17) and (3.19) and the «chain rule» (A.8).

Equation (4.5) is not the only form of the Bethe-Salpeter equation one finds in the literature. Two alternative forms are shown graphically in fig. 2*b*) and 2*c*). They can be obtained from eq. (4.5) as follows. The two-particle Green's function $G_2$ can be separated into a *free part* corresponding to the propagation of two single-particle excitations totally independent of one another and a *bound part* $\delta G_2$ [9]

$$G_2(1,2;1',2') = G_1(1,1')\,G_1(2,2') - G_1(1,2')\,G_1(2,1') + \delta G_2(1,2;1',2')\,, \tag{4.9}$$

whereby the bound part $\delta G_2$ satisfies the integral equation [9, 10]

$$\begin{aligned}\delta G_2(1,2;1',2') = -\int \mathrm{d}3456\, G_1(1,3)\,G_1(4,1')\,\Xi(3,5;4,6)\,\cdot \\ \cdot\, G_1(6,2')\,G_1(2,5) + \int \mathrm{d}3456\, G_1(1,3)\,G_1(4,1')\,\Xi(3,5;4,6)\,\delta G_2(6,2;5,2')\,.\end{aligned} \tag{4.10}$$

Otherwise, one can introduce the *many-particle T-matrix* defined as the solution of the integral equation [9, 11]

$$\begin{aligned}T(1,2;1',2') = \Xi(1,2;1',2') + \\ + \int \mathrm{d}3456\, \Xi(1,4;1',3)\,G_1(3,6)\,G_1(5,4)\,T(6,2;5,2')\,.\end{aligned} \tag{4.11}$$

Solving eq. (4.11) is equivalent to solving eq. (4.10) since the bound part $\delta G_2$ can be obtained by attaching a single-particle Green's function to each end point of $T$:

$$\begin{aligned}\delta G_2(1,2;1',2') = \\ = -\int \mathrm{d}3456\, G_1(1,3)\,G_1(4,1')\,T(3,5;4,6)\,G_1(6,2')\,G_1(2,5)\,.\end{aligned} \tag{4.12}$$

The spin variables can be eliminated from explicit consideration whenever the Hamiltonian is spin independent. The procedure is trivial for the single-particle Green's function, the vertex function, and the polarizability, but it requires some care for the two-particle Green's function or the $T$-matrix. In particular, the effective interaction entering the Bethe-Selpeter equation for the singlet channel differs from that for the triplet channels (appendix D).

Comparison of eqs. (3.22) and (4.1) shows that the polarizability $\chi$ can be obtained as a degenerate form of the two-particle correlation function $L$, namely,

$$\chi(1,2) = -i\hbar L(1,2;1^+,2^+)\,. \tag{4.13}$$

In this limit the Bethe-Selpeter equation (4.5) is equivalent to the set of equations (3.24), (3.26), and (3.18), thereby providing information on the density fluctuations of the system and related physical quantities (such as plasmons).

The full equation (4.5), on the other hand, is relevant to the study of bound-state problems (such as excitons) in the spirit of the original work of Gell-Mann and Low [12] (cf. sect. 11).

## 5. – Connection with linear-response theory.

The time-ordered correlation functions introduced thus far (cf. appendix C) do not directly represent the effects of the coupling between a system of particles and an external agent when causal boundary conditions are required. Specifically, if the system was in the ground state before the external agent acted, the *linear response* of the ground-state expectation value of a given operator $\hat{O}(\boldsymbol{x}, t)$ is known to be given by a Kubo formula [13]

$$\delta\langle\hat{O}(\boldsymbol{x}, t)\rangle = \frac{i}{\hbar}\int_{-\infty}^{t} \mathrm{d}t' \langle N|[\hat{H}'_{\mathrm{I}}(t'), \hat{O}_{\mathrm{I}}(\boldsymbol{x}, t)]|N\rangle . \tag{5.1}$$

Here

$$\hat{H}'_{\mathrm{I}}(t) = \exp[i\hat{H}t/\hbar]\,\hat{H}'(t)\,\exp[-i\hat{H}t/\hbar]\,, \tag{5.2a}$$

$$\hat{O}_{\mathrm{I}}(\boldsymbol{x}, t) = \exp[i\hat{H}t/\hbar]\,\hat{O}(\boldsymbol{x}, t)\,\exp[-i\hat{H}t/\hbar]\,, \tag{5.2b}$$

where $\hat{H}'(t)$ is the (weak) time-dependent interaction Hamiltonian between the system and the external agent. In particular, for an electromagnetic field $\hat{H}'(t)$ is given by eq. (C.1). In this case one is interested in the linear response of the density and current operators, given by eq. (C.2) and by

$$\hat{\boldsymbol{J}}(\boldsymbol{x}, t) = \hat{\boldsymbol{j}}(\boldsymbol{x}) - \frac{q}{mc}\boldsymbol{A}(\boldsymbol{r}, t)\,\hat{\rho}(\boldsymbol{x})\,, \tag{5.3}$$

respectively (cf. eq. (C.3)). To first order in the fields, one obtains for the total density and current:

$$\langle\hat{\rho}(1)\rangle_{\boldsymbol{A},\varphi} = \langle N|\hat{\rho}(1)|N\rangle + q\int \mathrm{d}2\left(\chi_{\mathrm{R}}(1, 2)\,\varphi(2) - \frac{1}{c}\vec{\chi}_{\mathrm{R}}(1, 2)\cdot\boldsymbol{A}(2)\right), \tag{5.4}$$

$$\langle\hat{\boldsymbol{J}}(1)\rangle_{\boldsymbol{A},\varphi} = -\frac{q}{mc}\langle N|\hat{\rho}(1)|N\rangle\,\boldsymbol{A}(1) + \\ + q\int \mathrm{d}2\left(\overleftarrow{\chi}_{\mathrm{R}}(1, 2)\,\varphi(2) - \frac{1}{c}\overleftrightarrow{\chi}_{\mathrm{R}}(1, 2)\cdot\boldsymbol{A}(2)\right), \tag{5.5}$$

where we have introduced the retarded counterparts of the correlation functions

(C.23) and (C.24):

$$\chi_{\mathrm{R}}(1,\ 2) = -\frac{i}{\hbar}\langle N|[\hat{\rho}'(1),\ \hat{\rho}'(2)]|N\rangle\,\theta(t_1 - t_2)\,, \tag{5.6a}$$

$$\overleftarrow{\chi}_{\mathrm{R}}(1,\ 2) = -\frac{i}{\hbar}\langle N|[\hat{\boldsymbol{j}}'(1),\ \hat{\rho}'(2)]|N\rangle\,\theta(t_1 - t_2)\,, \tag{5.6b}$$

$$\overleftrightarrow{\chi}_{\mathrm{R}}(1,\ 2) = -\frac{i}{\hbar}\langle N|[\hat{\boldsymbol{j}}'(1),\ \hat{\boldsymbol{j}}'(2)]|N\rangle\,\theta(t_1 - t_2)\,. \tag{5.6c}$$

Here the unit step function $\theta(t_1 - t_2)$ enforces the casual boundary conditions as it limits the knowledge of the interaction between the system and the external agent to antecedent times; the time-ordered correlation functions (C.23) and (C.24), on the other hand, require also the knowledge of the future of this interaction and thus do not have bearing on the experimental situation. However, the retarded correlation functions cannot be calculated through the set of coupled integral equations developed in appendix C (or, alternatively, by the Feynman-Dyson perturbation series) because the identities (C.4) and (C.5) hold only for time-ordered products of operators (or, alternatively, Wick's theorem applies only to these products). A connection between the two sets of correlation functions is then in order. This connection can be drawn by looking at the respective Lehmann representations after Fourier tranforming the time dependence.

For a general pair of time-ordered and retarded correlation functions

$$C_{\mathrm{T}}^{AB}(1,\ 2) \equiv -\frac{i}{\hbar}\langle N|T[\hat{A}'(1)\hat{B}'(2)]|N\rangle\,, \tag{5.7}$$

$$C_{\mathrm{R}}^{AB}(1,\ 2) \equiv -\frac{i}{\hbar}\langle N|[\hat{A}'(1),\ \hat{B}'(2)]|N\rangle\,\theta(t_1 - t_2)\,, \tag{5.8}$$

where $\hat{A}$ and $\hat{B}$ are Hermitian Bose-like operators, we obtain

$$C_{\mathrm{T}}^{AB}(\boldsymbol{x}_1,\ \boldsymbol{x}_2;\ \omega) = \sum_{s\neq 0}\left(\frac{A_s(\boldsymbol{x}_1)\,B_s^*(\boldsymbol{x}_2)}{\hbar\omega + E_0 - E_s + i\delta} - \frac{A_s^*(\boldsymbol{x}_1)\,B_s(\boldsymbol{x}_2)}{\hbar\omega + E_s - E_0 - i\delta}\right), \tag{5.9}$$

$$C_{\mathrm{R}}^{AB}(\boldsymbol{x}_1,\ \boldsymbol{x}_2;\ \omega) = \sum_{s\neq 0}\left(\frac{A_s(\boldsymbol{x}_1)\,B_s^*(\boldsymbol{x}_2)}{\hbar\omega + E_0 - E_s + i\delta} - \frac{A_s^*(\boldsymbol{x}_1)\,B_s(\boldsymbol{x}_2)}{\hbar\omega + E_s - E_0 + i\delta}\right). \tag{5.10}$$

Here the index $s$ labels the eigenstates $|N,\ s\rangle$ of the unperturbed Hamiltonian $\hat{H}$ ($s = 0$ corresponds to the ground state $|N\rangle$), $(E_s - E_0) > 0$ is an excitation energy,

$\delta \to 0^+$, and

$$A_s(\boldsymbol{x}) = \langle N|\hat{A}(\boldsymbol{x})|N,\, s\rangle\,. \tag{5.11}$$

Note the following properties (for real $\omega$):

$$\text{i)}\quad C_{\mathrm{R}}^{AB}(\boldsymbol{x}_1,\, \boldsymbol{x}_2;\, -\omega) = C_{\mathrm{R}}^{AB}(\boldsymbol{x}_1,\, \boldsymbol{x}_2;\, \omega)^*\,, \tag{5.12}$$

which implies that its real part is an even and its imaginary part is an odd function of $\omega$;

$$\text{ii)}\quad C_{\mathrm{T}}^{AB}(\boldsymbol{x}_1,\, \boldsymbol{x}_2;\, -\omega) = C_{\mathrm{T}}^{BA}(\boldsymbol{x}_2,\, \boldsymbol{x}_1;\, \omega)\,; \tag{5.13}$$

$$\text{iii)}\quad C_{\mathrm{R}}^{AB}(\boldsymbol{x}_1,\, \boldsymbol{x}_2;\, \omega) = C_{\mathrm{T}}^{AB}(\boldsymbol{x}_1,\, \boldsymbol{x}_2;\, \omega)\,, \tag{5.14}$$

for $\omega > 0$. One can thus evaluate $C_{\mathrm{T}}^{AB}(\boldsymbol{x}_1, \boldsymbol{x}_2; \omega)$ for $\omega > 0$ by standard many-body techniques and then obtain $C_{\mathrm{R}}^{AB}(\boldsymbol{x}_1, \boldsymbol{x}_2; \omega)$ for all values of $\omega$ through eqs. (5.12) and (5.14).

Further properties can be obtained when the operators $\hat{A}$ and $\hat{B}$ coincide with either $\hat{\rho}$ or $\hat{\boldsymbol{j}}$. In this case $\chi_{\mathrm{T}}(\boldsymbol{x}_1, \boldsymbol{x}_2; \omega)$ and $\overleftrightarrow{\chi}_{\mathrm{T}}(\boldsymbol{x}_1, \boldsymbol{x}_2; \omega)$ are even functions of $\omega$, while $\vec{\chi}_{\mathrm{T}}(\boldsymbol{x}_1, \boldsymbol{x}_2; \omega)$ is an odd function of $\omega$ (provided no magnetic field is present).

## 6. – Conserving approximations.

An approximate solution to the coupled set of integro-differential equations discussed in sects. 3 and 4 may or may not be consistent with the general (number, momentum, and energy) conservation laws satisfied by the exact solution. A particular approximation is then said to be conserving if it satisfies the restrictions imposed by the conservation laws. These restrictions have been first formulated by Baym and Kadanoff [11] in terms of sufficient conditions to be satisfied by the approximate self-energy operator $\Sigma$, and successively recast in a simple diagrammatic form by Baym [14]. Fulfillment of conservation criteria turns out to be essential to correctly describe transport phenomena (as, for instance, in the context of the Landau theory of Fermi liquids [9]); however, it may be less important in other contexts such as the determination of single-particle and bound electron-hole pairs excited states of a crystal. In any case, one should be aware of possible violations of conservation laws although it might be difficult to fulfill them in practice.

A sufficient condition to ensure fulfillment of conservation laws is that any approximation for the self-energy operator $\Sigma$ be «$\Phi$-derivable» in the sense that there exists a functional $\Phi$ such that [14]

$$\Sigma(1,2)=\frac{\delta\Phi}{\delta G_1(2,1)}\,. \tag{6.1}$$

$\Phi$ is meant to be a functional of the bare Coulomb potential $v(1,2)$ and of the generalized single-particle Green's function $G_1(1,2)$ (in the presence of an external field $U$), which has thus to be determined self-consistently via Dyson's equation (3.14). Examples that show how $\Phi$ can be constructed to reproduce known approximate expressions of $\Sigma$ are reported in fig. 3. Notice there that condition (6.1) requires certain diagrams for $\Sigma$ to be taken *together*, as for the terms *c*) and *f*). This feature, in turn, implies that the two alternative expressions (3.31) and (3.32) for the mass operator $M$ coincide for the given approximation, as anticipated in the discussion of eq. (3.11).

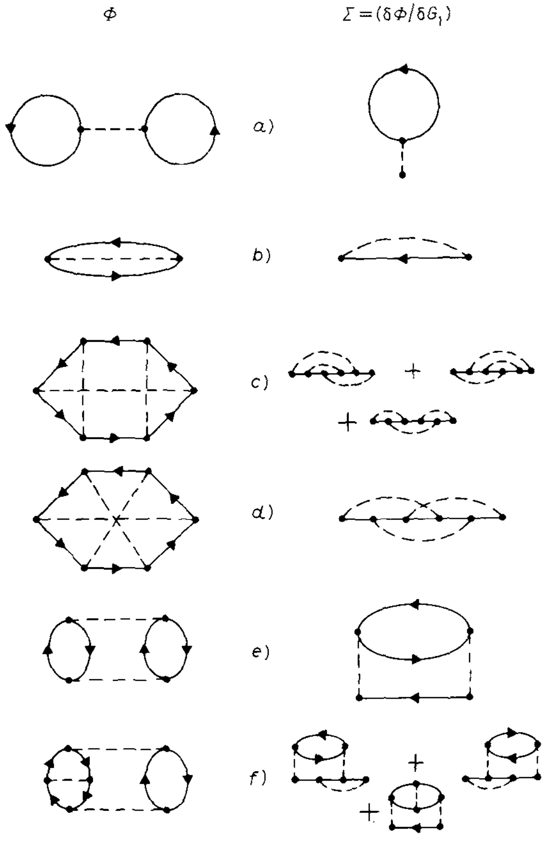

Fig. 3. – Examples of correspondence between diagrams for $\Phi$ and $\Sigma$. Straight lines here denote the self-consistent single-particle Green's function $G_1$ and broken lines denote the bare Coulomb potential $v$.

Conservation laws for the ground state follow directly when condition (6.1) is satisfied. In addition, conservation laws are also fulfilled within linear response if, for the given choice of $\Sigma$, the two-particle correlation function $L$ satisfies the Bethe-Salpeter equation (4.5) with kernel $\Xi = \delta\Sigma/\delta G_1$ (that is, with no terms omitted) [14]. In this case we can express (cf. eqs. (4.4) and (6.1)):

$$\Xi(1,\,2;\,1',\,2') = \frac{\delta^2 \Phi}{\delta G_1(2',\,2)\,\delta G_1(1',\,1)} = \Xi(2,\,1;\,2',\,1')\,, \tag{6.2}$$

which leads to the symmetry condition

$$L(1,\,2;\,1',\,2') = L(2,\,1;\,2',\,1') \tag{6.3}$$

for the approximate two-particle correlation function.

As an example, we consider the number conservation law expressed in terms of $G$

$$\begin{aligned} \frac{\partial}{\partial t_1} i\hbar G_1(1,\,1^+) + \nabla_1 \cdot \left[\frac{\hbar}{2im}(\nabla_1 - \nabla_2)\, i\hbar G_1(1,\,2)\right]_{2=1^+} &= \\ = \left[\left(\frac{\partial}{\partial t_1} + \frac{\partial}{\partial t_2}\right) i\hbar G_1(1,\,2) + \frac{\hbar^2}{2m}(\nabla_1^2 - \nabla_2^2)\, G_1(1,\,2)\right]_{2=1^+} &= 0\,. \end{aligned} \tag{6.4}$$

To recover this equation for the approximate $G_1$, we begin by subtracting the two alternative forms of Dyson's equation (3.14*a*) and (3.14*b*), to obtain

$$\begin{aligned} &\left(\frac{\partial}{\partial t_1} + \frac{\partial}{\partial t_2}\right) i\hbar G_1(1,\,2) + \frac{\hbar^2}{2m}(\nabla_1^2 - \nabla_2^2)\, G_1(1,\,2) - \\ &\quad - (V(\mathbf{r}_1) + U(1) - V(\mathbf{r}_2) - U(2))\, G_1(1,\,2) + \\ &\quad + \int \mathrm{d}3\,(G_1(1,\,3)\,\overline{\Sigma}(3,\,2) - \Sigma(1,\,3)\, G_1(3,\,2)) = 0\,, \end{aligned} \tag{6.5}$$

and then take the limit as $2 \to 1^+$. In this limit, one can readily show from eqs. (3.11) that

$$\lim_{2\to 1^+} \int \mathrm{d}3\,(G_1(1,\,3)\,\Sigma(3,\,2) - \Sigma(1,\,3)\, G_1(3,\,2)) = 0\,, \tag{6.6}$$

since $\Sigma = \overline{\Sigma}$ for a conserving approximation. Equation (6.4) thus follows.

Equation (6.6) can alternatively be obtained by noticing that the functional $\Phi$ is, by construction, invariant under the transformation

$$\begin{aligned} G_1(1,\,2) \to \exp[i\Lambda(1)]\, G_1(1,\,2)\, \exp[-i\Lambda(2)] &\simeq \\ \simeq G_1(1,\,2) + i(\Lambda(1) - \Lambda(2))\, G_1(1,\,2)&\,, \end{aligned} \tag{6.7}$$

to lowest order in the small function $\Lambda$. Variation of $\Phi$ then gives

$$\begin{aligned}(6.8)\qquad \delta\Phi &= \int \mathrm{d}12\, \frac{\delta\Phi}{\delta G_1(1,\,2)}\, \delta G_1(1,\,2^+) = \\ &= \int \mathrm{d}12\, \Sigma(2,\,1)\, i(\Lambda(1) - \Lambda(2^+))\, G_1(1,\,2^+) = \\ &= i\int \mathrm{d}1\, \Lambda(1^+) \int \mathrm{d}2 (G_1(1,\,2)\Sigma(2,\,1^+) - \Sigma(1,\,2)\, G_1(2,\,1^+)) = 0\,,\end{aligned}$$

where account has been taken of eqs. (6.1) and (6.7). (The need to replace $2 \to 2^+$ in the first line of eq. (6.8) originates from the Hartree-Fock term.) The arbitrariness of $\Lambda$ yields eventually eq. (6.6).

Physically, eq. (6.4) reduces to the continuity equation for the ground state in the limit of zero external field $U$ [15]. However, eq. (6.4) holds more generally for arbitrary $U$ and thus it contains information about the induced density and current within linear response. Specifically, taking the functional derivative of eq. (6.4) with respect to $U(3)$ and recalling eqs. (A.13) and (C.26), yields

$$\begin{aligned}(6.9)\qquad &\frac{\partial}{\partial t_1} i\hbar L(1,\,3;\,1^+,\,3^+) + \boldsymbol{\nabla}_1 \cdot i\hbar \left[\frac{\hbar}{2im} (\boldsymbol{\nabla}_1 - \boldsymbol{\nabla}_2)\, L(1,\,3;\,2,\,3^+)\right]_{2=1^+} = \\ &\qquad = -\left(\frac{\partial}{\partial t_1} \chi(1,\,3) + \boldsymbol{\nabla}_1 \cdot \overleftarrow{\chi}(1,\,3)\right) = 0\,,\end{aligned}$$

where the limit for vanishing $U$ is now understood.

Equation (6.9) holds for the approximate correlation functions, provided $L$ satisfies the Bethe-Salpeter equation (4.5) with kernel taken according to eq. (6.2). To interpret it as the continuity equation for the induced density and current within linear response, the connection established in sect. 5 between time-ordered and retarded correlation functions has to be recalled. In particular, by Fourier transforming the time dependence of eq. (6.9) and making use of the properties (5.12) and (5.14), it follows that (cf. eqs. (5.4) and (5.5))

$$(6.10)\qquad \frac{\partial}{\partial t_1} \langle \hat{\rho}(1) \rangle_U + \boldsymbol{\nabla}_1 \cdot \langle \hat{\boldsymbol{j}}(1) \rangle_U = \int \mathrm{d}2 \left(\frac{\partial}{\partial t_1} \chi_{\mathrm{R}}(1,\,2) + \boldsymbol{\nabla}_1 \cdot \overleftarrow{\chi}_{\mathrm{R}}(1,\,2)\right)_{U=0} U(2) = 0\,.$$

Equation (6.9) can also be obtained as a particular limit of a more general equation relating $\Sigma$ to $L$ which is satisfied by a «$\Phi$-derivable» approximation, as discussed in the next section.

## 7. – Gauge invariance, current conservation, and the Ward identities.

In this section we derive an identity relating the exact single- and two-particle Green's functions as well as any conserving approximation to these functions. This identity (which will be referred to as the «generalized Ward identity») will be shown to follow from the gauge invariance of the theory and to reduce to the continuity equation (6.9) for the induced density and current in a particular limit. The ordinary Ward identities [9] will also be recovered as special forms of the generalized Ward identity.

To derive the relationship between single- and two-particle Green's functions, we begin by coupling the system to the electromagnetic field according to eq. (C.1), where we replace [14]

$$\left\{\begin{aligned} &\boldsymbol{A}(\boldsymbol{r},t)\to\boldsymbol{\nabla}\Lambda(\boldsymbol{r},t),\\ &\varphi(\boldsymbol{r},t)\to-\frac{1}{c}\frac{\partial}{\partial t}\Lambda(\boldsymbol{r},t).\end{aligned}\right. \tag{7.1}$$

The resulting interaction Hamiltonian, which corresponds to vanishing electric and magnetic fields (gauge Hamiltonian), can then be utilized to define generalized Green's functions according to eqs. (2.9) and (2.10). In particular, the single-particle Green's function satisfies the following equation of motion:

$$\left[i\hbar\frac{\partial}{\partial t_1}+\frac{\hbar^2}{2m}(\boldsymbol{\nabla}_1+\boldsymbol{\nabla}_1\tilde{\Lambda}(1))^2-V(\boldsymbol{r}_1)+i\hbar\frac{\partial}{\partial t_1}\tilde{\Lambda}(1)\right]G_1(1,2;\tilde{\Lambda})-\\ -\int \mathrm{d}3\,\Sigma(1,3;\tilde{\Lambda})\,G_1(3,2;\tilde{\Lambda})=\delta(1,2), \tag{7.2}$$

where

$$\tilde{\Lambda}(1)=\frac{q}{i\hbar c}\Lambda(1). \tag{7.3}$$

Equation (7.2) can be obtained from eq. (3.14*a*) with the usual replacement in the presence of an electromagnetic field

$$\left\{\begin{aligned} &\boldsymbol{\nabla}\to\boldsymbol{\nabla}+\frac{q}{i\hbar c}\boldsymbol{A},\\ &V\to V+q\varphi,\end{aligned}\right. \tag{7.4}$$

where now $\boldsymbol{A}$ and $\varphi$ are taken according to eq. (7.1). The solution of eq. (7.2) can be expressed as [14]

$$G_1(1,2;\tilde{\Lambda})=\exp[-\tilde{\Lambda}(1)]\,G_1(1,2;\tilde{\Lambda}=0)\,\exp[\tilde{\Lambda}(2)], \tag{7.5}$$

which can be verified at every order of a diagrammatic expansion of $\Sigma$ in terms of $G_1$. Equation (7.5) implies that

$$\left.\frac{\delta G_1(1,\,2;\,\tilde{\Lambda})}{\delta\tilde{\Lambda}(3)}\right|_{\tilde{\Lambda}=0} = (\delta(2,\,3)-\delta(1,\,3))\,G_1(1,\,2) \tag{7.6}$$

for the exact generalized single-particle Green's function as well for any approximation to it.

The desired connection with the two-particle Green's function can then be established by expressing the functional derivative in eq. (7.6) in an alternative form by recalling eqs. (C.4) and (C.5). We write

$$\delta G_1(1,\,2;\,\tilde{\Lambda}) = -i\hbar\int \mathrm{d}3\left\{L(1,\,3;\,2,\,3^+)\frac{\partial}{\partial t_3}\tilde{\Lambda}(3)+\right. \\ \left.+\left[\frac{\hbar}{2im}(\nabla_3-\nabla_{3'})\,L(1,\,3;\,2,\,3')\right]_{3'=3^+}\cdot\nabla_3\tilde{\Lambda}(3)\right\}, \tag{7.7}$$

for an infinitesimal $\tilde{\Lambda}$. Integration by parts in eq. (7.7) yields

$$\left.\frac{\delta G_1(1,\,2;\,\tilde{\Lambda})}{\delta\tilde{\Lambda}(3)}\right|_{\tilde{\Lambda}=0} = i\hbar\left\{\frac{\partial}{\partial t_3}L(1,\,3;\,2,\,3^+)+\right. \\ \left.+\nabla_3\cdot\left[\frac{\hbar}{2im}(\nabla_3-\nabla_{3'})\,L(1,\,3;\,2,\,3')\right]_{3'=3^+}\right\}, \tag{7.8}$$

and comparison with eq. (7.6) leads eventually the *generalized Ward identity* in the form

$$\frac{\partial}{\partial t_3}L(1,\,3;\,2,\,3^+)+\nabla_3\cdot\left[\frac{\hbar}{2im}(\nabla_3-\nabla_{3'})\,L(1,\,3;\,2,\,3')\right]_{3'=3^+} = \\ =\frac{i}{\hbar}(\delta(1,\,3)-\delta(2,\,3))\,G_1(1,\,2), \tag{7.9}$$

where the limit $\tilde{\Lambda}=0$ is understood.

This equation holds for any approximate two-particle correlation function $L$, provided it satisfies the Bethe-Salpeter equation (4.5) with kernel $\Xi$ obtained from the approximate single-particle Green's function $G_1$ according to the prescription (4.4). However, in order to recover from eq. (7.9) the continuity equation (6.9) for the induced density and current within linear response, the kernel $\Xi$ has in addition to satisfy the symmetry requirement (6.2) which is met by any «$\Phi$-derivable» approximation. This is because the resulting symmetry property (6.3) for $L$ is required to relate the restrictions of local charge conservation (6.9) and of gauge invariance (7.9) [16].

The identity (7.9) can be obtained in an alternative way by expressing is left-hand side in terms of the density and current deviation operators (C.25)

$$\begin{aligned}(7.10)\qquad &\frac{\partial}{\partial t_3}L(1,\,3;\,2,\,3^+)+\boldsymbol{\nabla}_3\cdot\left[\frac{\hbar}{2im}(\boldsymbol{\nabla}_3-\boldsymbol{\nabla}_{3'})L(1,\,3;\,2,\,3')\right]_{3'=3^+}=\\ &=-\frac{1}{\hbar^2}\left\{\frac{\partial}{\partial t_3}\langle N|T[\hat{\rho}'(3)\,\hat{\Psi}(1)\,\hat{\Psi}^\dagger(2)]|N\rangle+\boldsymbol{\nabla}_3\cdot\langle N|T[\hat{\boldsymbol{j}}'(3)\,\hat{\Psi}(1)\,\hat{\Psi}^\dagger(2)]|N\rangle\right\}=\\ &=-\frac{1}{\hbar^2}\left\{\left\langle N\left|T\left[\left(\frac{\partial}{\partial t_3}\hat{\rho}'(3)+\boldsymbol{\nabla}_3\cdot\hat{\boldsymbol{j}}'(3)\right)\hat{\Psi}(1)\,\hat{\Psi}^\dagger(2)\right]\right|N\right\rangle-\right.\\ &\qquad\qquad\left.-\,i\hbar(\delta(1,\,3)-\delta(2,\,3))\,G_1(1,\,2)\right\},\end{aligned}$$

where the last term proportional to the single-particle Green's function originates from the time derivative of the time-ordering operator. Requiring the continuity equation for the density and current deviation operators to hold leads eventually to the result (7.9).

The generalized Ward identity (7.9) can also be rewritten in terms of the scalar and vector vertex functions through eqs. (C.8) and (C.9). Projection from the left and the right onto a pair of $G_1^{-1}$ with suitable arguments yields in fact

$$\begin{aligned}(7.11)\qquad &\frac{\partial}{\partial t_3}\mathit{\Gamma}(1,\,2;\,3)+\boldsymbol{\nabla}_3\cdot\boldsymbol{\Gamma}(1,\,2;\,3)=\frac{i}{\hbar}(\delta(2,\,3)-\delta(1,\,3))\,G_1^{-1}(1,\,2)=\\ &=\frac{i}{\hbar}(\delta(2,\,3)-\delta(1,\,3))\left\{\left[i\hbar\frac{\partial}{\partial t_1}+\frac{\hbar^2}{2m}\boldsymbol{\nabla}_1^2\right]\delta(1,\,2)-M(1,\,2)\right\}\end{aligned}$$

(cf. eqs. (B.4) with $U=0$, (2.2), (3.11), and (3.12)). Notice that the Hartree contribution to the self-energy operator (as well as the potential term) drops out from the right-hand side of eq. (7.11). This remark suggests that eq. (7.11) actually holds for the irreducible vertex functions introduced in appendix C. We can, in fact, express

$$(7.12a)\qquad \mathit{\Gamma}(1,\,2;\,3)=\tilde{\mathit{\Gamma}}(1,\,2;\,3)+\int \mathrm{d}45\,\tilde{\mathit{\Gamma}}(1,\,2;\,4)\,v(4,\,5)\,\chi(5,\,3)\,,$$

$$(7.12b)\qquad \boldsymbol{\Gamma}(1,\,2;\,3)=\tilde{\boldsymbol{\Gamma}}(1,\,2;\,3)+\int \mathrm{d}45\,\tilde{\boldsymbol{\Gamma}}(1,\,2;\,4)\,v(4,\,5)\,\vec{\chi}(5,\,3)\,,$$

that give

$$\begin{aligned}(7.13)\qquad &\frac{\partial}{\partial t_3}\mathit{\Gamma}(1,\,2;\,3)+\boldsymbol{\nabla}_3\cdot\boldsymbol{\Gamma}(1,\,2;\,3)=\frac{\partial}{\partial t_3}\tilde{\boldsymbol{\Gamma}}(1,\,2;\,3)+\boldsymbol{\nabla}_3\cdot\tilde{\boldsymbol{\Gamma}}(1,\,2;\,3)+\\ &\qquad+\int \mathrm{d}45\,\mathit{\Gamma}(1,\,2;\,4)\,v(4,\,5)\left[\frac{\partial}{\partial t_3}\chi(5,\,3)+\boldsymbol{\nabla}_3\cdot\vec{\chi}(5,\,3)\right].\end{aligned}$$

The continuity equation (6.9) for the induced density and current within linear response together with the symmetry properties of the correlation functions under the interchange of their arguments, guarantee the expression within brackets to vanish and allow us to replace the vertex functions in eq. (7.11) by their irreducible counterparts.

The ordinary Ward identities, which express a constraint between the derivatives of the self-energy operator and the vertex functions in the limit of long wave lenghts and small frequencies [9], can now be recovered from the generalized Ward identity (7.11) as follows. Let us consider, in particular, a translationally invariant system that admits the Fourier representations (D.13). After elimination of the spin variables eqs. (7.11) and (7.13) reduce thus to

$$q_0\tilde{\Gamma}(p;\, q) - \boldsymbol{q}\cdot\tilde{\boldsymbol{\Gamma}}(p;\, q) = q_0 - \frac{\hbar}{m}\boldsymbol{q}\cdot\boldsymbol{p} + \frac{1}{\hbar}[M(p-q/2) - M(p+q/2)]\,, \tag{7.14}$$

where $p = (\boldsymbol{p},\, p_0)$ and $q = (\boldsymbol{q},\, q_0)$. Taking the limit as $q \rightarrow 0$ (for given $p$) of eq. (7.14) yields

$$\tilde{\Gamma}(p;\, 0) = 1 - \frac{\partial M(p)}{\partial \hbar p_0} \tag{7.15a}$$

when $\boldsymbol{q}/q_0 \rightarrow 0$, and

$$\tilde{\boldsymbol{\Gamma}}(p;\, 0) = \frac{\hbar\boldsymbol{p}}{m} + \boldsymbol{\nabla}_{\hbar\boldsymbol{p}} M(p)\,, \tag{7.15b}$$

when $\boldsymbol{q}/q_0 \rightarrow \infty$. Notice that, on the Fermi surface, the Ward identities (7.15) relate the renormalized vertices to the wave function renormalization

$$a = \left[1 - \left.\frac{\partial M(p)}{\partial \hbar p_0}\right|_{\varepsilon_{\mathrm{F}}}\right]^{-1} \tag{7.16}$$

and to the effective mass of a quasi-particle

$$a\,\frac{m^*}{m} = \left[1 + \frac{m}{\hbar|\boldsymbol{p}_{\mathrm{F}}|}\,\frac{\partial}{\partial \hbar|\boldsymbol{p}|} M(|\boldsymbol{p}|,\, \varepsilon_{\mathrm{F}})\right|_{|\boldsymbol{p}_{\mathrm{F}}|}\Bigg]^{-1}\,. \tag{7.17}$$

Equation (7.15*a*), in particular, is needed, *e.g.*, to derive Landau's transport equation for a Fermi liquid from the Bethe-Salpeter equation [9].

Similar identities have been utilized in the theory of the inhomogeneous interacting electron gas to reveal the short-range density dependence of the mass operator [17], as well as in the theory of shallow impurities states in semiconductors [18]. For these inhomogeneous systems the identity corresponding to eq. (7.15*a*) can be obtained alternatively in the following way [19]. We may regard the scalar potential $U$ in eq. (3.14) as a slowly varying perturbation in time which is uniform throughout the system and set accordingly $U(1) = -\alpha q$ with $\alpha$ infinitesimal. This perturbation induces a change in the inverse single-particle Green's function which can be written in two ways. On the one hand, we can make use of the scalar (irreducible) vertex function (3.17) to write

$$\delta G_1^{-1}(1,\,2) = -\int \mathrm{d}3\tilde{\Gamma}(1,\,2;\,3)\,\delta V(3)\,, \tag{7.18}$$

with (cf. eq. (3.15))

$$\delta V(3) = -\alpha q - i\hbar\int \mathrm{d}2 v(3,\,2)\,\delta G_1(2,\,2^+)\,. \tag{7.19}$$

On the other hand, we can consider the shift (7.19) as generated by the gauge transformation (7.1) with $\Lambda(1) = \alpha c t_1$, $c$ being the velocity of light, and write according to eq. (7.6)

$$\delta G_1(1,\,2) = \frac{i}{\hbar}\,q\alpha(t_1 - t_2)\,G_1(1,\,2)\,. \tag{7.20}$$

Equation (7.20) yields (cf. eqs. (A.7), (B.2), and (B.4))

$$\delta G_1^{-1}(1,\,2) = \frac{i}{\hbar}\,q\alpha(t_1 - t_2)\,G_1^{-1}(1,\,2) = q\alpha\left[\delta(1,\,2) - \frac{i}{\hbar}(t_1 - t_2)\,M(1,\,2)\right], \tag{7.21}$$

as well as $\delta V(3) = -\alpha q$, since $\delta G_1(2,\,2^+) = 0$. Comparison of eq. (7.21) with eq. (7.18) leads to the Ward identity

$$\frac{i}{\hbar}(t_1 - t_2)\,M(1,\,2) = \delta(1,\,2) - \int \mathrm{d}3\tilde{\Gamma}(1,\,2;\,3)\,. \tag{7.22}$$

Upon taking the time Fourier transform, eq. (7.22) reads

$$\frac{\partial}{\partial\hbar\Omega}M(\boldsymbol{r}_1,\,\boldsymbol{r}_2;\,\Omega) = \delta(\boldsymbol{r}_1 - \boldsymbol{r}_2) - \int \mathrm{d}\boldsymbol{r}_3\,\tilde{\Gamma}(\boldsymbol{r}_1,\,\boldsymbol{r}_2;\,\boldsymbol{r}_3|\Omega,\,\omega\to 0)\,, \tag{7.23}$$

which reduces to eq. (7.15*a*) for a homogeneous system.

From eq. (7.9) it can also be shown that any «$\Phi$-derivable» approximation satisfies an important sum rule known as the Thomas-Reiche-Kuhn sum rule (cf. appendix E).

## 8. – Optical properties of semiconductors.

The purpose of this section is to apply the formal tools developed so far to the discussion of the optical properties of semiconductors. In particular, we shall combine the treatment of the *dynamics* of the many-body effects beyond the one-electron model with the *geometry* characterizing a crystalline semiconductor. After some general considerations which apply to semiconductors (or insulators) with arbitrary point-group symmetry and which can be formally carried out to all orders of (many-body) perturbation theory, we shall present numerical calculations for (cubic) covalent materials whereby the relevant many-body effect is the excitonic effect.

8'1. *Maxwell's equations and local-field effects.* – Charge densities and currents (over and above the ground-state values) can be partitioned into externally specified and induced contributions. The corresponding Maxwell's equations then read

$$\left\{\begin{aligned} &\nabla\cdot\boldsymbol{E}(\boldsymbol{r},\,t)=4\pi(\rho_{\text{ext}}(\boldsymbol{r},\,t)+\rho_{\text{ind}}(\boldsymbol{r},\,t))\,,\\ &\nabla\cdot\boldsymbol{B}(\boldsymbol{r},\,t)=0\,,\\ &\nabla\times\boldsymbol{E}(\boldsymbol{r},\,t)=-\frac{\partial}{\partial t}\boldsymbol{B}(\boldsymbol{r},\,t)\,,\\ &\nabla\times\boldsymbol{B}(\boldsymbol{r},\,t)=\frac{4\pi}{c}(\boldsymbol{J}_{\text{ext}}(\boldsymbol{r},\,t)+\boldsymbol{J}_{\text{ind}}(\boldsymbol{r},\,t))+\frac{1}{c}\frac{\partial}{\partial t}\boldsymbol{E}(\boldsymbol{r},\,t)\,.\end{aligned}\right. \tag{8.1}$$

Here the induced charge density and current can be obtained within linear response by multiplying the induced part of the number density (5.4) and current (5.5) by the electronic charge ($q=-e$). A comment about the nature of the scalar and vector potentials that enter these expressions is in order at this point. Although the choice of the gauge has been left unspecified in sect. 5 as well as in appendix C, the forms (2.1) and (C.1) for the unperturbed and interaction parts of the Hamiltonian, respectively, are actually consistent with the Coulomb (or transverse) gauge, in which

$$\nabla\cdot\boldsymbol{A}(\boldsymbol{r},\,t)=0\,. \tag{8.2}$$

The scalar and vector potentials entering eqs. (5.4) and (5.5) are thus to be understood as the *external* scalar potential and the *total* (transverse) vector potential which includes the induced contribution [20].

The Coulomb gauge yields a natural separation between the transverse (T) and longitudinal (L) parts of the electric field. We find it also convenient to introduce the so-called *perturbing electric field* [21]

$$\boldsymbol{E}^{\mathrm{P}}(\boldsymbol{r},\,t) \equiv -\frac{1}{c}\frac{\partial}{\partial t}\boldsymbol{A}(\boldsymbol{r},\,t) - \boldsymbol{\nabla}\varphi^{\mathrm{ext}}(\boldsymbol{r},\,t) = \boldsymbol{E}^{\mathrm{ext}}(\boldsymbol{r},\,t) + \boldsymbol{E}^{\mathrm{ind}}_{\mathrm{T}}(\boldsymbol{r},\,t) = \\ = \boldsymbol{E}(\boldsymbol{r},\,t) - \boldsymbol{E}^{\mathrm{ind}}_{\mathrm{L}}(\boldsymbol{r},\,t)\,, \tag{8.3}$$

in terms of which the induced charge density and current can be expressed. To this end, we need to exploit the generalized Ward identity (7.9) and the symmetry condition (6.3), to obtain

$$\begin{cases} -i\omega\chi_{\mathrm{R}}(\boldsymbol{r}_1,\,\boldsymbol{r}_2;\,\omega) + \boldsymbol{\nabla}_1\cdot\overleftarrow{\chi}_{\mathrm{R}}(\boldsymbol{r}_1,\,\boldsymbol{r}_2;\,\omega) = 0\,, \\ -i\omega\overrightarrow{\chi}_{\mathrm{R}}(\boldsymbol{r}_1,\,\boldsymbol{r}_2;\,\omega) + \boldsymbol{\nabla}_1\cdot\overleftrightarrow{\chi}_{\mathrm{R}}(\boldsymbol{r}_1,\,\boldsymbol{r}_2;\,\omega) + \dfrac{1}{m}\langle N|\hat{\rho}(\boldsymbol{r}_2)|N\rangle\,\boldsymbol{\nabla}_1\delta(\boldsymbol{r}_1-\boldsymbol{r}_2) = 0\,, \end{cases} \tag{8.4}$$

and

$$\begin{cases} i\omega\chi_{\mathrm{R}}(\boldsymbol{r}_1,\,\boldsymbol{r}_2;\,\omega) + \boldsymbol{\nabla}_2\cdot\overrightarrow{\chi}_{\mathrm{R}}(\boldsymbol{r}_1,\,\boldsymbol{r}_2;\,\omega) = 0\,, \\ i\omega\overleftarrow{\chi}_{\mathrm{R}}(\boldsymbol{r}_1,\,\boldsymbol{r}_2;\,\omega) + \boldsymbol{\nabla}_2\cdot\overleftrightarrow{\chi}_{\mathrm{R}}(\boldsymbol{r}_1,\,\boldsymbol{r}_2;\,\omega) + \dfrac{1}{m}\langle N|\hat{\rho}(\boldsymbol{r}_1)|N\rangle\,\boldsymbol{\nabla}_2\delta(\boldsymbol{r}_2-\boldsymbol{r}_1) = 0\,. \end{cases} \tag{8.5}$$

In eqs. (8.4) and (8.5) advantage has been taken of the time translational invariance of the unperturbed system by introducing the time Fourier transform, and the analytic continuation from time-ordered to retarded correlation functions has been performed according to the prescriptions of sect. 5. Recall also that eqs. (8.4) and (8.5) hold for any conserving ($\Phi$-derivable) approximation to the correlation functions.

Equations (8.4) ensure that the induced charge density and current obtained from eqs. (5.4) and (5.5) satisfy the continuity equation. Equations (8.5), on the other hand, enable us to rewrite

$$\begin{cases} \rho_{\mathrm{ind}}(\boldsymbol{r};\,\omega) = -\dfrac{q^2}{i\omega}\displaystyle\int \mathrm{d}\boldsymbol{r}'\,\overrightarrow{\chi}_{\mathrm{R}}(\boldsymbol{r},\,\boldsymbol{r}';\,\omega)\cdot\boldsymbol{E}^{\mathrm{P}}(\boldsymbol{r}';\,\omega)\,, \\ \boldsymbol{J}_{\mathrm{ind}}(\boldsymbol{r};\,\omega) = -i\omega\displaystyle\int \mathrm{d}\boldsymbol{r}'\,\overleftrightarrow{\alpha}(\boldsymbol{r},\,\boldsymbol{r}';\,\omega)\cdot\boldsymbol{E}^{\mathrm{P}}(\boldsymbol{r}';\,\omega)\,, \end{cases} \tag{8.6}$$

where we have introduced the so-called *quasi-polarizability* tensor

$$\overleftrightarrow{\alpha}(\boldsymbol{r},\,\boldsymbol{r}';\,\omega) \equiv -\frac{q^2}{\omega^2}\left(\overleftrightarrow{\chi}_{\mathrm{R}}(\boldsymbol{r},\,\boldsymbol{r}';\,\omega) + \frac{1}{m}\langle N|\hat{\rho}(\boldsymbol{r})|N\rangle\,\delta(\boldsymbol{r}-\boldsymbol{r}')\,\overleftrightarrow{\mathbf{1}}\right), \tag{8.7}$$

$\overleftrightarrow{\mathbf{1}}$ being the unit dyadic. In deriving eqs. (8.6) the surface contributions that originate from an integration by parts have been assumed to vanish.

It is common practice when dealing with dielectric materials to implement Maxwell's equations by introducing the polarization and displacement vectors

$$(8.8)\qquad \begin{cases} \boldsymbol{P}(\boldsymbol{r};\,\omega) = -\dfrac{1}{i\omega}\boldsymbol{J}_{\text{ind}}(\boldsymbol{r};\,\omega)\,, \\[2ex] \boldsymbol{D}(\boldsymbol{r};\,\omega) = \boldsymbol{E}(\boldsymbol{r};\,\omega) + 4\pi\boldsymbol{P}(\boldsymbol{r};\,\omega)\,. \end{cases}$$

(We assume throughout the absence of magnetic phenomena.) Notice that in eq. (8.8) $\boldsymbol{E}(\boldsymbol{r};\,\omega)$ is the *total* electric field, while in eqs. (8.6) only the perturbing electric field (8.3) enters, thereby justifying calling the tensor (8.7) the quasi-polarizability.

The Coulomb gauge allows us also to express the scalar potential in terms of the instantaneous charge density and the vector potential in terms of the sole transverse currents, as they satisfy the equations [22]

$$(8.9)\qquad \begin{cases} \nabla^2\varphi(\boldsymbol{r};\,\omega) = -4\pi(\rho_{\text{ext}}(\boldsymbol{r};\,\omega) + \rho_{\text{ind}}(\boldsymbol{r};\,\omega))\,, \\[2ex] \left(\nabla^2 + \dfrac{\omega^2}{c^2}\right)\boldsymbol{A}(\boldsymbol{r};\,\omega) = -\dfrac{4\pi}{c}(\boldsymbol{J}_{\text{T}}^{\text{ext}}(\boldsymbol{r};\,\omega) + \boldsymbol{J}_{\text{T}}^{\text{ind}}(\boldsymbol{r};\,\omega))\,. \end{cases}$$

In what follows we shall assume that $\boldsymbol{J}_{\text{T}}^{\text{ext}} = 0$ inside the material.

All equations considered so far hold for the *microscopic fields* which exhibit large and irregular variations on the atomic scale. This phenomenon occurs in a crystal irrespective of the fact that the external fields may vary only on a macroscopic scale corresponding to several crystal cells. These features (which are called *local-field effects*) thus render the response to an electromagnetic field of a crystal different from that of a homogeneous material. The difference can be expressed by stating that any response function of the crystal satisfies the (geometrical) property

$$(8.10)\qquad f(\boldsymbol{r}+\boldsymbol{n},\, \boldsymbol{r}'+\boldsymbol{n};\,\omega) = f(\boldsymbol{r},\, \boldsymbol{r}';\,\omega)$$

for any vector $\boldsymbol{n}$ of the Bravais lattice; for a homogeneous system, on the other hand, there is no restriction on the translation that appears at the left-hand side of eq. (8.10).

To fully exploit the symmetry property (8.10), it is convenient to introduce the space Fourier transform, which reads

$$(8.11)\qquad f(\boldsymbol{r},\, \boldsymbol{r}';\,\omega) = \\ = \frac{1}{\Omega}\sum_{\boldsymbol{k}}^{\text{BZ}}\sum_{\boldsymbol{G}\boldsymbol{G}'} \exp[i(\boldsymbol{k}+\boldsymbol{G})\cdot\boldsymbol{r}]\, f(\boldsymbol{k}+\boldsymbol{G},\, \boldsymbol{k}+\boldsymbol{G}';\,\omega)\, \exp[-i(\boldsymbol{k}+\boldsymbol{G}')\cdot\boldsymbol{r}']\,.$$

Here $\Omega$ is the volume occupied by the crystal, $\boldsymbol{k}$ is a Bloch wave vector confined to the first Brillouin zone (BZ), and $\boldsymbol{G}$ and $\boldsymbol{G}'$ are reciprocal lattice vectors. The appearence of the *same* $\boldsymbol{k}$ in the two exponential factors at the right-hand side of eq. (8.11) enables us to consider $\boldsymbol{k}$ itself, besides $\omega$, as a *parameter* in the Fourier transform of eqs. (8.6)-(8.9).

Microscopic fields are not, however, the quantities which are dealt with in ordinary electrodynamics where one considers field quantities that vary on a macroscopic scale and are thus experimentally accessible. To obtain the macroscopic from the microscopic fields an *averaging procedure* is necessary which has the result of smoothing out the irregular fluctuations of the microscopic quantities [23]. A suitable averaging procedure for functions which, once represented by the Fourier series

$$(8.12) \qquad g(\boldsymbol{r};\,\omega)=\frac{1}{\sqrt{\Omega}}\sum_{\boldsymbol{k}}^{\mathrm{BZ}}\sum_{\boldsymbol{G}}\exp[i(\boldsymbol{k}+\boldsymbol{G})\cdot\boldsymbol{r}]\,g(\boldsymbol{k}+\boldsymbol{G};\,\omega)\,,$$

contain only small Bloch wave vectors (*i.e.*, $|\boldsymbol{k}|\ll|\boldsymbol{G}|$), is to take the average over a unit cell of the cell-periodic part only [24]

$$(8.13) \qquad \bar{g}(\boldsymbol{n};\,\omega)\equiv\frac{1}{\Omega_c}\int\limits_{\Omega_c[\boldsymbol{n}]}\mathrm{d}\boldsymbol{r}\,g(\boldsymbol{r};\,\omega)\simeq\frac{1}{\sqrt{\Omega}}\sum_{\boldsymbol{k}}^{\mathrm{BZ}}\exp[i\boldsymbol{k}\cdot\boldsymbol{n}]\,g(\boldsymbol{k}+0;\,\omega)\,.$$

Here $\Omega_c[\boldsymbol{n}]$ is the unit cell centred at $\boldsymbol{n}$, $\Omega_c$ is its volume, and the approximation in the last line neglects the variation of $\exp[i\boldsymbol{k}\cdot\boldsymbol{r}]$ over the unit cell. Consistently, one may replace $\boldsymbol{n}$ in eq. (8.13) by the continuous variable $\boldsymbol{r}$.

The averaging procedure (8.13) suffices to eliminate the rapidly varying fields from eqs. (8.8) and (8.9), *provided* the external fields are slowly varying over the unit cell, but it fails, in general, for eqs. (8.6) where the average of a product needs to be taken. In practice, however, we can neglect the microscopic components ($\boldsymbol{G}\neq 0$) of the perturbing electric field for values of the frequency $\omega$ restricted to the optical range [21]. In fact, combining the Fourier transforms of eqs. (8.8) and (8.9) yields

$$(8.14) \qquad \boldsymbol{E}_{\mathrm{T}}(\boldsymbol{k}+\boldsymbol{G};\,\omega)=\frac{(\omega^2/c^2)}{(\boldsymbol{k}+\boldsymbol{G})^2}\boldsymbol{D}_{\mathrm{T}}(\boldsymbol{k}+\boldsymbol{G};\,\omega)\,,$$

which tipically gives ($\boldsymbol{G}\neq 0$)

$$(8.15) \qquad \frac{|\boldsymbol{E}_{\mathrm{T}}(\boldsymbol{k}+\boldsymbol{G};\,\omega)|}{|\boldsymbol{E}_{\mathrm{T}}(\boldsymbol{k}+0;\,\omega)|}\lesssim 10^{-5}\,,$$

for $\hbar\omega\approx 5\,\mathrm{eV}$. Similarly, the microscopic components of the longitudinal part of the displacement vector can be neglected, since one may show that

$$(8.16) \qquad \boldsymbol{D}_{\mathrm{L}}(\boldsymbol{k}+\boldsymbol{G};\,\omega)=\boldsymbol{E}_{\mathrm{L}}^{\mathrm{ext}}(\boldsymbol{k}+\boldsymbol{G};\,\omega)\,.$$

8'2. *Macroscopic dielectric tensor.* – The optical properties of semiconductors can be conveniently described in terms of the macroscopic dielectric tensor $\overleftrightarrow{\epsilon}_{\mathrm{M}}(\boldsymbol{k};\,\omega)$ which relates the macroscopic components of the displacement vector and of the total electric field:

$$\boldsymbol{D}(\boldsymbol{k}+0;\,\omega)=\overleftrightarrow{\epsilon}_{\mathrm{M}}(\boldsymbol{k};\,\omega)\cdot\boldsymbol{E}(\boldsymbol{k}+0;\,\omega)\,. \tag{8.17}$$

$\overleftrightarrow{\epsilon}_{\mathrm{M}}(\boldsymbol{k};\,\omega)$ can, in turn, be expressed in terms of many-body response functions by relating it to the macroscopic component $\overleftrightarrow{\alpha}(\boldsymbol{k}+0,\,\boldsymbol{k}+0;\,\omega)$ of the quasi-polarizability tensor (8.7). To this end, we need first to relate the macroscopic components of the total and of the perturbing electric fields via

$$\boldsymbol{E}(\boldsymbol{k}+0;\,\omega)=[\overleftrightarrow{1}-4\pi(\hat{k}\hat{k})\cdot\overleftrightarrow{\alpha}(\boldsymbol{k}+0,\,\boldsymbol{k}+0;\,\omega)]\cdot\boldsymbol{E}^{\mathrm{P}}(\boldsymbol{k}+0;\,\omega)\,, \tag{8.18}$$

where $(\hat{k}\hat{k})$ is the longitudinal projection operator. Inverting this equation in favour of $\boldsymbol{E}^{\mathrm{P}}(\boldsymbol{k}+0;\,\omega)$ and using eq. (8.8) we find eventually

$$\overleftrightarrow{\epsilon}_{\mathrm{M}}(\boldsymbol{k};\,\omega)=\overleftrightarrow{1}+4\pi\overleftrightarrow{\alpha}(\boldsymbol{k}+0,\,\boldsymbol{k}+0;\,\omega)\cdot[\overleftrightarrow{1}-4\pi(\hat{k}\hat{k})\cdot\overleftrightarrow{\alpha}(\boldsymbol{k}+0,\,\boldsymbol{k}+0;\,\omega)]^{-1}\,. \tag{8.19}$$

The matrix within brackets at the right-hand side of eq. (8.19) may then be explicitly inverted, to give [21]

$$\begin{aligned}\overleftrightarrow{\epsilon}_{\mathrm{M}}(\boldsymbol{k};\,\omega)&=\overleftrightarrow{1}+4\pi\overleftrightarrow{\alpha}(\boldsymbol{k}+0,\,\boldsymbol{k}+0;\,\omega)\,\cdot\\&\cdot\left[\overleftrightarrow{1}+\frac{4\pi(\hat{k}\hat{k})\cdot\overleftrightarrow{\alpha}(\boldsymbol{k}+0,\,\boldsymbol{k}+0;\,\omega)}{1-4\pi\hat{k}\cdot\overleftrightarrow{\alpha}(\boldsymbol{k}+0,\,\boldsymbol{k}+0;\,\omega)\cdot\hat{k}}\right].\end{aligned} \tag{8.20}$$

There still remains to evaluate the left and right longitudinal contractions of the tensor $\overleftrightarrow{\alpha}(\boldsymbol{k}+0,\,\boldsymbol{k}+0;\,\omega)$. This can be readily done by taking the space Fourier transform of eqs. (8.5*b*), (8.4*b*), and (8.4*a*). We obtain, in the order,

$$\overleftrightarrow{\alpha}(\boldsymbol{k}+0,\,\boldsymbol{k}+0;\,\omega)\cdot\hat{k}=-\frac{q^2}{\omega k}\overleftarrow{\chi}_{\mathrm{R}}(\boldsymbol{k}+0,\,\boldsymbol{k}+0;\,\omega)\,, \tag{8.21a}$$

$$\hat{k}\cdot\overleftrightarrow{\alpha}(\boldsymbol{k}+0,\,\boldsymbol{k}+0;\,\omega)=-\frac{q^2}{\omega k}\overrightarrow{\chi}_{\mathrm{R}}(\boldsymbol{k}+0,\,\boldsymbol{k}+0;\,\omega)\,, \tag{8.21b}$$

$$\hat{k}\cdot\overleftrightarrow{\alpha}(\boldsymbol{k}+0,\,\boldsymbol{k}+0;\,\omega)\cdot\hat{k}=-\frac{q^2}{k^2}\chi_{\mathrm{R}}(\boldsymbol{k}+0,\,\boldsymbol{k}+0;\,\omega)\,. \tag{8.21c}$$

Insertion of eqs. (8.21) into eq. (8.20) allows us to calculate the macroscopic dielectric tensor by many-body techniques.

In eq. (8.20) the parameter $\boldsymbol{k}$ is assumed to be restricted in such a way that $|\boldsymbol{k}|^{-1}$ is much larger than the characteristic microscopic lenght scale, *i.e.* the dimension of the crystal cell. The frequency $\omega$, on the other hand, ranges over the optical region and thus it is quite comparable with the semiconductor band gap. One may then envisage eliminating $\boldsymbol{k}$ from eq. (8.20) by formally taking the limit as $\boldsymbol{k} \to 0$, while keeping $\omega$ finite. In performing the limit, however, some care should be exerted owing to the divergence of the (Fourier transform of the) bare Coulomb potential in this limit. We shall show that the macroscopic dielectric tensor is well-behaved in this limit, irrespective of the divergence.

To single out from the correlation functions the part containing the divergence of the bare Coulomb potential, it is convenient to rearrange the integral equations they satisfy (cf. eqs. (3.24) and (C.31) for the time-ordered counterparts) in the following way. We first introduce the *proper correlation functions* (denoted by a circumflex) as being the solutions to the equations

$$\text{(8.22}a\text{)}\qquad \hat{\chi}_{\mathrm{R}}(\boldsymbol{k}+\boldsymbol{G},\ \boldsymbol{k}+\boldsymbol{G}';\ \omega) = \\ = \tilde{\chi}_{\mathrm{R}}(\boldsymbol{k}+\boldsymbol{G},\ \boldsymbol{k}+\boldsymbol{G}';\ \omega) + \sum_{\boldsymbol{G}''\neq 0} \tilde{\chi}_{\mathrm{R}}(\boldsymbol{k}+\boldsymbol{G},\ \boldsymbol{k}+\boldsymbol{G}'';\ \omega)\, v(\boldsymbol{k}+\boldsymbol{G}'')\, \hat{\chi}_{\mathrm{R}}(\boldsymbol{k}+\boldsymbol{G}'',\ \boldsymbol{k}+\boldsymbol{G}';\ \omega)\,,$$

$$\text{(8.22}b\text{)}\qquad \hat{\overrightarrow{\chi}}_{\mathrm{R}}(\boldsymbol{k}+\boldsymbol{G},\ \boldsymbol{k}+\boldsymbol{G}';\ \omega) = \\ = \tilde{\overrightarrow{\chi}}_{\mathrm{R}}(\boldsymbol{k}+\boldsymbol{G},\ \boldsymbol{k}+\boldsymbol{G}';\ \omega) + \sum_{\boldsymbol{G}''\neq 0} \hat{\chi}_{\mathrm{R}}(\boldsymbol{k}+\boldsymbol{G},\ \boldsymbol{k}+\boldsymbol{G}'';\ \omega)\, v(\boldsymbol{k}+\boldsymbol{G}'')\, \tilde{\overrightarrow{\chi}}_{\mathrm{R}}(\boldsymbol{k}+\boldsymbol{G}'',\ \boldsymbol{k}+\boldsymbol{G}';\ \omega)\,,$$

$$\text{(8.22}c\text{)}\qquad \hat{\overleftarrow{\chi}}_{\mathrm{R}}(\boldsymbol{k}+\boldsymbol{G},\ \boldsymbol{k}+\boldsymbol{G}';\ \omega) = \\ = \tilde{\overleftarrow{\chi}}_{\mathrm{R}}(\boldsymbol{k}+\boldsymbol{G},\ \boldsymbol{k}+\boldsymbol{G}';\ \omega) + \sum_{\boldsymbol{G}''\neq 0} \tilde{\overleftarrow{\chi}}_{\mathrm{R}}(\boldsymbol{k}+\boldsymbol{G},\ \boldsymbol{k}+\boldsymbol{G}'';\ \omega)\, v(\boldsymbol{k}+\boldsymbol{G}'')\, \hat{\chi}_{\mathrm{R}}(\boldsymbol{k}+\boldsymbol{G}'',\ \boldsymbol{k}+\boldsymbol{G}';\ \omega)\,,$$

$$\text{(8.22}d\text{)}\qquad \hat{\overleftrightarrow{\chi}}_{\mathrm{R}}(\boldsymbol{k}+\boldsymbol{G},\ \boldsymbol{k}+\boldsymbol{G}';\ \omega) = \tilde{\overleftrightarrow{\chi}}_{\mathrm{R}}(\boldsymbol{k}+\boldsymbol{G},\ \boldsymbol{k}+\boldsymbol{G}';\ \omega) + \\ + \sum_{\boldsymbol{G}''\neq 0} \tilde{\overleftarrow{\chi}}_{\mathrm{R}}(\boldsymbol{k}+\boldsymbol{G},\ \boldsymbol{k}+\boldsymbol{G}'';\ \omega)\, v(\boldsymbol{k}+\boldsymbol{G}'')\, \tilde{\overrightarrow{\chi}}_{\mathrm{R}}(\boldsymbol{k}+\boldsymbol{G}'',\ \boldsymbol{k}+\boldsymbol{G}';\ \omega) + \\ + \sum_{\boldsymbol{G}''\neq 0}\ \sum_{\boldsymbol{G}'''\neq 0} \tilde{\overleftarrow{\chi}}_{\mathrm{R}}(\boldsymbol{k}+\boldsymbol{G},\ \boldsymbol{k}+\boldsymbol{G}'';\ \omega)\, v(\boldsymbol{k}+\boldsymbol{G}'')\,\cdot \\ \cdot\, \hat{\chi}_{\mathrm{R}}(\boldsymbol{k}+\boldsymbol{G}'',\ \boldsymbol{k}+\boldsymbol{G}''';\ \omega)\, v(\boldsymbol{k}+\boldsymbol{G}''')\, \tilde{\overrightarrow{\chi}}_{\mathrm{R}}(\boldsymbol{k}+\boldsymbol{G}''',\ \boldsymbol{k}+\boldsymbol{G}';\ \omega)\,.$$

Here $v(\boldsymbol{k}+\boldsymbol{G}) = 4\pi e^2/|\boldsymbol{k}+\boldsymbol{G}|^2$ and the retarded irreducible correlation functions (denoted by a tilde) are obtained by analytic continuation from the time-ordered counterparts introduced in appendix C. Owing to the absence in eqs. (8.22) of the factor $v(\boldsymbol{k}+0)$ which would be the source of the divergence in the limit $\boldsymbol{k} \to 0$, the proper correlation functions can be interpreted as the correlation functions of a hypothetical medium whereby the interparticle potential is replaced by a Coulomb potential with a small-momentum cutoff [25]. These functions are thus well-behaved in the limit $\boldsymbol{k} \to 0$.

The $\boldsymbol{G} = \boldsymbol{G}' = 0$ elements of the correlation functions that enter the expression (8.20) of the macroscopic dielectric tensor can be cast in a form which isolates the divergent factor $v(\boldsymbol{k}+0)$ explicitly [26]:

$$(8.23a)\qquad \chi_R(\boldsymbol{k}+0,\ \boldsymbol{k}+0;\ \omega)=\frac{\hat{\chi}_R(\boldsymbol{k}+0,\ \boldsymbol{k}+0;\ \omega)}{1-v(\boldsymbol{k}+0)\,\hat{\chi}_R(\boldsymbol{k}+0,\ \boldsymbol{k}+0;\ \omega)}\,,$$

$$(8.23b)\qquad \vec{\chi}_R(\boldsymbol{k}+0,\ \boldsymbol{k}+0;\ \omega)=$$

$$=\hat{\vec{\chi}}_R(\boldsymbol{k}+0,\ \boldsymbol{k}+0;\ \omega)+\frac{\hat{\chi}_R(\boldsymbol{k}+0,\ \boldsymbol{k}+0;\ \omega)\,v(\boldsymbol{k}+0)}{1-v(\boldsymbol{k}+0)\,\hat{\chi}_R(\boldsymbol{k}+0,\ \boldsymbol{k}+0;\ \omega)}\,\hat{\vec{\chi}}_R(\boldsymbol{k}+0,\ \boldsymbol{k}+0;\ \omega)\,,$$

$$(8.23c)\qquad \overleftarrow{\chi}_R(\boldsymbol{k}+0,\ \boldsymbol{k}+0;\ \omega)=$$

$$=\hat{\overleftarrow{\chi}}_R(\boldsymbol{k}+0,\ \boldsymbol{k}+0;\ \omega)+\hat{\overleftarrow{\chi}}_R(\boldsymbol{k}+0,\ \boldsymbol{k}+0;\ \omega)\frac{v(\boldsymbol{k}+0)\,\hat{\chi}_R(\boldsymbol{k}+0,\ \boldsymbol{k}+0;\ \omega)}{1-v(\boldsymbol{k}+0)\,\hat{\chi}_R(\boldsymbol{k}+0,\ \boldsymbol{k}+0;\ \omega)}\,,$$

$$(8.23d)\qquad \overleftrightarrow{\chi}_R(\boldsymbol{k}+0,\ \boldsymbol{k}+0;\ \omega)=$$

$$=\hat{\overleftrightarrow{\chi}}_R(\boldsymbol{k}+0,\ \boldsymbol{k}+0;\ \omega)+\hat{\overleftarrow{\chi}}_R(\boldsymbol{k}+0,\ \boldsymbol{k}+0;\ \omega)\frac{v(\boldsymbol{k}+0)\,\hat{\vec{\chi}}_R(\boldsymbol{k}+0,\ \boldsymbol{k}+0;\ \omega)}{1-v(\boldsymbol{k}+0)\,\hat{\chi}_R(\boldsymbol{k}+0,\ \boldsymbol{k}+0;\ \omega)}\,.$$

We are now in a position to rewrite the macroscopic dielectric tensor (8.20) in a form suitable for taking the limit $\boldsymbol{k}\to 0$. Inserting eqs. (8.23) into eqs. (8.21) and into the Fourier transform of eq. (8.7) and entering the results into eq. (8.20), we obtain after straightforward algebraic manipulation:

$$(8.24)\qquad \overleftrightarrow{\epsilon}_M(\boldsymbol{k};\ \omega)=\left(1-\frac{\omega_p^2}{\omega^2}\right)\overleftrightarrow{\mathbf{1}}-\frac{4\pi e^2}{\omega^2}\hat{\overleftrightarrow{\chi}}_R(\boldsymbol{k}+0,\ \boldsymbol{k}+0;\ \omega)\,,$$

which is indeed well-behaved in the limit $\boldsymbol{k}\to 0$. Equation (8.24) is formally valid to all orders of (many-body) perturbation theory and for crystals of arbitrary point-group symmetry [27]. For cubic materials eq. (8.24) takes a particularly simple form, to be discussed next.

8'3. *Cubic materials.* – For materials with cubic symmetry the macroscopic dielectric tensor (8.24) is equivalent to a scalar in the limit $\boldsymbol{k}\to 0$, *i.e.* it is diagonal with equal elements:

$$(8.25)\qquad \lim_{\boldsymbol{k}\to 0}\overleftrightarrow{\epsilon}_M(\boldsymbol{k};\ \omega)=\epsilon_M(\omega)\,\overleftrightarrow{\mathbf{1}}\,.$$

Here $\epsilon_M(\omega)$ can be obtained, in particular, from the longitudinal-longitudinal element of the matrix (8.20) by taking into account eqs. (8.21*c*) and (8.23*a*):

$$(8.26)\qquad \epsilon_M(\omega)=1-\lim_{\boldsymbol{k}\to 0}v(\boldsymbol{k}+0)\,\chi_R(\boldsymbol{k}+0,\ \boldsymbol{k}+0;\ \omega)\,,$$

where

$$\hat{\chi}_{\mathrm{R}}(\boldsymbol{k}+0,\ \boldsymbol{k}+0;\ \omega) \underset{\boldsymbol{k}\to 0}{\widetilde{\quad}}\ k^2\,\hat{\chi}_{\mathrm{R}}(\omega)\,, \tag{8.27}$$

for $\overleftrightarrow{\epsilon}_{\mathrm{M}}(\boldsymbol{k};\ \omega)$ to be well-behaved in this limit.

Equations (8.25) and (8.27) can be proved by exploiting the Lehmann representation (5.10) of the proper correlation functions (8.22*d*) and (8.22*a*), in the order. For completeness, we sketch the proof below.

i) *Proof of eq.* (8.25). Equation (8.25) results from the following symmetry property of the proper current-current correlation function:

$$\mathscr{R}^{-1}\cdot\hat{\overleftrightarrow{\chi}}_{\mathrm{R}}(\mathscr{R}\boldsymbol{k},\ \mathscr{R}\boldsymbol{k};\ \omega)\cdot\mathscr{R} = \hat{\overleftrightarrow{\chi}}_{\mathrm{R}}(\boldsymbol{k},\ \boldsymbol{k};\ \omega)\,, \tag{8.28}$$

where $\mathscr{R}$ is the rotation part of a symmetry transformation $\{\mathscr{R}|\boldsymbol{w}\}$ of the crystal. Equation (8.28), in turn, follows from the invariance under this transformation of the set of projection operators (built from many-body eigenstates of given energy) that enter the Lehmann representation. Taking the limit as $\boldsymbol{k}\to 0$ of both sides of eq. (8.28) and choosing successively $\mathscr{R}$ to be, *e.g.*, a rotation by $\pi$ about the $x$-axis, a rotation by $\pi$ about the $y$-axis, and a rotation by $2\pi/3$ about the 111-axis [28], one may readily prove that $\hat{\overleftrightarrow{\chi}}_{\mathrm{R}}(0,\ 0;\ \omega)$ is equivalent to a scalar.

ii) *Proof of eq.* (8.27). Equation (8.27) follows from the Lehmann representation of the proper density-density correlation function together with the property

$$\int \mathrm{d}\boldsymbol{r}\,\langle N|\hat{\rho}(\boldsymbol{r})|N,\ s\rangle = 0\,, \tag{8.29}$$

for $s \neq 0$ (cf. eqs. (5.10) and (5.11)) and the fact that the system possesses an energy gap. (*QED*)

The result (8.25) simplifies considerably the discussion of the optical properties of cubic semiconductors. In particular, one may write for the induced current (cf. eqs. (8.6*b*), (8.16), (8.18), and (8.20))

$$\lim_{\boldsymbol{k}\to 0}\boldsymbol{J}_{\mathrm{ind}}(\boldsymbol{k}+0;\ \omega) = -\,i\omega\left(\frac{\epsilon_{\mathrm{M}}(\omega)-1}{4\pi}\right)\left\{\begin{matrix}\boldsymbol{E}^{\mathrm{P}}_{\mathrm{T}}(0;\ \omega)\\ \dfrac{\boldsymbol{E}^{\mathrm{ext}}_{\mathrm{L}}(0;\ \omega)}{\epsilon_{\mathrm{M}}(\omega)}\end{matrix}\right\}, \tag{8.30}$$

where the transverse and longitudinal components have been explicitly indicated. Equation (8.30) implies, in particular, the well-known results that there is no transverse screening effect in the long wavelength limit and that a transverse perturbing electric field excites only transverse induced currents [25]. It then follows that we can find purely transverse solutions to Maxwell's equations (8.9), whereby $\varphi(\boldsymbol{r};\,\omega)=0$. Setting

$$A(\boldsymbol{r};\,\omega)=\boldsymbol{A}_0\exp\left[i\mathscr{k}\cdot\boldsymbol{r}\right] \tag{8.31}$$

and taking

$$\boldsymbol{J}_{\mathrm{T}}^{\mathrm{ind}}(\boldsymbol{r};\,\omega)=-i\omega\left(\frac{\epsilon_{\mathrm{M}}(\omega)-1}{4\pi}\right)\frac{i\omega}{c}\boldsymbol{A}(\boldsymbol{r};\,\omega)\,, \tag{8.32}$$

we find that the propagation vector $\mathscr{k}$ satisfies the *dispersion relation*

$$\mathscr{k}^2=\frac{\omega^2}{c^2}\,\epsilon_{\mathrm{M}}(\omega)\,. \tag{8.33}$$

In writing eq. (8.32), we have assumed that the real and imaginary parts of $\mathscr{k}$ are small enough for the space Fourier transform of eq. (8.31) to contain only small wave vectors $\boldsymbol{k}$. In this way the same constant $\epsilon_{\mathrm{M}}(\omega)$ is pertinent to all Fourier components of the wavepacket (8.31).

Conventionally, one writes the propagation vector $\mathscr{k}$ in terms of the index of refraction ($n$) and of the extinction coefficients ($\varkappa$)

$$\mathscr{k}=\hat{s}\,\frac{\omega}{c}(n+i\varkappa)\,, \tag{8.34}$$

where $\hat{s}$ is the unit vector in the direction of propagation. One can then express the average energy flux in the medium corresponding to the (real part of the) solution (8.31) through a Poynting's vector of the form

$$\langle\boldsymbol{S}\rangle=\hat{s}\,\frac{c}{8\pi}\,n\,\frac{\omega^2}{c^2}\,A_0^2\,\exp\left[-2\,\frac{\omega}{c}\,\varkappa\hat{s}\cdot\boldsymbol{r}\right]. \tag{8.35}$$

The coefficient of the exponentially decreasing factor in eq. (8.35) is called the *absorption coefficient* $\eta$ [39], and may be also expressed in terms of the imaginary part $\epsilon_2(\omega)$ of the macroscopic dielectric function $\epsilon_{\mathrm{M}}(\omega)$ by using the dispersion relation (8.33):

$$\eta(\omega)=\frac{\omega}{c}\,\frac{\epsilon_2(\omega)}{n(\omega)}\,. \tag{8.36}$$

This expression for $\eta$ can alternatively be obtained by calculating the power absorbed by the medium. To this end, we identify the rate at which the electromagnetic field does work on the system as the time rate of change of the mean value of the system Hamiltonian (2.1) [24]

$$\frac{\mathrm{d}\mathscr{W}}{\mathrm{d}t}=\frac{\mathrm{d}}{\mathrm{d}t}\langle\Psi(t)|\hat{H}|\Psi(t)\rangle=\frac{i}{\hbar}\langle\Psi(t)|[\hat{H}'(t),\,(\hat{H}+\hat{H}'(t))]|\Psi(t)\rangle\,, \tag{8.37}$$

where $|\Psi(t)\rangle$ is the wave function of the system driven by the electromagnetic field and $\hat{H}'(t)$ is the interaction Hamiltonian (C.1) (without the diamagnetic term). Standard manipulations lead to

$$\begin{aligned}\frac{\mathrm{d}\mathscr{W}}{\mathrm{d}t}=&-\int\mathrm{d}\boldsymbol{r}\,\boldsymbol{\nabla}\varphi^{\mathrm{ext}}(\boldsymbol{r},\,t)\cdot\boldsymbol{J}_{\mathrm{ind}}(\boldsymbol{r},\,t)+\\&+\frac{1}{c}\int\mathrm{d}\boldsymbol{r}\,\boldsymbol{A}(\boldsymbol{r},\,t)\cdot\frac{\partial}{\partial t}\left[\boldsymbol{J}_{\mathrm{ind}}(\boldsymbol{r},\,t)+\frac{e^2}{mc}\langle N|\hat{\rho}(\boldsymbol{r})|N\rangle\,\boldsymbol{A}(r,\,t)\right],\end{aligned} \tag{8.38}$$

where use has been made of the continuity equation and a surface term originating from integration by parts has been dropped. To recover from eq. (8.38) the classical expression involving only the induced current and the (perturbing) electric field, we should perform the *time average* of eq. (8.38) over the time interval $(-T,\,+T)$ during which the perturbation acts on the system. (For periodic disturbances, it is actually enough to average over one cycle.) We obtain

$$\left\langle\frac{\mathrm{d}\mathscr{W}}{\mathrm{d}t}\right\rangle\equiv\frac{1}{2T}\int_{-T}^{+T}\mathrm{d}t'\frac{\mathrm{d}\mathscr{W}}{\mathrm{d}t'}=\frac{1}{2T}\int_{-T}^{+T}\mathrm{d}t'\int\mathrm{d}\boldsymbol{r}\,\boldsymbol{J}_{\mathrm{ind}}(\boldsymbol{r},\,t')\cdot\boldsymbol{E}^{\mathrm{P}}(\boldsymbol{r},\,t')\,, \tag{8.39}$$

where we have performed an integration by parts over $t'$ and recalled eq. (8.3).

Equation (8.39) holds quite generally for any type of material. For a cubic semiconductor we may consider a solution of the form

$$\begin{cases}\boldsymbol{E}^{\mathrm{P}}_{\mathrm{T}}(\boldsymbol{r};\,\omega)=\pi[\boldsymbol{E}^{\mathrm{P}}_{\mathrm{T}}(\boldsymbol{r})\,\delta(\omega-\omega_0)+\boldsymbol{E}^{\mathrm{P}}_{\mathrm{T}}(\boldsymbol{r})^*\,\delta(\omega+\omega_0)]\,,\\[2ex]\boldsymbol{E}^{\mathrm{P}}_{\mathrm{T}}(\boldsymbol{r})=i\dfrac{\omega_0}{c}\boldsymbol{A}_0\exp[i\boldsymbol{k}\cdot\boldsymbol{r}]\,,\end{cases} \tag{8.40}$$

$(\omega_0>0)$, for which

$$\left\langle\frac{\mathrm{d}\mathscr{W}}{\mathrm{d}t}\right\rangle=\frac{\omega_0}{8\pi}\,\epsilon_2(\omega_0)\int\mathrm{d}\boldsymbol{r}|\boldsymbol{E}^{\mathrm{P}}_{\mathrm{T}}(\boldsymbol{r})|^2\,. \tag{8.41}$$

Defining the absorption coefficient as the ratio between the (time-averaged) energy absorbed by the system (per unit time and per unit volume) and the energy flux in the medium (for the same unit volume), we are able to recover eq. (8.36) from eq. (8.41).

One may also verify that the (time-averaged) energy absorbed by the system per unit time can be obtained directly for a transverse vector potential corresponding to eq. (8.40) by calculating the transition probability per unit time from the Golden rule. This calculation shows, in addition, that

$$\overleftrightarrow{\chi}_{\mathrm{R}}(\boldsymbol{k}+0,\ \boldsymbol{k}+0;\ \omega)_{\mathrm{T}} = \hat{\overleftrightarrow{\chi}}_{\mathrm{R}}(\boldsymbol{k}+0,\ \boldsymbol{k}+0;\ \omega)_{\mathrm{T}}\,, \tag{8.42}$$

for the transverse submatrices in the limit $\boldsymbol{k} \to 0$. This result can be interpreted by saying that the proper density-density correlation function describes the response of a (cubic) semiconductor (or insulator) to a *transverse* electric field of long wavelength [25]. Notice that eq. (8.42) could have alternatively been obtained from eq. (8.23*d*) by showing that the second term at the right-hand side of that equation vanishes by symmetry in the long-wavelength limit [30].

8.4. *Time-dependent-screened-Hartree-Fock approximation in a local-orbital basis.* – The result (8.26) for the macroscopic dielectric function holds quite generally whatever form of the proper density-density correlation function is inserted at its right-hand side. We now discuss some numerical results which have been obtained for (cubic) covalent crystals such as diamond [31] and silicon [32, 33], and more recently for GaP [34], whereby the important many-body mechanism is the screened interaction within an electron-hole pair created in the polarization process. Parallel calculations of the photoabsorption cross-section in atomic systems within the RPAE approximation have also emphasized the importance of the above mechanism [35], although methods for different systems rely on different computational schemes. In particular, for semiconductors the use of a *local-orbital basis* to represent single-particle wave functions has made it possible the inclusion of the excitonic effect on top of local-field effects.

As discussed in sects. **2**-**4**, the dynamics of the many-body processes occurring in the system response is embodied in the choice of the functional form of the self-energy operator, since the effective two-particle interaction can be obtained from it by functional differentiation. Consistency with conservation laws further restricts the choice of the self-energy, as discussed in sect. **6**. For the purpose of describing the optical properties of semiconductors it is apparently sufficient to take for the non-Hartree part of the self-energy operator (cf. eqs. (3.11) and (3.12))

$$M(1,\ 2) = i\hbar W(1^+,\ 2)\, G_1(1,\ 2)\,, \tag{8.43}$$

as well as to neglect the variation of the dynamically screened interaction while calculating the functional derivative:

$$-\frac{\delta M(1,\ 2)}{\delta G_1(3,\ 4)} \simeq i\hbar\, \delta(1,\ 3)\, \delta(2,\ 4)\, W(1^+,\ 2)\,. \tag{8.44}$$

Equation (8.44) would become exact if $W$ in eq. (8.43) would be replaced by the bare Coulomb potential. In this case the system response is said to be approximated within the time-dependent-Hartree-Fock approximation, which has been used with success for several atomic systems. For semiconductors, however, the screening of the electron-hole attraction is an essential feature which cannot be neglected in calculating the optical spectra. The same conclusion will consistently be reached when discussing the single-particle energies (sect. **9**) and the (bound) excitonic levels (sect. **11**).

The form (8.43) for the mass operator (the so-called GW approximation) has been first discussed by Hedin in conjunction with properties of the electron gas [36]. This form is consistent with conservation criteria *provided* that the dynamically screened interaction is evaluated within the random-phase-approximation (RPA), *i.e.*, by approximating the (irreducibile) scalar vertex function that enters the expression (3.26) of the irreducibile polarizability by its lowest-order expression. An example is given in fig. 3*e*). Going beyond the RPA approximation (by introducing, *e.g.*, a screened electron-hole interaction in the bubbles) requires, in principle, the addition of other terms to the mass operator in order to be consistent with conservation criteria (cf. fig. 3*f*)). By the same token, the approximation (8.44) where some terms at the right-hand side have been dropped, violates in principle the conservation criteria. In practice, however, in calculating the optical response one usually approximates the dynamically screened interaction by a static screened potential obtained from a phenomenological dielectric function

$$W(1^+, 2) \simeq W_s(\boldsymbol{r}_1, \boldsymbol{r}_2)\,\delta(t_1^+ - t_2)\,, \tag{8.45}$$

and keeps the form (8.44) for the kernel of the Bethe-Salpeter equation. Consistency with conservation criteria is then limited to a numerical check on the accuracy to which the longitudinal sum rule is satisfied. Further comments on the practical importance of a formal violation of conservation criteria in the calculation of the band structure of covalent semiconductors will be given in sect. **9**.

We pass now to solve the integral equation (C.16) whose kernel (C.15) is approximated by eqs. (8.44) and (8.45). It is convenient to eliminate at the outset both the spin variables according to the prescriptions of appendix D and the time variables by first pairing them as in eq. (C.18) and then taking the Fourier transform with respect to the resulting relative time. We obtain

$$\begin{aligned}\tilde{L}(\boldsymbol{r}_1, \boldsymbol{r}_2; \boldsymbol{r}_1', \boldsymbol{r}_2'|\omega) = \tilde{L}_0(\boldsymbol{r}_1, \boldsymbol{r}_2; \boldsymbol{r}_1', \boldsymbol{r}_2'|\omega) +{}& \\ + \frac{i\hbar}{2}\int \mathrm{d}\boldsymbol{r}_3\,\mathrm{d}\boldsymbol{r}_4\,\tilde{L}_0(\boldsymbol{r}_1, \boldsymbol{r}_4; \boldsymbol{r}_1', \boldsymbol{r}_3|\omega)\,W_s(\boldsymbol{r}_3, \boldsymbol{r}_4)\,\tilde{L}(\boldsymbol{r}_3, \boldsymbol{r}_2; \boldsymbol{r}_4, \boldsymbol{r}_2'|\omega)\,,&\end{aligned} \tag{8.46}$$

where we have introduced the notation

$$(8.47)\qquad \tilde{L}_0(\boldsymbol{r}_1, \boldsymbol{r}_2; \boldsymbol{r}_1', \boldsymbol{r}_2'|\omega) = 2 \int_{-\infty}^{+\infty} \frac{\mathrm{d}\omega'}{2\pi} G_1(\boldsymbol{r}_1, \boldsymbol{r}_2'; \omega + \omega')\, G_1(\boldsymbol{r}_2, \boldsymbol{r}_1'; \omega')$$

for the noninteracting part. Notice that the factor of two at the right-hand side of eq. (8.47) originates from the spin degeneracy. Notice also that in eq. (8.46) the frequency $\omega$ is a parameter.

To proceed further, we represent all single-particle Green's functions entering eq. (8.46) in the *quasi-particle approximation* of the form

$$(8.48)\qquad G_1(\boldsymbol{r}_1, \boldsymbol{r}_2; \omega) \simeq \sum_k \frac{u_k(\boldsymbol{r}_1)\, u_k(\boldsymbol{r}_2)^*}{\hbar\omega - \varepsilon_k + i\delta \operatorname{sgn}(\varepsilon_k - \varepsilon_{\mathrm{F}})},$$

where $\delta \to 0^+$ and the Fermi level $\varepsilon_{\mathrm{F}}$ is placed within the gap. In eq. (8.48) the $u_k(\boldsymbol{r})$ are (orthonormalized) single-particle wave functions which are assumed to be known by a previous solution of a band eigenvalue problem. In practice, they are approximated by a $X\alpha$ or a local-density calculation. Although eq. (8.48) is not the most general form for a single-particle Green's function, it turns out to be a suitable approximation to describe the optical properties of semiconductors. In sect. **9** we shall justify the choice (8.48) as well as its internal consistency.

Entering eq. (8.48) into eq. (8.47) yields

$$(8.49a)\qquad \tilde{L}_0(\boldsymbol{r}_1, \boldsymbol{r}_2; \boldsymbol{r}_1', \boldsymbol{r}_2'|\omega) = \\ = \sum_{k_1 k_2 k_1' k_2'} u_{k_1}(\boldsymbol{r}_1)\, u_{k_2}(\boldsymbol{r}_2)\, \tilde{L}_0(k_1, k_2; k_1', k_2'|\omega)\, u_{k_1'}(\boldsymbol{r}_1')^*\, u_{k_2'}(\boldsymbol{r}_2')^*,$$

where

$$(8.49b)\qquad \tilde{L}_0(k_1, k_2; k_1', k_2'|\omega) = \\ = \delta_{k_1 k_2'} \delta_{k_2 k_1'} \frac{2i}{\hbar} \left[ \frac{\theta(\varepsilon_{k_2} - \varepsilon_{\mathrm{F}})\, \theta(\varepsilon_{\mathrm{F}} - \varepsilon_{k_2'})}{\varepsilon_{k_2'} - \varepsilon_{k_2} + i\delta + \hbar\omega} - \frac{\theta(\varepsilon_{k_2'} - \varepsilon_{\mathrm{F}})\, \theta(\varepsilon_{\mathrm{F}} - \varepsilon_{k_2})}{\varepsilon_{k_2'} - \varepsilon_{k_2} - i\delta + \hbar\omega} \right].$$

Here the step functions discriminate conduction bands from valence bands states. (Notice that the infinitesimal imaginary parts in the energy denominators in eq. (8.49*b*) correspond still to time-ordered quantities. Analytic continuation to retarded quantities will eventually be performed by replacing $i\delta \to -i\delta$ in the second energy denominator within brackets). We may similarly expand

$$(8.50)\qquad \tilde{L}(\boldsymbol{r}_1, \boldsymbol{r}_2; \boldsymbol{r}_1', \boldsymbol{r}_2'|\omega) = \sum_{k_1 k_2 k_1' k_2'} u_{k_1}(\boldsymbol{r}_1)\, u_{k_2}(\boldsymbol{r}_2)\, \tilde{L}(k_1, k_2; k_1', k_2'|\omega)\, u_{k_1'}(\boldsymbol{r}_1')^*\, u_{k_2'}(\boldsymbol{r}_2')^*,$$

and transform eq. (8.46) into an integral equation for the coefficients at the right-hand side of eq. (8.50) by invoking the assumed orthonormality of the single-particle wave functions. A more handy *matrix equation* can instead be obtained by representing the single-particle wave functions in eqs. (8.49*a*) and (8.50) in a local-orbital basis [31]:

$$u_{nk}(\boldsymbol{r}) = \mathcal{N}^{-1/2} \sum_{\mu \boldsymbol{l}} \exp[i\boldsymbol{k}\cdot\boldsymbol{l}]\, \phi_\mu(\boldsymbol{r}-\boldsymbol{l})\, c_{\mu n}(\boldsymbol{k}) . \tag{8.51}$$

Here we have specified the label $k$ to signify the pair $(n, \boldsymbol{k})$ where $n$ is a band index and $\boldsymbol{k}$ is a Bloch wave vector, $\mathcal{N}$ is the number of lattice sites, and the orbital $\phi_\mu(\boldsymbol{r}-\boldsymbol{l})$ is localized about the lattice site $\boldsymbol{l}$. In eq. (8.51) it is understood that the set $\{\mu\}$ is sufficient to describe the valence and conduction bands which are coupled by optical excitations.

The following steps allow us then to transform the Bethe-Salpeter equation (8.46) into a matrix equation:

i) set $\boldsymbol{r}_1 = \boldsymbol{r}_1'$ and $\boldsymbol{r}_2 = \boldsymbol{r}_2'$ in the light of eq. (C.18);

ii) multiply both sides of eq. (8.46) by $\Omega^{-1} \exp[-i(\boldsymbol{q}+\boldsymbol{G})\cdot\boldsymbol{r}_2] \cdot \exp[i(\boldsymbol{q}+\boldsymbol{G}')\cdot\boldsymbol{r}_1]$, where $\boldsymbol{q}$ now stands for a Bloch wave vector, and integrate over $\boldsymbol{r}_1$ and $\boldsymbol{r}_2$;

iii) use the symmetry properties of the screened interaction $W_s(\boldsymbol{r}_3, \boldsymbol{r}_4)$ when shifting both coordinates by the same lattice vector as well as when interchanging $\boldsymbol{r}_3 \rightleftarrows \boldsymbol{r}_4$.

After suitable shift of integration and of (discrete) summation variables, we obtain eventually

$$\begin{aligned} \frac{1}{\Omega_0} \sum_{c,c'} A_c(\boldsymbol{q}+\boldsymbol{G}) \Big\{ & N_{cc'}(\boldsymbol{q};\,\omega) - N^0_{cc'}(\boldsymbol{q};\,\omega) - \\ & - \frac{i\hbar}{2} \sum_{c''c'''} N_{cc''}(\boldsymbol{q};\,\omega)\, V^{sx}_{c''c'''}(\boldsymbol{q})\, N^0_{c'''c'}(\boldsymbol{q};\,\omega) \Big\} A^*_{c'}(\boldsymbol{q}+\boldsymbol{G}') = 0 . \end{aligned} \tag{8.52}$$

In eq. (8.52) $\Omega_0$ is the volume of the Wigner-Seitz cell, the collective index «$c$» stands for the triad $(\boldsymbol{l}, \nu, \mu)$ which appears in the form factors

$$A_c(\boldsymbol{q}+\boldsymbol{G}) = \int \mathrm{d}\boldsymbol{r}\, \phi^*_\nu(\boldsymbol{r}) \exp[-i(\boldsymbol{q}+\boldsymbol{G})\cdot\boldsymbol{r}]\, \phi_\mu(\boldsymbol{r}-\boldsymbol{l}) , \tag{8.53}$$

and we have introduced the matrices

$$\begin{aligned} N_{cc'}(\boldsymbol{q};\,\omega) = \frac{1}{\mathcal{N}} \sum_{\boldsymbol{k}\boldsymbol{k}'}^{\mathrm{BZ}} \sum_{n_1 n_2 n_3 n_4} & c^*_{\nu n_2}(\boldsymbol{k})\, c_{\mu n_1}(\boldsymbol{k}+\boldsymbol{q}) \exp[i(\boldsymbol{k}+\boldsymbol{q})\cdot\boldsymbol{l}] \cdot \\ & \cdot \tilde{L}(n_3 \boldsymbol{k}',\, n_1 \boldsymbol{k}+\boldsymbol{q};\, n_4 \boldsymbol{k}'+\boldsymbol{q},\, n_2 \boldsymbol{k}|\omega) \exp[-i(\boldsymbol{k}'+\boldsymbol{q})\cdot\boldsymbol{l}']\, c^*_{\mu' n_4}(\boldsymbol{k}'+\boldsymbol{q})\, c_{\nu' n_3}(\boldsymbol{k}') , \end{aligned} \tag{8.54}$$

$$(8.55)\qquad N^0_{cc'}(\boldsymbol{q};\,\omega)=\frac{1}{\mathcal{N}}\sum_{\boldsymbol{k}}^{\mathrm{BZ}}\sum_{n_1n_2}c^*_{\nu n_2}(\boldsymbol{k})\,c_{\mu n_1}(\boldsymbol{k}+\boldsymbol{q})\,\exp[i(\boldsymbol{k}+\boldsymbol{q})\cdot(\boldsymbol{l}-\boldsymbol{l}')]\,\cdot$$
$$\cdot\frac{2i}{\hbar}\left[\frac{\theta(\varepsilon_{n_2}(\boldsymbol{k})-\varepsilon_{\mathrm{F}})\,\theta(\varepsilon_{\mathrm{F}}-\varepsilon_{n_1}(\boldsymbol{k}+\boldsymbol{q}))}{\varepsilon_{n_1}(\boldsymbol{k}+\boldsymbol{q})-\varepsilon_{n_2}(\boldsymbol{k})+i\delta-\hbar\omega}-\right.$$
$$\left.-\frac{\theta(\varepsilon_{\mathrm{F}}-\varepsilon_{n_2}(\boldsymbol{k}))\,\theta(\varepsilon_{n_1}(\boldsymbol{k}+\boldsymbol{q})-\varepsilon_{\mathrm{F}})}{\varepsilon_{n_1}(\boldsymbol{k}+\boldsymbol{q})-\varepsilon_{n_2}(\boldsymbol{k})-i\delta-\hbar\omega}\right]c_{\nu'n_2}(\boldsymbol{k})\,c^*_{\mu'n_1}(\boldsymbol{k}+\boldsymbol{q}),$$

$$(8.56)\qquad V^{sx}_{cc'}(\boldsymbol{q})=\sum_{\boldsymbol{m}}\exp[-i\boldsymbol{q}\cdot\boldsymbol{m}]\,\cdot$$
$$\cdot\left\langle\phi^*_\nu(\boldsymbol{r}'-\boldsymbol{m})\,\phi_\mu(\boldsymbol{r}-\boldsymbol{l}-\boldsymbol{m})\middle|W_s(\boldsymbol{r},\,\boldsymbol{r}')\middle|\,\phi^*_{\nu'}(\boldsymbol{r}')\,\phi_{\mu'}(\boldsymbol{r}-\boldsymbol{l}')\right\rangle,$$

which represent the irreducible polarizability, its RPA approximation, and the screened interaction in the local-orbital basis, respectively. For reasons that will soon become clear, eq. (8.56) is called the (screened) *exchange* Coulomb matrix.

Equation (8.52) can, in general, be satisfied if the matrix within braces vanishes identically. This is the desired matrix equation, which can be formally solved to give

$$(8.57)\qquad N=N^0\left[1-\frac{i\hbar}{2}V^{sx}N^0\right]^{-1}$$

in matrix notation. The practical convenience of this computational scheme is apparent at this point whenever the spatial localization of the orbitals $\phi$ drastically limits the range of the index $c$ in eq. (8.52) (cf. eq. (8.53)). In the limiting case of extreme localization one may, in particular, recover the classical Clausius-Mossotti relation from eq. (8.57) and below (cf. appendix F).

Within the above approximations, the irreducible polarizability takes on the form

$$(8.58)\qquad \tilde{\chi}(\boldsymbol{q}+\boldsymbol{G},\,\boldsymbol{q}+\boldsymbol{G}';\,\omega)=\frac{1}{\Omega_0}\sum_{cc'}A_c(\boldsymbol{q}+\boldsymbol{G})(-i\hbar)N_{cc'}(\boldsymbol{q};\,\omega)A^*_{c'}(\boldsymbol{q}+\boldsymbol{G}').$$

The proper polarizability, which is needed to evaluate the macroscopic dielectric function (8.26), may be similarly expressed as

$$(8.59)\qquad \hat{\chi}(\boldsymbol{q}+\boldsymbol{G},\,\boldsymbol{q}+\boldsymbol{G}';\,\omega)=\frac{1}{\Omega_0}\sum_{cc'}A_c(\boldsymbol{q}+\boldsymbol{G})\,\hat{S}_{cc'}(\boldsymbol{q};\,\omega)\,A^*_{c'}(\boldsymbol{q}+\boldsymbol{G}'),$$

where $\hat{S}$ is called the (proper) screening matrix. $\hat{S}$ can be determined by entering eqs. (8.58) and (8.59) into the integral equation (8.22*a*). One finds

$$(8.60)\qquad \hat{S}=(-i\hbar)N[1+i\hbar\hat{V}^CN]^{-1}=(-i\hbar)N^0\left[1+\left(\frac{1}{2}V^{sx}-\hat{V}^C\right)(-i\hbar)N^0\right]^{-1}$$

in matrix notation, where in the last line use has been made of eq. (8.57), and

$$\hat{V}^{C}_{cc'}(\boldsymbol{q}) = \frac{1}{\Omega_0} \sum_{\boldsymbol{G}\neq 0} A^*_c(\boldsymbol{q}+\boldsymbol{G})\, v(\boldsymbol{q}+\boldsymbol{G})\, A_{c'}(\boldsymbol{q}+\boldsymbol{G}) \tag{8.61}$$

is the (proper) Coulomb matrix. By adding to the right-hand side of eq. (8.61) the missing term with $\boldsymbol{G}=0$, one obtains the full Coulomb matrix which will be needed in sect. **9**. The latter can also be cast in the form (8.56) with the interchange $\boldsymbol{r} \rightleftarrows \boldsymbol{r}'$ between the first and the last orbital. This justifies calling eq. (8.56) the (screened) exchange counterpart of the Coulomb matrix.

The limit as $\boldsymbol{q} \to 0$ can be taken in eq. (8.59), whereby the property (8.27) results from eq. (8.53) and the orthogonality of orbitals referring to valence and conduction bands.

Details of the calculations are given in refs. [31-34]. Here we only comment on the main features of the results. One is interested in comparing the experimental spectrum of $\epsilon_2(\omega)$ with the calculated spectrum obtained within alternative approximations based on the result (8.60), namely, i) the time-dependent-screened-Hartree-Fock approximation (TDSHF) that takes eq. (8.60) as it stands, ii) the random-phase-approximation (RPA) that neglects the excitonic effect and thus sets $V^{sx}=0$ in eq. (8.60), and iii) the RPA with the further neglect of local-field effects ($\overline{\text{RPA}}$) that sets also $V^C=0$ in eq. (8.60) [37]. Figures 4 and 5 show the results for diamond and silicon, respectively. Common trends for both materials are that passing from the $\overline{\text{RPA}}$ to the RPA approximation furthers the discrepancy with experiment, while good agreement with experiment is re-established by the inclusion of the excitonic effect (TDSHF). Notice how these effects are more pronounced for diamond than for silicon, as expected from the different degree of localization of the orbitals. Similar results are found for GaP [34].

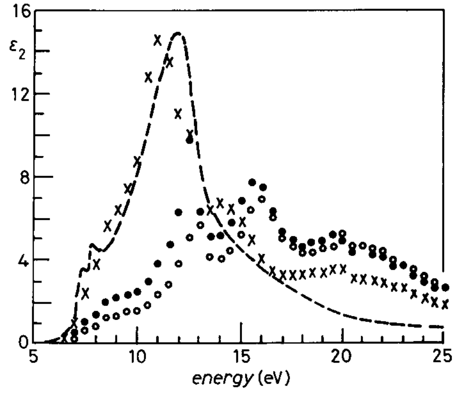

Fig. 4. – Imaginary part of the dielectric function *vs.* energy for diamond (adapted from ref. [31]). The experimental spectrum is compared with three different calculations (see text). --- experiment, ··· $\overline{\text{RPA}}$, ooo RPA, ××× TDSHF.

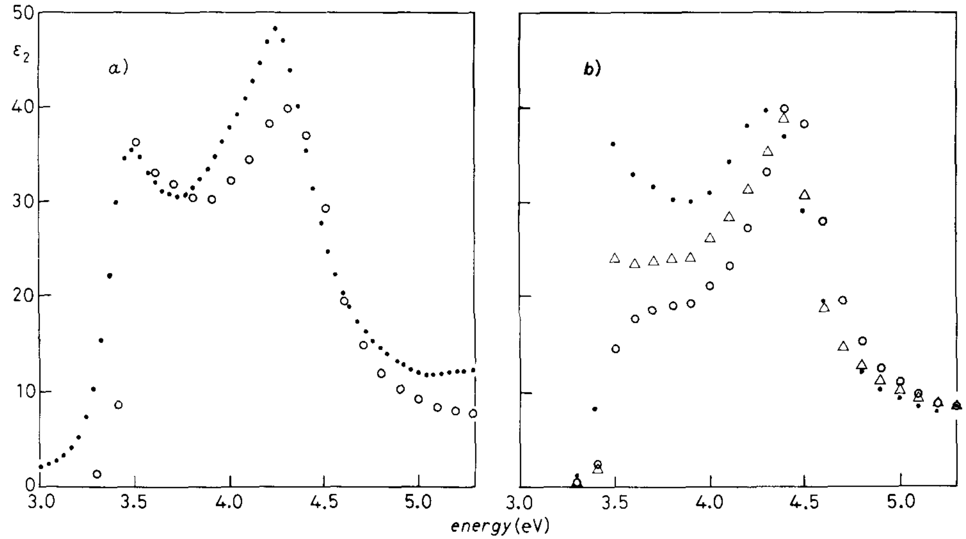

Fig. 5. – Imaginary part of the dielectric function versus energy for silicon (from ref. [35]). *a*) The experimental spectrum (···) is compared with the TDSHF calculation (○○○); *b*) comparison of three different calculations (see text). ··· TDSHF, ○○○RPA, △△△ $\overline{\text{RPA}}$.

As a «rule of thumb», the excitonic effect tends to pull the strength of the absorption coefficient toward the low-energy side [38], a feature which can also be accounted for by the use of a simplified model [39]. The numerical results also show the appropriateness of describing the absorption *above* the fundamental gap in terms of localized orbitals, since large regions of $\boldsymbol{k}$-space contribute to the main peaks. This has to be contrasted with the description of excitonic bound states *below* the fundamental gap whereby the use of the so-called effective-mass-approximation is found to be appropriate for semiconductors (cf. sect. **11**).

## 9. – Single-particle energy levels.

In the previous section the underlying single-particle band structure needed for calculating the optical spectra of semiconductors (cf. eqs. (8.48) and (8.51)) has been assumed to be known and emphasis has been placed on two-particle effects over and above band-structure effects. Many-body techniques, however, allow us *also* to determine single-particle band structures of semiconductors. This study, on the one hand, is necessary for a consistency check on the optical spectra, and, on the other hand, has some interest of its own because single-particle energy levels can be directly probed whenever two-particle effects can be disregarded. In particular, assessing the role of many-body effects on the band structure of semiconductors bears on the so-called «band-gap problem» that arises from the inability of conventional local-density calculations to reproduce the experimental band gaps of semiconductors [40]. It turns out that the *ansatz* (8.43) for the mass operator is sufficient for an accurate description of the band structure of (covalent) semiconductors and wide-gap insulators, at least for the cases studied thus far [41-44], this finding being consistent with the relevance of the excitonic effect on the optical spectra.

The starting point for the connection between the single-particle Green's function and the band structure is the observation that the poles of the time Fourier transform of the single-particle Green's function (in the absence of an external time-dependent potential) correspond to the energies of excitation of quasi-electrons and quasi-holes [45]. As the poles might be complex, these are approximate excited states of the $(N+1)$-particle and $(N-1)$-particle system, respectively. A suitable algorithm to locate these poles starts by taking the time Fourier transform of Dyson's eq. (3.14) with $U=0$

$$(9.1)\qquad [\hbar\omega - h(\boldsymbol{r})]\,G_1(\boldsymbol{r}, \boldsymbol{r}'; \omega) - \int \mathrm{d}\boldsymbol{r}''\,\Sigma(\boldsymbol{r}, \boldsymbol{r}''; \omega)\,G_1(\boldsymbol{r}'', \boldsymbol{r}'; \omega) = \delta(\boldsymbol{r}-\boldsymbol{r}')\,,$$

and then proceeds by considering the associated right and left eigenvalue problems [17]

$$(9.2a)\qquad h(\boldsymbol{r})\,\psi_\nu(\boldsymbol{r}; \omega) + \int \mathrm{d}\boldsymbol{r}'\,\Sigma(\boldsymbol{r}, \boldsymbol{r}'; \omega)\,\psi_\nu(\boldsymbol{r}'; \omega) = \mathcal{E}_\nu(\omega)\,\psi_\nu(\boldsymbol{r}; \omega)\,,$$

$$(9.2b)\qquad h(\boldsymbol{r})\,\tilde{\psi}_\nu(\boldsymbol{r}; \omega) + \int \mathrm{d}\boldsymbol{r}'\,\tilde{\psi}_\nu(\boldsymbol{r}'; \omega)\,\Sigma(\boldsymbol{r}', \boldsymbol{r}; \omega) = \mathcal{E}_\nu(\omega)\,\tilde{\psi}_\nu(\boldsymbol{r}; \omega)\,,$$

whereby $\omega$ is regarded as a parameter. In these equations, the self-energy acts as a nonlocal and energy-dependent potential [46]. The eigensolutions of eqs. (9.2) are assumed to form a complete set and to satisfy the orthonormality relation

$$(9.3)\qquad \int \mathrm{d}\boldsymbol{r}\,\tilde{\psi}_\nu(\boldsymbol{r}; \omega)\,\psi_{\nu'}(\boldsymbol{r}; \omega) = \delta_{\nu\nu'}\,.$$

The single-particle Green's function can thus be expressed in the bilinear form

$$(9.4)\qquad G_1(\boldsymbol{r}, \boldsymbol{r}'; \omega) = \sum_\nu \frac{\psi_\nu(\boldsymbol{r}; \omega)\,\tilde{\psi}_\nu(\boldsymbol{r}'; \omega)}{\hbar\omega - \mathcal{E}_\nu(\omega)}\,.$$

Equation (9.4) can be considerably simplified when the resonances occurring at $\hbar\omega \sim \mathcal{E}_\nu(\omega)$ are *narrow*. In this case, one usually adopts the so-called quasi-particle approximation [47] which assumes that the singularities originating from the energy denominator in eq. (9.4) form the *dominant contribution* to the single-particle Green's function:

$$(9.5)\qquad G_1(\boldsymbol{r}, \boldsymbol{r}'; \omega) \simeq \sum_\nu g_\nu \frac{\psi_\nu(\boldsymbol{r}; \mathrm{Re}\{\omega_\nu\})\,\tilde{\psi}_\nu(\boldsymbol{r}'; \mathrm{Re}\{\omega_\nu\})}{\hbar\omega - \hbar\omega_\nu}\,,$$

where $\omega_\nu$ are determined by the condition

$$\mathcal{E}_\nu(\omega_\nu) = \hbar\omega_\nu \tag{9.6}$$

and we have introduced the renormalization factor

$$g_\nu = \left[1 - \left.\frac{\mathrm{d}\mathcal{E}_\nu(\omega)}{\mathrm{d}\omega}\right|_{\omega_\nu}\right]^{-1}. \tag{9.7}$$

Since the skew-Hermitian part of the self-energy operator changes from being a positive operator to being a negative operator as $\hbar\omega$ increases through the chemical potential [47] (which for a semiconductor lies within the energy gap $\varepsilon_g$), the imaginary part of $\mathcal{E}_\nu$ changes sign correspondingly. This remark implies, in particular, that if the self-energy did not depend on $\omega$, its skew-Hermitian part would vanish and consequently eq. (9.5) would become exact with $g_\nu = 1$. This is indeed the case for the Hartree-Fock approximation

$$\begin{aligned}\Sigma_{\mathrm{HF}}(\boldsymbol{r}, \boldsymbol{r}') = -i\hbar\,\delta(\boldsymbol{r}-\boldsymbol{r}')\,2\int \mathrm{d}\boldsymbol{r}''\,v(\boldsymbol{r}-\boldsymbol{r}'')\int_{-\infty}^{+\infty}\frac{\mathrm{d}\omega'}{2\pi}\exp[i\omega'\delta]\,G_1(\boldsymbol{r}'', \boldsymbol{r}''; \omega') +{}\\ + i\hbar v(\boldsymbol{r}-\boldsymbol{r}')\int_{-\infty}^{+\infty}\frac{\mathrm{d}\omega'}{2\pi}\exp[i\omega'\delta]\,G_1(\boldsymbol{r}, \boldsymbol{r}'; \omega'),\end{aligned} \tag{9.8}$$

where the factor of two in the Hartree term originates from the spin sum and the convergence factor in the frequency integrals selects the contribution of the states below the chemical potential in eq. (9.5).

The Hartree-Fock approximation represents conceptually a good reference level to study many-body effects since it corresponds to the «best» single-particle picture whereby each particle is assumed to move under the influence of the *average* interaction with all other particles [48]. However, when applied to real materials it gives, *e.g.*, energy gaps that are by far too large compared with the experimental values. For instance, in the case of diamond one obtains a value of 15.0 eV for the gap [49] which is about twice the experimental value (7.3 eV). The reason for this serious deficiency of the Hartree-Fock approximation can be traced in the lack of relaxation processes which should accompany the primary single-particle excitation, namely, the rearrangement of the passive electrons to the addition of an extra electron or to the creation of a hole. The success in describing the optical properties (sect. 8) suggests that the ansatz (8.43), which replaces the bare Coulomb interaction $v$ of the Fock term with the dynamically screened interaction $W$, can actually account for the above polarization processes in semiconductors. Moreover, to address important questions such as the influence of the energy dependence of the dielectric matrix on the self-energy shifts and the goodness of the quasi-particle approximation in semiconductors, we will keep the full time dependence of eq. (8.43) in the calculation and resort to a static approximation of the type (8.45) only for comparison.

The adding of correlation effects within the GW approximation (8.43) on top of a Hartree-Fock band structure was the line followed in the original calculation for diamond [41] which was chosen as a prototype of covalent materials. The reasons for this choice were essentially the availability of accurate Hartree-Fock calculations for this light-core material as well as the appropriateness of a local-orbital representation for the valence and conduction bands which is needed for an accurate description of the screening properties (cf. subsect. 8·4). Later work [42-44] has used as starting point local-density band-structure calculations which have the advantage of being more readily available than Hartree-Fock calculations. Here we follow the approach of the prototype calculation for diamond [41] for pedagogical reasons.

The local-orbital representation (8.51) for the single-particle wave functions allows us to reduce the quasi-particle equation (9.2) to an algebraic eigenvalue problem for the coefficients $c_{\mu n}(\boldsymbol{k})$ [50]

$$(9.9)\qquad \sum_{\mu'}\big(\langle\mu|\varepsilon(\boldsymbol{k})|\mu'\rangle + \langle\mu|M(\boldsymbol{k};\,E_n(\boldsymbol{k}))|\mu'\rangle\big)\,c_{\mu' n}(\boldsymbol{k}) = E_n(\boldsymbol{k})\,c_{\mu n}(\boldsymbol{k})\,.$$

Here we have introduced the notation

$$(9.10a)\qquad \langle\mu|\varepsilon(\boldsymbol{k})|\mu'\rangle = \sum_{\boldsymbol{l}} \exp[i\boldsymbol{k}\cdot\boldsymbol{l}]\,\langle\phi_\mu(\boldsymbol{r})|h_{\text{av}}(\boldsymbol{r})|\phi_{\mu'}(\boldsymbol{r}-\boldsymbol{l})\rangle\,,$$

$$(9.10b)\qquad \langle\mu|M(\boldsymbol{k};\,E)|\mu'\rangle = \sum_{\boldsymbol{l}} \exp[i\boldsymbol{k}\cdot\boldsymbol{l}]\,\langle\phi_\mu(\boldsymbol{r})|M(\boldsymbol{r},\,\boldsymbol{r}';\,E)|\phi_{\mu'}(\boldsymbol{r}'-\boldsymbol{l})\rangle\,,$$

where $h_{\text{av}}(\boldsymbol{r})$ contains the Coulomb effects both of the nuclei and of the average electronic charge distribution in the ground state (Hartree term). Notice that the condition (9.6) has already been taken into account in eq. (9.9).

For the expressions (9.10) to be of practical importance the summations over the lattice sites $\boldsymbol{l}$ should be rapidly converging. This is certainly the case for the matrix elements of the local Hamiltonian in eq. (9.10*a*), provided the local orbitals are sufficiently localized, while for the convergence of eq. (9.10*b*) the short-range property in $|\boldsymbol{r}-\boldsymbol{r}'|$ of the mass operator in required in addition [17]). Crystal symmetry also considerably reduces the number of independent matrix elements in eqs. (9.10). For diamond a minimal set of ten independent matrix elements has proven sufficient [41].

The expression of the mass operator within the GW approximation to be inserted in eq. (9.10*b*), namely

$$(9.11)\qquad M(\boldsymbol{r},\,\boldsymbol{r}';\,E) = \frac{i}{2\pi}\int_{-\infty}^{+\infty} \mathrm{d}E'\,\exp[iE'\delta]\,G_1(\boldsymbol{r},\,\boldsymbol{r}';\,E+E')\,W(\boldsymbol{r},\,\boldsymbol{r}';\,E')$$

can be split in terms of the Hartree-Fock $M_{\mathrm{HF}}$ (the second term at the right-hand side of eq. (9.8)) and of a remainder $M'$, whereby the dynamically screened interaction in eq. (9.11) is replaced by

$$W'(\boldsymbol{r}, \boldsymbol{r}'; E) = \int \mathrm{d}\boldsymbol{r}_1 \, \mathrm{d}\boldsymbol{r}_2 \, v(\boldsymbol{r} - \boldsymbol{r}_1) \chi_{\mathrm{T}}(\boldsymbol{r}_1, \boldsymbol{r}_2; E) v(\boldsymbol{r}_2 - \boldsymbol{r}'), \tag{9.12}$$

$\chi_{\mathrm{T}}$ being the (time-ordered) polarizability matrix. The matrix elements of $M_{\mathrm{HF}}$ can thus be determined by fitting a Hartree-Fock band structure calculation [49]. The matrix elements of $M'$, on the other hand, need to be explicitly evaluated. To this end, it is convenient to exploit the local-orbital representation for $\chi_{\mathrm{T}}$ which is obtained from eq. (8.59) by replacing the proper screening matrix $\hat{S}$ with the full screening matrix $S$ that contains also the term with $\boldsymbol{G} = 0$. This is because, contrary to the description of the optical properties where the limit $\boldsymbol{q} \to 0$ is in order, the short-range nature of the electronic correlations requires an accurate description of $\chi_{\mathrm{T}}(\boldsymbol{q} + \boldsymbol{G}, \boldsymbol{q} + \boldsymbol{G}'; E)$ for *all* $\boldsymbol{q}$. The result can then be expressed in terms of the matrix

$$W'_{m\sigma\tau, m'\sigma'\tau'}(\boldsymbol{q}; E) = \sum_{l\nu\mu} \sum_{l'\nu'\mu'} V_{m\sigma\tau, l\nu\mu}(\boldsymbol{q}) S_{l\nu\mu, l'\nu'\mu'}(\boldsymbol{q}; E) V_{l'\nu'\mu', m'\sigma'\tau'}(\boldsymbol{q}), \tag{9.13}$$

where now the indices $(\sigma, \tau)$ refer either to a pair of bonding or antibonding orbitals, or to a bonding and an antibonding orbital. Details of the calculation are

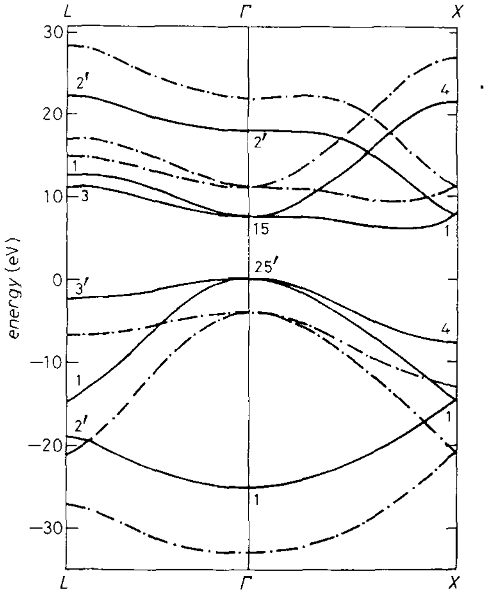

Fig. 6. – Quasi-particle band structure of diamond calculated within the Hartree-Fock approximation (dashed-dotted line) and within the GW approximation with the screening taken within the TDSHF approximation (full line) (from ref. [19]).

given in ref. [41] where the numerical methods adopted to make the scheme working in practice are also described.

The quasi-particle valence and conduction band structure of diamond (that is, the *real* part of the eigenvalues $E_n(\boldsymbol{k})$ of eq. (9.9)) is shown in fig. 6 for two symmetry directions. The label TDSHF signifies, as in sect. 8, that both local-field effects and the electron-hole attraction have been included in the screening properties entering eq. (9.13). The Hartree-Fock band structure from ref. [49] is also shown for comparison. In fig. 7 the quasi-particle band structure TDSHF is compared with the RPA simplified form obtained by neglecting the electron-hole attraction in the screening properties. Several interesting features can be inferred from these calculations.

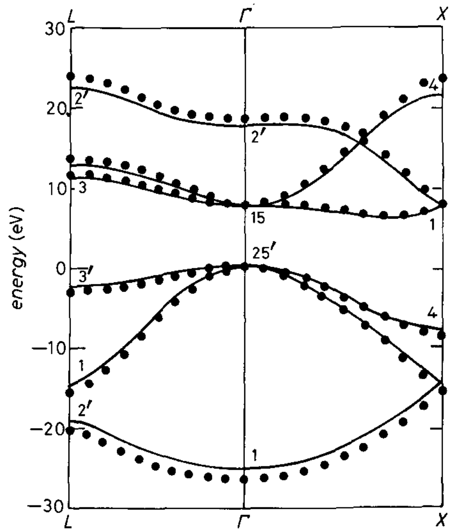

Fig. 7. – Quasi-particle band structure of diamond calculated within the GW approximation with the screening taken within the TDSHF approximation (full line) and within the RPA approximation (dotted line) (from ref. [19]).

i) Self-energy corrections to the Hartree-Fock eigenvalues are positive for holes and negative for electrons, thereby reducing the amount of energy required to produce an electron-hole pair. In particular, a drastic reduction of the diamond band gap at $\Gamma$ occurs from the Hartree-Fock value (15.0 eV) to the final correlated value (7.4 eV) within the TDSHF approximation, in very good agreement with the experimental value. Notice also that the magnitude of self-energy corrections for the valence bands is larger than for the conduction bands, thereby matching a general «rule of thumb» that to larger effective masses correspond larger self-energy corrections.

ii) The magnitude of the self-energy corrections within the RPA approximation is smaller than the corresponding value within the TDSHF approximation; in particular, the RPA band gap is increased by about 1 eV compared with the full calculation. This is consistent with the *ab initio* values obtained for the long-wavelength static dielectric constant $\epsilon_0$ within the RPA (4.25) and TDSHF (6.10) approximations, respectively, thereby fulfilling the other «rule of thumb» that self-energy corrections increase with $\epsilon_0$. Thus, although it formally violates conservation criteria, the TDSHF approximation gives in practice better results for the quasi-particle band structure and for the optical properties than the RPA approximation (cf. also sect. 8).

iii) At any given $\boldsymbol{k}$, the magnitude of self-energy corrections increases away from the gap region, resulting in a narrowing of the valence bandwidth. In particular, the Hartree-Fock bandwidth (29.0 eV) is reduced to 25.2 eV by the TDSHF calculation, a value which is rather close to the experimental value of 24.2 eV. To assess the importance of the energy dependence of the self-energy operator across the valence bands, an additional calculation has been performed where the energy dependence of the matrix elements (9.13) has been (almost) neglected by taking their values at $E = 0$ and cutting off the energy integration of eq. (9.11) past the plasma resonance. The result is that, while the energy gap is found practically unchanged with respect to the full calculation, the valence band width now comes out to be essentially unrenormalized with respect to the Hartree-Fock value. This suggests that an energy-independent approximation works well at energies about the gap, while the energy-dependence of the self-energy becomes progressively important as soon as we leave the gap region moving down through the valence bands. This finding corresponds to an increasing weight of the plasma resonance in the energy integration of eq. (9.11) with respect to the low-lying electron-hole continuum, as one proceeds deep in the valence bands. To make a further check on this point, the contribution of the plasma resonance to the full calculation has been neglected by terminating the energy integration before the onset of the plasma resonance. No variation has been consistently found on the gap. Similar results have been found for silicon [42], confirming that quasi-particle properties in the vicinity of the gap are essentially entirely determined by coupling to electron-hole excitations.

iv) The self-energy corrections of figs. 6 and 7 show a weak, although noticeable, $\boldsymbol{k}$-dependence, being in general more pronounced away from the centre of the Brillouin zone. This is consistent with the short-range property of the mass operator discussed after eqs. (9.10) and indicates that self-energy corrections are essentially dominated by large albeit rigid shifts of the valence and conduction bands.

A comment on the self-consistency of the single-particle Green's function is in order at this point. For the purpose of evaluating the matrix elements of the mass operator, the single-particle Green's function entering eq. (9.11) has been represented in the form (8.48) with the bands taken from a previous $X\alpha$

calculation which is closer to the final result than the Hartree-Fock calculation. Once the new quasi-particle band structure has been obtained by solving eq. (9.9), however, the calculation should in principle be repeated using again for $G_1$ an approximate expression of the type (8.48), until self-consistency is attained. While in the original calculation for diamond this kind of self-consistency has not been achieved, later work [44] has verified that iteration causes only a small further change for the spectrum which is whithin the estimated numerical error (0.2 eV).

We finally discuss the decay of (valence) quasi-holes in diamond which can be calculated whenever the approximation for the mass operator is energy dependent. Within the GW approximation the mechanism responsible for this decay is the Coulomb interaction among the electrons which leads to radiationless transitions to final states with more than one hole in the valence bands (intra-band multiple Auger processes). Clearly, these processes must be consistent with energy conservation and the decay rate must vanish below a threshold, rising sharply beyond it. For diamond the decay rate can be estimated to become noticeable about 10 eV *below* the top of the valence bands. In fig. 8 the *imaginary* part of the eigenvalues $E_n(\boldsymbol{k})$ of eq. (9.9) is shown versus the real part along two symmetry directions. (Recall that the corresponding lifetime of the approximate $(N-1)$-particles states is given by $(2Im\{E_n(\boldsymbol{k})\})^{-1}$.) The characteristic value of about 1 eV for this quantity sets an intrinsic limit of consistency on the validity of the quasi-particle approximation which has extensively been used in our calculations.

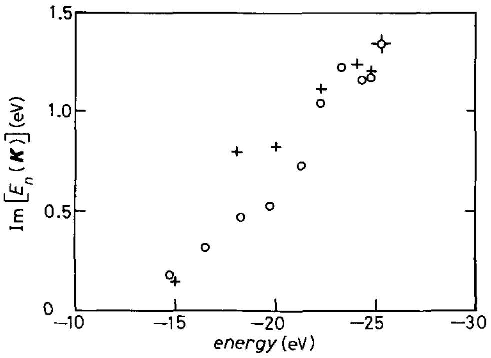

Fig. 8. – Imaginary part of quasi-hole levels in diamond along two different symmetry directions within the TDSHF approximation (from ref. [19]). ○ along $\Delta$, + along $\Lambda$.

Some of above results can be understood, at least *qualitatively*, in an analytical way. To this end, we represent the (time-ordered) polarizability matrix $\chi_T$ entering eq. (9.12) in the form (5.9) (where $A$ and $B$ are now identified with the density operator), and we perform the energy integration in eq. (9.11) by suitably closing the contour in the complex energy plane. We obtain for the diagonal matrix elements of the remainder $M'$

$$(9.14)\qquad \int \mathrm{d}\boldsymbol{r}\,\mathrm{d}\boldsymbol{r}'\,u_k^*(\boldsymbol{r})\,M'(\boldsymbol{r},\boldsymbol{r}';\varepsilon_k)\,u_k(\boldsymbol{r}')=$$

$$=\sum_{s\neq 0}\sum_{k'}\left|\int \mathrm{d}\boldsymbol{r}\,\mathrm{d}\boldsymbol{r}'\,u_k^*(\boldsymbol{r})\,u_{k'}(\boldsymbol{r})\,v(\boldsymbol{r}-\boldsymbol{r}')\,\rho_s(\boldsymbol{r}')\right|^2\left[\frac{\theta(\varepsilon_{\mathrm{F}}-\varepsilon_{k'})}{\varepsilon_k-\varepsilon_{k'}+\omega_s-i\delta}+\frac{\theta(\varepsilon_{k'}-\varepsilon_{\mathrm{F}})}{\varepsilon_k-\varepsilon_{k'}-\omega_s+i\delta}\right],$$

where $\omega_s$ are the excitation energies of sect. 5. For $\varepsilon_k$ at the top of the valence bands the first term within brackets at the right-hand side of eq. (9.14) dominates over the second one, yielding a positive self-energy shift, while for $\varepsilon_k$ at the bottom of the conduction bands is the second term that dominates over the first one, yielding a negative self-energy shift. Combination of the two effects results then in a net narrowing of the band gap compared with the Hartree-Fock value. However, if one neglected the energy dependence of the screened interaction altogether and took $W'(\boldsymbol{r},\boldsymbol{r}';E)$ outside the energy integral in eq. (9.11), one would obtain a self-energy correction

$$(9.15)\qquad \int \mathrm{d}\boldsymbol{r}\,\mathrm{d}\boldsymbol{r}'\,u_k^*(\boldsymbol{r})\,M'(\boldsymbol{r},\boldsymbol{r}';\varepsilon_k)\,u_k(\boldsymbol{r}')\simeq$$

$$\simeq\sum_{s\neq 0}\sum_{k'}\theta(\varepsilon_{\mathrm{F}}-\varepsilon_{k'})\left|\int \mathrm{d}\boldsymbol{r}\,\mathrm{d}\boldsymbol{r}'\,u_k^*(\boldsymbol{r})\,u_{k'}(\boldsymbol{r})\,v(\boldsymbol{r}-\boldsymbol{r}')\,\rho_s(\boldsymbol{r}')\right|^2\frac{2}{\omega_s},$$

which is manifestly positive for both electrons and holes [51]. The fact that *some* sort of energy dependence of the screened interaction should be retained is borne out, in particular, in the prescription for obtaining the COHSEX approximation [5], which is sometimes used for comparison with the full dynamical calculations [41, 44].

To get additional insight, we may further simplify eq. (9.14) by neglecting the local-field effects in the screening (although they are important for getting good quantitative results), and by approximating the low-lying electron-hole continuum and the plasma resonance (in which the energy range covered by the dielectric function is usually partitioned) by two modes with dispersion $\omega_1(\boldsymbol{q})$ and $\omega_2(\boldsymbol{q})$, respectively. We thus take

$$(9.16)\qquad \epsilon_{\mathrm{T}}^{-1}(\boldsymbol{q};\omega)=1+\frac{\Omega_1^2}{\omega^2-(\omega_1(\boldsymbol{q})-i\delta)^2}+\frac{\Omega_2^2}{\omega^2-(\omega_2(\boldsymbol{q})-i\delta)^2},$$

where the sign of the infinitesimal imaginary frequency corresponds to a time-ordered quantity, and the coefficients $\Omega_1$ and $\Omega_2$ are related to the plasma frequency by the sum rule (E.5)

$$(9.17)\qquad \Omega_1^2+\Omega_2^2=\omega_{\mathrm{p}}^2.$$

The self-energy shift now becomes

$$(9.18)\qquad \int \mathrm{d}\boldsymbol{r}\,\mathrm{d}\boldsymbol{r}'\, u_k^*(\boldsymbol{r})\, M'(\boldsymbol{r}, \boldsymbol{r}'; \varepsilon_k)\, u_k(\boldsymbol{r}') \simeq$$

$$\simeq \int \frac{\mathrm{d}\boldsymbol{q}}{(2\pi)^3}\, v(\boldsymbol{q}) \sum_{k'} \left| \int \mathrm{d}\boldsymbol{r}\, u_k^*(\boldsymbol{r}) \exp[i\boldsymbol{q}\cdot\boldsymbol{r}]\, u_{k'}(\boldsymbol{r}) \right|^2 \cdot$$

$$\cdot \sum_{s=1}^{2} \frac{\Omega_s^2}{2\omega_s(\boldsymbol{q})} \left[ \frac{\theta(\varepsilon_{\mathrm{F}} - \varepsilon_{k'})}{\varepsilon_k - \varepsilon_{k'} + \omega_s(\boldsymbol{q}) - i\delta} + \frac{\theta(\varepsilon_{k'} - \varepsilon_{\mathrm{F}})}{\varepsilon_k - \varepsilon_{k'} - \omega_s(\boldsymbol{q}) + i\delta} \right],$$

which shows at glance that the valence bandwidth $\Delta\varepsilon_{\mathrm{val}}$ is shrinked by the plasma resonance for $\Delta\varepsilon_{\mathrm{val}} < \omega_2(\boldsymbol{q})$. A corresponding analysis can be done for the imaginary part of the self-energy shift.

## 10. – Screening of static impurities.

The mass operator considered in the previous section was assumed to possess the full symmetry of the crystal. In real materials this symmetry is often destroyed by the presence of impurities which may sit either at crystalline sites (substitutional impurities) or at interstitial sites (interstitial impurities). In both cases, the electronic density rearranges about the impurities which, therefore, test the screening properties of the crystal both locally and at large distances.

In the simplest case of a single *weak* impurity the theory of linear response to an external (static) scalar potential can be applied. In fact, the change in the self-energy operator to lowest order in the (bare) impurity potential $v_{\mathrm{imp}}(\boldsymbol{r})$ is given by

$$(10.1)\qquad \Sigma_I(1, 2) - \Sigma(1, 2) = -\int \mathrm{d}3 \left( \delta(1, 2)\,\delta(1, 3) + \frac{\delta G_1^{-1}(1, 2)}{\delta U(3)} \right) v_{\mathrm{imp}}(3) =$$

$$= -\delta(1, 2)\, v_{\mathrm{imp}}(1) + \int \mathrm{d}3\, \Gamma(1, 2; 3)\, v_{\mathrm{imp}}(3),$$

where $\Sigma$ is the self-energy operator of the perfect crystal. Equation (10.1) has been obtained by combining Dyson's equation in the form (B.4) with the definition (C.6) for the reducible scalar vertex function. Notice that, upon insertion of eq. (10.1) into eq. (3.14), the first term at the right-hand side of eq. (10.1) cancels with the potential term. One may thus regard the second term at the right-hand side of eq. (10.1) as the effective change in the self-energy operator over and above the perfect crystal expression [18].

The *screened impurity potential* can be introduced at this point by recalling the definitions (3.17) for the irreducible scalar vertex function and (3.19) for the inverse (longitudinal) dielectric matrix. One obtains

$$(10.2)\qquad \int d3\,\Gamma(1,2;3)\,v_{\mathrm{imp}}(3) = -\int d3\frac{\delta G_1^{-1}(1,2)}{\delta U(3)}v_{\mathrm{imp}}(3) =$$
$$= -\int d34\frac{\delta G_1^{-1}(1,2)}{\delta V(3)}\frac{\delta V(3)}{\delta U(4)}v_{\mathrm{imp}}(4) = \int d34\,\tilde{\Gamma}(1,2;3)\,\epsilon^{-1}(3,4)\,v_{\mathrm{imp}}(4) =$$
$$= \int d3\,\tilde{\Gamma}(1,2;3)\,\phi_{\mathrm{imp}}(3)\,,$$

where use has been made of the «chain rule» (A.8) and

$$(10.3)\qquad \phi_{\mathrm{imp}}(1) = \int d2\,\epsilon^{-1}(1,2)\,v_{\mathrm{imp}}(2) = \int d\boldsymbol{r}_2\,\epsilon^{-1}(\boldsymbol{r}_1,\boldsymbol{r}_2;\,\omega=0)\,v_{\mathrm{imp}}(\boldsymbol{r}_2)$$

is the (statically screened) impurity potential. Since at zero frequency the time-ordered inverse dielectric matrix in eq. (10.3) coincides with its retarded counterpart (cf. sect. 5), eq. (10.3) could have alternatively been obtained within linear response theory as the change in the Hartree potential resulting from the induced charge density about the (static) impurity [52]. Retaining only the effects of the impurity potential (10.3) corresponds to approximating $\tilde{\Gamma}(1,2;3)=\delta(1,2)\,\delta(1,3)$ in eq. (10.2), *i.e.* to neglecting vertex corrections. It has been shown [18] that for a Coulombic impurity, whereby the Hartree potential (10.3) is $O(r^{-1})$ at large distance $r$ from the impurity, vertex corrections produce terms of shorter range $[O(r^{-2})]$. Within the GW approximation used previously, this feature results from the converge properties of the single-particle Green's function far from the impurity centre.

We do not enter here into the question whether vertex corrections within linear screening or nonlinear screening effects (due to higher terms in the expansion (10.1)) might be relevant to the calculation of specific impurity levels [53]. Rather we focus on the impurity potential (10.3) (or, equivalently, on the corresponding induced charge density) and take advantage of the knowledge of $\epsilon^{-1}(\boldsymbol{r},\boldsymbol{r}';\omega)$ developed in sects. 8 and 9 to determine the size of the corrections introduced by local-field and excitonic effects. Details of the calculations are given in refs. [33] and [54] where embedding a pointlike impurity with positive unit charge both at substitutional and interstitial positions in crystalline diamond and silicon was considered. Different levels of approximation are again identified by the acronyms TDSHF, RPA, and $\overline{\mathrm{RPA}}$ where the latter now means neglecting the electron-hole attraction and taking $\epsilon^{-1}$ diagonal in the reciprocal lattice vectors. Figures 9 and 10 show the induced-charge density along two different directions for a substitutional impurity in diamond and silicon, respectively. These results demonstrate that in diamond *both* local field and excitonic effects introduce corrections of comparable magnitude. In addition, since these corrections are of the same magnitude of the isotropic $\overline{\mathrm{RPA}}$ screening, both effects are crucial for a microscopic description of the impurity screening. In silicon, on the other hand, there is a smaller difference between the RPA and the TDSHF approximations. Similar trends show up also at large distances from the impurity centre as it results, *e.g.*, from the value of the total induced-charge density $Q_{\text{ind}} = (1 - \epsilon_0)/\epsilon_0$. For silicon one gets the values $\epsilon_0 = 10.9$ in the $\overline{\text{RPA}}$, $\epsilon_0 = 10.3$ in the RPA, and $\epsilon_0 = 11.6$ in the TDSHF, that give values of $Q_{\text{ind}}$ within a 1% range. For diamond, there is about a 10% difference among the corresponding values of $Q_{\text{ind}}$.

The fact that the electronic charge in silicon is more easily polarizable than in diamond manifests also in the strong *anysotropy* of the screening charge distribution which is more pronounced in diamond than in silicon. By analysing the contour plots in selected crystal planes [54, 33], one finds that charge flux toward the impurity in diamond is preferentially directed along the bonds, while in silicon this asymmetry is less pronounced.

Finally, a parallel study conducted for an interstitial impurity shows that in both materials the screening is locally more efficient for the substitutional than for the interstitial case [54, 33].

Although the screened impurity potential (10.3) considered in this section was strictly static, other self-energy terms beyond the Hartree potential entail in general dynamical screening effects through the frequency dependence of the dielectric matrix. On the other hand, in the theory of excitons which is

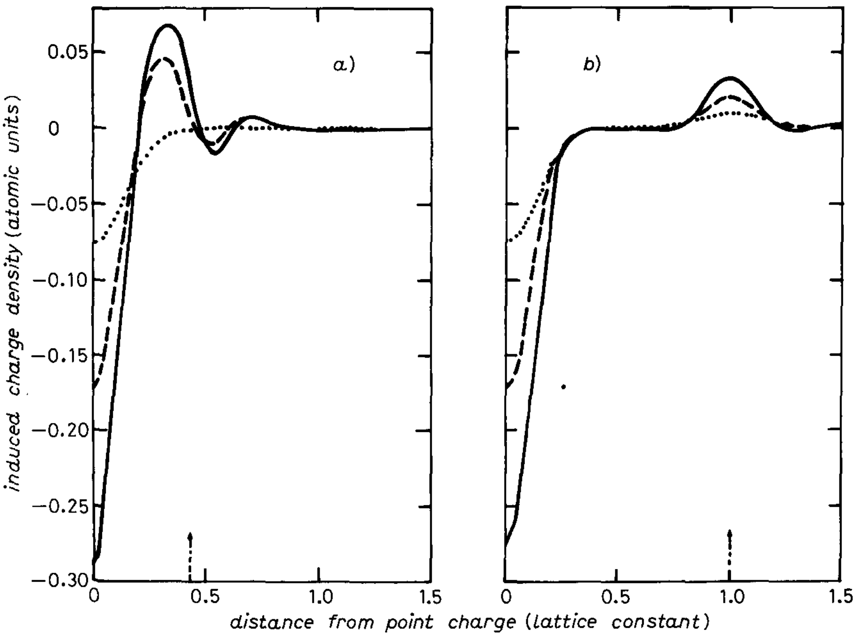

Fig. 9. – Induced charge density, $\rho_{\text{ind}}$, about a positive substitutional impurity in diamond, along two different directions (from ref. [33]). For the meaning of various approximations see text. *a*) (1.1.1)-direction, *b*) (1.0.0)-direction; ··· $\overline{\text{RPA}}$, --- RPA, —— TDSHF.

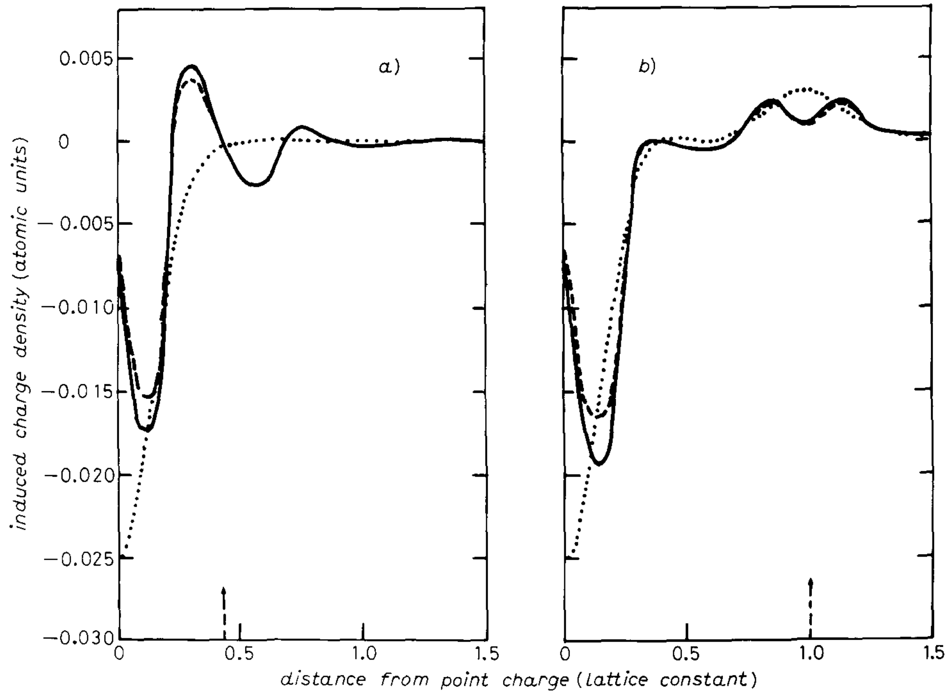

Fig. 10. – Same as in fig. 9 for silicon.

considered in the next section (whereby bound states originate from the interaction of an excited electron with the hole left behind), the static linear-response screening of eq. (10.3) is replaced by an «effective» screening function that depends self-consistently on the excitonic binding energy.

## 11. – Excitonic states.

We have seen in sect. 5 from the Lehmann representation of the density-density correlation function that the poles of this function occur at the exact excitation energies of the subset of states which are coupled to the ground state through the density operator. For a crystalline semiconductor above the fundamental single-particle energy gap $\varepsilon_g$ these poles merge into a continuum and one may apply the methods of sect. 8 to calculate the strength of the absorption coefficient at any given frequency. It is *below* this edge, however, that the most striking two-particle effects over and above single-particle excitations take place, with the appearence of sharp peaks in the absorption coefficient that correspond to bound electron-hole pairs [55]. This new kind of states is associated with truly isolated poles of the density-density correlation function and is produced by the same many-body mechanism which is responsible for the shift of the single-particle peaks in the continuum toward the low-energy side. In this section we describe an algorithm to locate these poles, which reduces the Bethe-Salpeter integral equation for the two-particle correlation function to an effective eigenvalue problem [12, 10, 8]. The need for this kind of algorithm arises also to circumvent the uncertainties in the single-particle band structure that might in practice be even larger than the spacing of the bound excitonic levels we are looking for. We shall, in fact, regard the underlying single-particle band structure as given (at worst, by fitting the energy gap to the experimental value) and concentrate on two-particle effects by calculating the excitonic binding energies.

The derivation of the effective eigenvalue problem starts from the analysis of the linear combinations of the four time variables in the two-particle Green's function $G_2(1, 2; 1', 2')$ to identify its particle-hole portion for the relevant types of excited states. One may take, in particular, the symmetric combinations

$$\tau_1 = t_1 - t_{1'}, \qquad \tau_2 = t_2 - t_{2'}, \qquad \tau = t^1 - t^2 \tag{11.1}$$

with $t^1 = (1/2)(t_1 + t_{1'})$ and $t^2 = (1/2)(t_2 + t_{2'})$, as independent time variables, and conveniently group the 24 terms of the two-particle Green's function into 6 classes with 4 terms each, as discussed in appendix G. The 8 terms that contain the phase factors $\exp[i(E_s - E_0)t^1]$ and $\exp[i(E_s - E_0)t^2]$ are then called the particle-hole Green's function. Upon setting $t_{2'} = t_2 + \delta(\delta \to 0^+)$ and Fourier transforming the variable $t_2$, we obtain

$$\begin{aligned}
&L^{\mathrm{ph}}(\boldsymbol{x}_1, \boldsymbol{x}_2; \boldsymbol{x}_{1'}, \boldsymbol{x}_{2'} | t_1, t_{1'}; \omega) \equiv \\
&\equiv - \int_{-\infty}^{+\infty} \mathrm{d}t_2 \exp[-i\omega t_2] L^{\mathrm{ph}}(\boldsymbol{x}_1 t_1, \boldsymbol{x}_2 t_2; \boldsymbol{x}_{1'} t_{1'}, \boldsymbol{x}_{2'} t_2^+) = \\
&= -\frac{i}{\hbar} \exp[-i\omega(t^1 - |\tau_1|/2)] \cdot \\
&\cdot \sum_s \frac{\chi_s^{\mathrm{ph}}(\boldsymbol{x}_1, \boldsymbol{x}_{1'}; \tau_1) \tilde{\chi}_s^{\mathrm{ph}}(\boldsymbol{x}_2, \boldsymbol{x}_{2'}; -\delta)}{\hbar\omega - (E_s - E_0) + i\eta} \exp\left[-i\frac{(E_s - E_0)|\tau_1|}{2\hbar}\right] + \\
&+ \frac{i}{\hbar} \exp[-i\omega(t^1 + |\tau_1|/2)] \cdot \\
&\cdot \sum_s \frac{\chi_s^{\mathrm{ph}}(\boldsymbol{x}_2, \boldsymbol{x}_{2'}; -\delta) \tilde{\chi}_s^{\mathrm{ph}}(\boldsymbol{x}_1, \boldsymbol{x}_{1'}; \tau_1)}{\hbar\omega + (E_s - E_0) - i\eta} \exp\left[-i\frac{(E_s - E_0)|\tau_1|}{2\hbar}\right],
\end{aligned} \tag{11.2}$$

where $\eta \to 0^+$ and the transform of the single-particle factor in eq. (4.1) has been dropped, since it vanishes provided $\omega$ is nonzero.

The Bethe-Salpeter equation (4.5) can be Fourier transformed accordingly. Assuming a particular (simple) pole at $\hbar\omega_s = E_s - E_0 > 0$ to be *isolated* from the other singularities in the complex $\omega$ plane, we may pick up the corresponding residue by integrating over an infinitesimal contour enclosing the pole. We obtain

$$(11.3)\qquad \chi_s^{\rm ph}(\boldsymbol{x}_1, \boldsymbol{x}_{1'}; \tau_1)\exp[-i\omega_s t^1] = \\ = \int {\rm d}33'44' G_1(1, 3)\, G_1(3', 1')\, \Xi(3, 4'; 3', 4)\, \chi_s^{\rm ph}(\boldsymbol{x}_4, \boldsymbol{x}_{4'}; \tau_4)\exp[-i\omega_s t^4],$$

which can be regarded as a (homogeneous) *bound-state equation* for the right-hand particle-hole amplitudes (G.3*a*).

Equation (11.3) holds for $\hbar\omega_s < \varepsilon_g$, whereby the single-particle term at the right-hand side of eq. (4.5) gives no contribution and the pole at $\hbar\omega_s$ lies on the real energy axis. It can, therefore, be applied in the present form to determine binding energies of valence excitons. For core excitons, on the other hand, for which the core hole decays by Auger effect and the associated poles have finite imaginary widths, the procedure to obtain an effective eigenvalue equation requires a suitable generalization [56].

Equation (11.3) holds quite generally regardless of the specific form of the effective two-particle interaction $\Xi$ which embodies the dynamics of the bound electron-hole pair. Similarly to the calculation of the optical properties described in sect. 8, we take $\Xi$ of the form (cf. eqs. (4.4), (3.11), (3.12), and (8.44))

$$(11.4)\qquad \Xi(3, 4'; 3', 4) \simeq -i\hbar\delta(3, 3')\,\delta(4^+, 4')\, v(3, 4) + \\ + i\hbar\delta(3, 4)\,\delta(3', 4')\, W(3^+, 3');$$

we now keep, however, the full time dependence of the dynamically screened interaction $W$ without resorting to the static approximation (8.45). In this way, we can address studying the effects of dynamical screening on the excitonic binding energy $E_s^{\rm B}$ over and above the effective-mass limit in which $E_s^{\rm B}$ is much smaller than the energy gap $\varepsilon_g$ and $\Xi$ reduces to a Coulomb potential modified by the (static) macroscopic dielectric constant $\epsilon_0$ of the insulating medium [10].

We further represent the single-particle Green's functions entering eq. (11.3) by the quasi-particle approximation (8.48) that we known from sect. 9 to work well whenever the relevant single-particle excitations occur in the neighbourhood of the energy gap. We can then: i) project both sides of eq. (11.3) onto $u_c(\boldsymbol{x}_1)\, u_v^*(\boldsymbol{x}_{1'})$, where $c$ and $v$ stand for conduction- and valence-band quantum numbers, respectively, and make use of the assumed orthonormality of the single-particle wave functions; ii) take the limit as $\tau_1 = 0^-$ and drop the common factor $\exp[-i\omega_s t_1]$; iii) multiply both sides by $[\varepsilon_c - \varepsilon_v - \hbar\omega_s]$. The result is

$$(11.5)\qquad [\varepsilon_c-\varepsilon_v-\hbar\omega_s]\int \mathrm{d}\boldsymbol{x}_1\,\mathrm{d}\boldsymbol{x}_{1'}\,u_c^*(\boldsymbol{x}_1)\,u_v(\boldsymbol{x}_{1'})\,\chi_s^{\mathrm{ph}}(\boldsymbol{x}_1,\,\boldsymbol{x}_{1'};\,-\delta)=$$
$$=-\int \mathrm{d}\boldsymbol{x}_2\,\mathrm{d}\boldsymbol{x}_{2'}\,u_c^*(\boldsymbol{x}_2)\,u_v(\boldsymbol{x}_2)\,v(\boldsymbol{r}_2-\boldsymbol{r}_{2'})\,\chi_s^{\mathrm{ph}}(\boldsymbol{x}_{2'},\,\boldsymbol{x}_{2'};\,-\delta)+$$
$$+\int \mathrm{d}\boldsymbol{x}_2\,\mathrm{d}\boldsymbol{x}_{2'}\,u_c^*(\boldsymbol{x}_2)\,u_v(\boldsymbol{x}_{2'})\int_{-\infty}^{+\infty}\mathrm{d}\tau\,\exp[i\omega_s\tau/2]\,W(\boldsymbol{x}_2,\,\boldsymbol{x}_{2'};\,\tau^+)\,\cdot$$
$$\cdot[\theta(\tau)\exp[i\tau\varepsilon_v/\hbar]+\theta(-\tau)\exp[i\tau(\varepsilon_c-\hbar\omega_s)/\hbar]]\,\chi_s^{\mathrm{ph}}(\boldsymbol{x}_2,\,\boldsymbol{x}_{2'};\,\tau)\,.$$

For the states of interest to us we can insert into eq. (11.5) an approximate expression for the right-hand particle-hole amplitudes which is obtained from the definition (G.3*a*) by expanding the field operators in terms of the single-particle wave functions $u_k(\boldsymbol{x})$ introduced above and retaining the same approximation that has led to the energy denominators of eq. (8.48). We thus set

$$(11.6)\qquad \chi_s^{\mathrm{ph}}(\boldsymbol{x},\,\boldsymbol{x}';\,\tau)\simeq-\exp[i\omega_s|\tau|/2]\sum_{v'c'}u_{c'}(\boldsymbol{x})\,u_{v'}^*(\boldsymbol{x}')\,A_s(v',\,c')\,\cdot$$
$$\cdot[\theta(\tau)\exp[-i\varepsilon_{c'}\tau]+\theta(-\tau)\exp[-i\varepsilon_{v'}\tau]]\,,$$

where the expansion coefficients $A_s(v,\,c)$ can be expressed as transition matrix elements in terms of creation and destruction operators

$$(11.7)\qquad A_s(v,\,c)=\langle N|\hat{a}_v^\dagger\hat{a}_c|N,\,s\rangle\,.$$

The unknown excitation energies $\hbar\omega_s$ and the associated expansion coefficients $A_s(v,\,c)$ of eq. (11.6) are then determined as the eigenvalues and the associated eigenvectors of the eigenvalue problem (11.5). In fact, inserting eq. (11.6) into eq. (11.5) and performing the integration over $\tau$ yield

$$(11.8)\qquad [\varepsilon_c-\varepsilon_v-\hbar\omega_s]A_s(v,\,c)+\sum_{v'c'}A_s(v',\,c')\Bigg\{\langle c,\,v'|v|v,\,c'\rangle-$$
$$-i\int_{-\infty}^{+\infty}\frac{\mathrm{d}\hbar\omega}{2\pi}\exp[-i\omega\delta]\,\langle c,\,v'|W(\omega)|c',\,v\rangle\,\cdot$$
$$\cdot\left(\frac{1}{\hbar(\omega_s-\omega)-(\varepsilon_{c'}-\varepsilon_v)+i\delta}+\frac{1}{\hbar(\omega_s+\omega)-(\varepsilon_c-\varepsilon_{v'})+i\delta}\right)\Bigg\}=0$$

($\delta\to0^+$), where we have introduced the notation

$$(11.9a)\qquad \langle c,\,v'|v|v,\,c'\rangle=\int\mathrm{d}\boldsymbol{x}\,\mathrm{d}\boldsymbol{x}'\,u_c^*(\boldsymbol{x})\,u_{v'}^*(\boldsymbol{x}')\,v(\boldsymbol{r}-\boldsymbol{r}')\,u_v(\boldsymbol{x})\,u_{c'}(\boldsymbol{x}')\,,$$

$$(11.9b)\qquad \langle c,\,v'|W(\omega)|c',\,v\rangle=\int\mathrm{d}\boldsymbol{x}\,\mathrm{d}\boldsymbol{x}'\,u_c^*(\boldsymbol{x})\,u_{v'}^*(\boldsymbol{x}')\,W(\boldsymbol{x},\,\boldsymbol{x}';\,\omega)\,u_{c'}(\boldsymbol{x})\,u_v(\boldsymbol{x}')\,,$$

for the Coulomb matrix elements and their (dynamically screened) exchange counterparts (cf. also eq. (8.56)).

Equation (11.8) constitutes a self-consistent eigenvalue problem whereby the Hamiltonian matrix and its eigenvectors $A_s$ depend on the eigenvalue $\hbar\omega_s$, akin to the eigenvalue problem (9.2) for single-particle energy levels supplemented by the condition (9.6). Moreover, the Hamiltonian matrix in eq. (11.8) is Hermitian consistently with the assumption that the eigenvalue $\hbar\omega_s$ lies on the real energy axis below the threshold of the single-particle continuum.

Equation (11.8) should be read as follows. The first term describes an uncorrelated electron-hole pair for which the two-particle interaction is effectively switched off. Interaction effects are contained in the two terms within braces. The first term is independent of the screening properties of the medium and, being of short-range character, does not affect the excitonic binding energy when the excitonic radius is relatively large. This term is responsible for the longitudinal-transverse splitting of excitonic states and induces a mixing of different spin-orbit eigenstates, to be discussed below. The second term within braces in eq. (11.8) bounds the electron-hole pair since at large electron-hole distances it reduces to an attractive Coulomb potential screened by $\epsilon_0$. Dynamical screening effects occur at shorter distances. To show this, we recast this term in a more meaningful form by making use of the relation between the time-ordered (T) and retarded (R) density-density correlation functions (cf. sect. 5)

$$\mathrm{Re}\{\chi_{\mathrm{T}}(\boldsymbol{r}, \boldsymbol{r}'; \omega)\} = \mathrm{Re}\{\chi_{\mathrm{R}}(\boldsymbol{r}, \boldsymbol{r}'; \omega)\}, \tag{11.10a}$$

$$\mathrm{Im}\{\chi_{\mathrm{T}}(\boldsymbol{r}, \boldsymbol{r}'; \omega)\} = \mathrm{sgn}(\omega)\, \mathrm{Im}\{\chi_{\mathrm{R}}(\boldsymbol{r}, \boldsymbol{r}'; \omega)\} \tag{11.10b}$$

($\omega$ real), of the property

$$\mathrm{Im}\{\chi_{\mathrm{R}}(\boldsymbol{r}, \boldsymbol{r}'; -\omega)\} = -\,\mathrm{Im}\{\chi_{\mathrm{R}}(\boldsymbol{r}, \boldsymbol{r}'; \omega)\}, \tag{11.11}$$

and of the Kramers-Krönig relation

$$\mathrm{Re}\{\chi_{\mathrm{R}}(\boldsymbol{r}, \boldsymbol{r}'; \omega)\} = \frac{P}{\pi} \int_{-\infty}^{+\infty} \mathrm{d}\omega' \, \frac{\mathrm{Im}\{\chi_{\mathrm{R}}(\boldsymbol{r}, \boldsymbol{r}'; \omega')\}}{\omega' - \omega}, \tag{11.12}$$

where $P$ means that the principal part is to be taken in the integration of the singularity. We obtain

$$\begin{aligned} & i \int_{-\infty}^{+\infty} \frac{\mathrm{d}\hbar\omega}{2\pi} \exp[-i\omega\delta] \langle c, v'|W(\omega)|c', v\rangle \,\cdot \\ & \qquad \cdot \left( \frac{1}{\hbar(\omega_s - \omega) - (\varepsilon_{c'} - \varepsilon_v) + i\delta} + \frac{1}{\hbar(\omega_s + \omega) - (\varepsilon_c - \varepsilon_{v'}) + i\delta} \right) = \\ & = \int \mathrm{d}\boldsymbol{x}\, \mathrm{d}\boldsymbol{x}'\, u_c^*(\boldsymbol{x})\, u_{c'}(\boldsymbol{x}) \int \mathrm{d}\boldsymbol{r}''\, \epsilon^{-1}_{v'c, vc'}(\boldsymbol{r}, \boldsymbol{r}''; \omega_s)\, v(\boldsymbol{r}'' - \boldsymbol{r}')\, u_v(\boldsymbol{x}')\, u_{v'}^*(\boldsymbol{x}'), \end{aligned} \tag{11.13}$$

where we have introduced the *effective inverse dielectric matrix*

$$\text{(11.14)} \qquad \epsilon^{-1}_{v'c,vc'}(\boldsymbol{r}, \boldsymbol{r}'; \omega_s) = \delta(\boldsymbol{r}-\boldsymbol{r}') + \int \mathrm{d}\boldsymbol{r}''\, v(\boldsymbol{r}-\boldsymbol{r}'') \int_0^\infty \frac{\mathrm{d}\hbar\omega}{\pi} \cdot$$

$$\cdot (-1)\, \mathrm{Im}\,\{\chi_{\mathrm{R}}(\boldsymbol{r}'', \boldsymbol{r}'; \omega)\} \left( \frac{1}{\hbar(\omega_s-\omega)-(\varepsilon_{c'}-\varepsilon_v)+i\delta} + \frac{1}{\hbar(\omega_s-\omega)-(\varepsilon_c-\varepsilon_{v'})+i\delta} \right) .$$

The diagonal ($c = c'$ and $v = v'$) elements of expression (11.14) can be interpreted as describing the density response of the system with a hole in the state $v$ probed by an electron excited into a conduction-band state $c$. Equation (11.14) has to be contrasted with the ordinary inverse dielectric matrix of linear response theory, namely,

$$\text{(11.15)} \qquad \epsilon^{-1}_{\mathrm{R}}(\boldsymbol{r}, \boldsymbol{r}'; \omega) = \delta(\boldsymbol{r}-\boldsymbol{r}') + \int \mathrm{d}\boldsymbol{r}''\, v(\boldsymbol{r}-\boldsymbol{r}'') \int_0^\infty \frac{\mathrm{d}\omega'}{\pi} \cdot$$

$$\cdot (-1)\, \mathrm{Im}\,\{\chi_{\mathrm{R}}(\boldsymbol{r}'', \boldsymbol{r}'; \omega')\} \left( \frac{1}{\omega-\omega'+i\delta} + \frac{1}{\omega+\omega'+i\delta} \right),$$

whereby an external (test) charge probes the density response of the system in the ground state. The effective and the ordinary dielectric matrices coincide, however, in the *static limit* when the differences $\hbar\omega_s - (\varepsilon_{c'} - \varepsilon_v)$ and $\hbar\omega_s - (\varepsilon_c - \varepsilon_{v'})$ can be neglected in comparison with the characteristic energies in the loss matrix $-\mathrm{Im}\,\{\chi_{\mathrm{R}}(\boldsymbol{r}, \boldsymbol{r}'; \omega)\}$, which are at least of the order of the energy gap $\varepsilon_{\mathrm{g}}$. In other words, whenever $E^{\mathrm{B}} \ll \varepsilon_{\mathrm{g}}$ the effective potential at the right-hand side of eq. (11.13) reduces to a statically screened Coulomb potential with asymptotic form $e^2|\boldsymbol{r}-\boldsymbol{r}'|^{-1}\,\epsilon_0^{-1}$ for large values of $|\boldsymbol{r}-\boldsymbol{r}'|$. Deviations from static screening need otherwise to be considered.

Numerical solution to the effective eigenvalue equation (11.8) could be tackled by converting it into a local-orbital representation along the approach described in subsect. 8.4. This procedure, which is appropriate to intermediate binding [57], is sketched in the appendix of ref. [56]. Here we restrict ourselves to considering the leading corrections to the effective-mass limit of eq. (11.8), whereby one follows the steps yielding the usual effective-mass equation for excitons [55], but retains the full effective inverse dielectric function and not just its static limit.

For a crystalline semiconductor, a Bloch wave vector $\boldsymbol{Q}$ can be associated with the many-particle state $|N, s\rangle$ of eq. (11.7), wherein the single-particle labels $v$ and $c$ stand for the triad of a band index $n$, a Bloch wave vector $\boldsymbol{k}$, and a spin index $\sigma$. Translational symmetry also requires $\boldsymbol{k}_c = \boldsymbol{k}_v + \boldsymbol{Q}$ in eq. (11.7) (up to equivalence in reciprocal space) and identifies $\boldsymbol{Q}$ as a good quantum number for the eigenvectors of eq. (11.8). In the following, we shall adopt for simplicity the model of a semiconductor with simple (*i.e.*, nondegenerate) valence and conductor bands. Consistently with the effective-mass limit, we assume

$A_s(\sigma_v,\ \sigma_c;\ \boldsymbol{k}_v,\ \boldsymbol{Q})$ to be sharply peaked about a particular value of $\boldsymbol{k}_v$ (say $\boldsymbol{k}_0$) that coincides with an extremum (maximum) of the simple band $\varepsilon_v(\boldsymbol{k}_v)$. By the same token, $\boldsymbol{k}_v + \boldsymbol{Q}$ is confined to a small neighbourhood of an extremum (minimum) of $\varepsilon_c(\boldsymbol{k}_c)$ which we take at vanishing $\boldsymbol{Q}$ for the excitonic state to be excited by an electromagnetic field.

The eigenvalue equation (11.8) can now be transformed into a differential equation by multiplying both sides by $(2\pi)^{-3}\exp[i\boldsymbol{k}_v\cdot\boldsymbol{r}]$ and integrating over the whole $\boldsymbol{k}_v$-space, and by expanding the single-particle band eigenvalues about the relevant extrema up to quadratic order. One obtains

$$
\begin{aligned}
(11.16)\qquad & -\frac{\hbar^2}{2}\left(\frac{1}{m_v^*}+\frac{1}{m_c^*}\right)\boldsymbol{\nabla}^2 F_s(\sigma_v,\ \sigma_c;\ \boldsymbol{r}) + \\
& + \sum_{\sigma_{v'}\sigma_{c'}} \int \frac{\mathrm{d}\boldsymbol{k}_v}{(2\pi)^3}\exp[i(\boldsymbol{k}_v-\boldsymbol{k}_0)\cdot\boldsymbol{r}] \int \frac{\mathrm{d}\boldsymbol{k}_{v'}}{(2\pi)^3} A_s(\sigma_{v'},\ \sigma_{c'};\ \boldsymbol{k}_{v'})\,\mathcal{N}^2\Omega_0\,\cdot \\
& \cdot\Bigg\{\lim_{\boldsymbol{Q}\to 0}\langle\sigma_c\boldsymbol{k}_v+\boldsymbol{Q},\ \sigma_{v'}\boldsymbol{k}_{v'}|v|\sigma_v\boldsymbol{k}_v,\ \sigma_{c'}\boldsymbol{k}_{v'}+\boldsymbol{Q}\rangle + \\
& + i\int_{-\infty}^{+\infty}\frac{\mathrm{d}\hbar\omega}{2\pi}\exp[-i\omega\delta]\,\langle\sigma_c\boldsymbol{k}_v,\ \sigma_{v'}\boldsymbol{k}_{v'}|W(\omega)|\sigma_{c'}\boldsymbol{k}_{v'},\ \sigma_v\boldsymbol{k}_v\rangle\,\cdot \\
& \cdot\left(\frac{1}{E_s^{\mathrm{B}}+\dfrac{\hbar^2}{2m_c^*}(\boldsymbol{k}_{v'}-\boldsymbol{k}_0)^2+\dfrac{\hbar^2}{2m_v^*}(\boldsymbol{k}_v-\boldsymbol{k}_0)^2+\hbar\omega-i\delta}+\right. \\
& \left.+\frac{1}{E_s^{\mathrm{B}}+\dfrac{\hbar^2}{2m_c^*}(\boldsymbol{k}_v-\boldsymbol{k}_0)^2+\dfrac{\hbar^2}{2m_v^*}(\boldsymbol{k}_{v'}-\boldsymbol{k}_0)-\hbar\omega-i\delta}\right)\Bigg\} = \\
& \qquad\qquad = -E_s^{\mathrm{B}}F_s(\sigma_v,\ \sigma_c;\ \boldsymbol{r}),
\end{aligned}
$$

where $m_v^*$ and $m_c^*$ are the effective masses associated with the (isotropic) valence band maximum and conduction band minimum, respectively,

$$
(11.17)\qquad E_s^{\mathrm{B}} = \varepsilon_c(\boldsymbol{k}_0) - \varepsilon_v(\boldsymbol{k}_0) - \hbar\omega_s
$$

is the excitonic binding energy referred to the relevant single-particle energy gap, and

$$
(11.18)\qquad F_s(\sigma_v,\ \sigma_c;\ \boldsymbol{r}) = \int\frac{\mathrm{d}\boldsymbol{k}_v}{(2\pi)^3}\exp[i(\boldsymbol{k}_v-\boldsymbol{k}_0)\cdot\boldsymbol{r}]A_s(\sigma_v,\ \sigma_c;\ \boldsymbol{k}_v)
$$

is the envelope function. Notice that the limit $\boldsymbol{Q}\to 0$ has been explicitly indicated for the Coulomb matrix elements in eq. (11.16), since they behave pathologically in the neighbourhood of $\boldsymbol{Q}=0$. To extract this behaviour, the Bloch functions entering the Coulomb matrix elements can be represented in terms of Wannier functions (cf. eq. (8.51) where a single local orbital is now associated with each simple band), yielding

$$\langle \sigma_c \boldsymbol{k}_v + \boldsymbol{Q},\ \sigma_{v'} \boldsymbol{k}_{v'} | v | \sigma_v \boldsymbol{k}_v,\ \sigma_{c'} \boldsymbol{k}_{v'} + \boldsymbol{Q} \rangle \simeq \delta_{\sigma_v \sigma_c} \delta_{\sigma_{v'} \sigma_{c'}} \mathcal{N}^{-1} J_{vc}(\boldsymbol{Q}), \tag{11.19a}$$

$$J_{vc}(\boldsymbol{Q}) = \sum_{l} \exp[i\boldsymbol{Q} \cdot \boldsymbol{l}] \int \mathrm{d}\boldsymbol{r}\, \mathrm{d}\boldsymbol{r}'\, \phi_v(\boldsymbol{r})\, \phi_c^*(\boldsymbol{r})\, v(\boldsymbol{r} - \boldsymbol{r}')\, \phi_v^*(\boldsymbol{r}' - \boldsymbol{l})\, \phi_c(\boldsymbol{r}' - \boldsymbol{l}), \tag{11.19b}$$

where only dipole-like excitations on the same lattice site have been retained. Assuming further that dipole like excitations at $\boldsymbol{l} \neq 0$ do not overlap with the one in the central cell ($\boldsymbol{l} = 0$), we can expand the Coulomb integrals in eq. (11.19*b*) into multipoles and retain only the leading dipole-dipole interaction terms:

$$J_{vc}(\boldsymbol{Q}) \simeq \int \mathrm{d}\boldsymbol{r}\, \mathrm{d}\boldsymbol{r}'\, \phi_v(\boldsymbol{r})\, \phi_c^*(\boldsymbol{r})\, v(\boldsymbol{r} - \boldsymbol{r}')\, \phi_v^*(\boldsymbol{r}')\, \phi_c(\boldsymbol{r}') + \\ + \sum_{\boldsymbol{l} \neq 0} \exp[i\boldsymbol{Q} \cdot \boldsymbol{l}] \frac{[\boldsymbol{d}_{vc}^* \cdot \boldsymbol{d}_{vc} - 3(\hat{\boldsymbol{l}} \cdot \boldsymbol{d}_{vc}^*)(\hat{\boldsymbol{l}} \cdot \boldsymbol{d}_{vc})]}{|\boldsymbol{l}|^3}, \tag{11.20}$$

where we have introduced the dipole moment of the excitation $v \rightarrow c$

$$\boldsymbol{d}_{vc} = e \int \mathrm{d}\boldsymbol{r}\, \phi_v^*(\boldsymbol{r})\, \boldsymbol{r}\, \phi_c(\boldsymbol{r}). \tag{11.21}$$

For a cubic material in the small $\boldsymbol{Q}$ limit the dipolar sum in eq. (11.20) acquires the form [58]

$$\sum_{\boldsymbol{l} \neq 0} \exp[i\boldsymbol{Q} \cdot \boldsymbol{l}] \frac{[\boldsymbol{d}_{vc}^* \cdot \boldsymbol{d}_{vc} - 3(\hat{\boldsymbol{l}} \cdot \boldsymbol{d}_{vc}^*)(\hat{\boldsymbol{l}} \cdot \boldsymbol{d}_{vc})]}{|\boldsymbol{l}|^3} = \\ = \frac{4\pi}{3\Omega_0} \left[ \frac{3(\boldsymbol{Q} \cdot \boldsymbol{d}_{vc}^*)(\boldsymbol{Q} \cdot \boldsymbol{d}_{vc})}{Q^2} - \boldsymbol{d}_{vc}^* \cdot \boldsymbol{d}_{vc} \right], \tag{11.22}$$

which is a piecewice continuous at $\boldsymbol{Q} = 0$ and has a rapid angular variation about this point.

Within the above approximations, the second term at the left-hand side of eq. (11.16) becomes

$$\sum_{\sigma_{v'} \sigma_{c'}} \int \frac{\mathrm{d}\boldsymbol{k}_v}{(2\pi)^3} \exp[i(\boldsymbol{k}_v - \boldsymbol{k}_0) \cdot \boldsymbol{r}] \int \frac{\mathrm{d}\boldsymbol{k}_{v'}}{(2\pi)^3} A_s(\sigma_{v'}, \sigma_{c'}; \boldsymbol{k}_{v'})\, \mathcal{N} \Omega_0 \cdot \\ \cdot \lim_{\boldsymbol{Q} \to 0} \langle \sigma_c \boldsymbol{k}_v + \boldsymbol{Q},\ \sigma_{v'} \boldsymbol{k}_{v'} | v | \sigma_v \boldsymbol{k}_v,\ \sigma_{c'} \boldsymbol{k}_{v'} + \boldsymbol{Q} \rangle \simeq \\ \simeq \delta(\boldsymbol{r})\, \Omega_0 \lim_{\boldsymbol{Q} \to 0} J_{vc}(\boldsymbol{Q})\, \delta_{\sigma_v \sigma_c} \sum_{\sigma_{v'} \sigma_{c'}} F_s(\sigma_{v'}, \sigma_{c'}; \boldsymbol{r})\, \delta_{\sigma_{v'} \sigma_{c'}}. \tag{11.23}$$

This term, being of short-range character, does not affect the excitonic binding energy when the excitonic radius is relatively large. This term, however, is responsible for the longitudinal-transverse splitting of the excitonic states, since eq. (11.22) has different values when $\boldsymbol{d}_{vc}$ is parallel or orthogonal to $\boldsymbol{Q}$ [59], and it induces a mixing of different spin-orbit eigenstates that leads to an inversion of the 2:1 intensity ratio [60].

The dynamically screened exchange matrix elements (11.9*b*) that enter the last term at the left-hand side of eq. (11.16) may instead be approximated by neglecting both the variation of the periodic part of the Bloch functions about the extrema and the local field effects. One obtains

$$\langle \sigma_c \boldsymbol{k}_v,\ \sigma_{v'} \boldsymbol{k}_{v'} | W(\omega) | \sigma_{c'} \boldsymbol{k}_{v'},\ \sigma_v \boldsymbol{k}_v \rangle \simeq \delta_{\sigma_c \sigma_{c'}} \delta_{\sigma_v \sigma_{v'}} \frac{1}{\Omega} W(\boldsymbol{k}_v - \boldsymbol{k}_{v'};\ \omega)\,, \tag{11.24}$$

where

$$W(\boldsymbol{q};\ \omega) = v(\boldsymbol{q})\, \epsilon_{\mathrm{T}}^{-1}(\boldsymbol{q};\ \omega) \tag{11.25}$$

is the Fourier transform of the dynamically screened interaction obtained by neglecting off-diagonal screening. Alternative procedures may be followed at this point to evaluate the integrals over wavevector and frequency in the last term at the left-hand side of eq. (11.16), yielding, *e.g.*, the Haken potential (cf. appendix H) or the asymptotic dynamically screened Coulomb potential. To obtain the latter, we neglect the dispersion of the single-particle energy levels in the energy denominators and make use of a simplified form of eqs. (11.13) and (11.14). The last term at the left-hand side of eq. (11.16) then becomes

$$\begin{aligned} &\sum_{\sigma_{v'} \sigma_{c'}} \int \frac{\mathrm{d}\boldsymbol{k}_v}{(2\pi)^3} \exp[i(\boldsymbol{k}_v - \boldsymbol{k}_0) \cdot \boldsymbol{r}] \int \frac{\mathrm{d}\boldsymbol{k}_{v'}}{(2\pi)^3} A_s(\sigma_{v'},\ \sigma_{c'};\ \boldsymbol{k}_{v'}) \sqrt{\Omega_0}\, \cdot \\ &\qquad \cdot i \int_{-\infty}^{+\infty} \frac{\mathrm{d}\hbar\omega}{2\pi} \exp[-i\omega\delta] \langle \sigma_c \boldsymbol{k}_v,\ \sigma_{v'} \boldsymbol{k}_{v'} | W(\omega) | \sigma_{c'} \boldsymbol{k}_{v'},\ \sigma_v \boldsymbol{k}_v \rangle\, \cdot \\ &\qquad \cdot \left( \frac{1}{E_s^{\mathrm{B}} + \frac{\hbar^2}{2m_c^*} (\boldsymbol{k}_{v'} - \boldsymbol{k}_0)^2 + \frac{\hbar^2}{2m_v^*} (\boldsymbol{k}_v - \boldsymbol{k}_0) + \hbar\omega - i\delta} + \right. \\ &\qquad \left. + \frac{1}{E_s^{\mathrm{B}} + \frac{\hbar^2}{2m_c^*} (\boldsymbol{k}_v - \boldsymbol{k}_0)^2 + \frac{\hbar^2}{2m_v^*} (\boldsymbol{k}_{v'} - \boldsymbol{k}_0)^2 - \hbar\omega - i\delta} \right) \simeq \\ &\qquad \simeq \left[ - \int \frac{\mathrm{d}\boldsymbol{q}}{(2\pi)^3} \exp[i\boldsymbol{q} \cdot \boldsymbol{r}]\, v(\boldsymbol{q})\, \tilde{\epsilon}^{-1}(\boldsymbol{q};\ E_s^{\mathrm{B}}) \right] F_s(\sigma_v,\ \sigma_c;\ \boldsymbol{r})\,, \end{aligned} \tag{11.26}$$

where we have introduced the wave vector dependent effective inverse dielectric function

$$\tilde{\epsilon}^{-1}(\boldsymbol{q}; E_s^{\mathrm{B}}) = 1 - \frac{2}{\pi}\int_0^\infty \mathrm{d}\hbar\omega\, \frac{(-1)\,\mathrm{Im}\,\{\epsilon_{\mathrm{R}}^{-1}(\boldsymbol{q};\omega)\}}{\hbar\omega + E_s^{\mathrm{B}}}. \tag{11.27}$$

Dynamical effects thus modify the statically screened electron-hole attractive interaction, which is usually considered in the effective mass limit for excitons [55], by replacing it with the more attractive interaction within brackets at the right-hand side of eq. (11.26). Notice that the static limit can be recovered by setting $E_s^{\mathrm{B}} = 0$ in eq. (11.27). A plot of $\tilde{\epsilon}_0(E_s^{\mathrm{B}}) \equiv [\tilde{\epsilon}^{-1}(\boldsymbol{q}=0;\ E_s^{\mathrm{B}})]^{-1}$ is shown in fig. 11 for the loss function $-\mathrm{Im}\,\{\epsilon_{\mathrm{R}}^{-1}(\boldsymbol{q};\omega)\}$ corresponding to silicon.

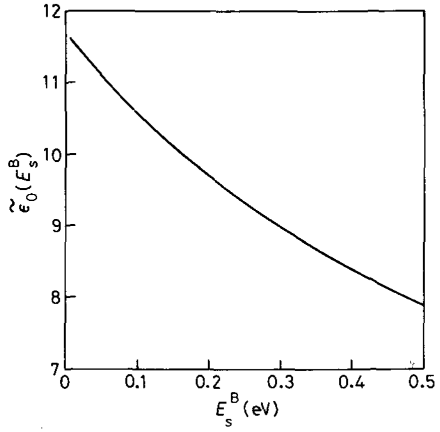

Fig. 11. – Effective dielectric function (silicon) for vanishing momentum transfer versus the excitonic binding energy $E_s^{\mathrm{B}}$ (adapted from ref. [56]).

Inserting the results (11.23) and (11.26) into eq. (11.16), we obtain eventually the desired differential equation for the envelope function

$$\begin{aligned} -\frac{\hbar^2}{2}\left(\frac{1}{m_v^*}+\frac{1}{m_c^*}\right)\nabla^2 F_s(\sigma_v,\sigma_c;\boldsymbol{r}) &+ \\ + \delta(\boldsymbol{r})\,\Omega_0 \lim_{\boldsymbol{Q}\to 0} J_{vc}(\boldsymbol{Q})\,\delta_{\sigma_v\sigma_c} &\sum_{\sigma_{v'}\sigma_{c'}} F_s(\sigma_{v'},\sigma_{c'};\boldsymbol{r})\,\delta_{\sigma_{v'}\sigma_{c'}} - \\ - \int \frac{\mathrm{d}\boldsymbol{q}}{(2\pi)^3} \exp[i\boldsymbol{q}\cdot\boldsymbol{r}]\,v(\boldsymbol{q})\,\tilde{\epsilon}^{-1}(\boldsymbol{q};E_s^{\mathrm{B}})\,F_s(\sigma_v,\sigma_c;\boldsymbol{r}) &= -E_s^{\mathrm{B}} F_s(\sigma_v,\sigma_c;\boldsymbol{r}). \end{aligned} \tag{11.28}$$

The spin structure of eq. (11.28) can be organized into a singlet solution, for which $F_s(\uparrow, \uparrow; \boldsymbol{r}) = F_s(\downarrow, \downarrow; \boldsymbol{r})$, and a triplet solution, for which $F_s(\uparrow, \uparrow; \boldsymbol{r}) = -F_s(\downarrow, \downarrow; \boldsymbol{r})$. In accordance with the results of appendix $D$, only the singlet solution is affected by the longitudinal-transverse splitting. (In particular, only the singlet transverse excitonic state can be excited optically.)

Numerical solution to eq. (11.28) shows that the inclusion of dynamical screening effects within the effective mass limit leads to a negligible increase of the binding energy over the corresponding static value. However, in the case of core excitons a suitable modification of eq. (11.28) to include band structure effects (such as intervalley mixing and centrall-cell corrections) in an effective manner by modifying the screened Coulomb potential at short electron-hole separation, leads typically to a (20 ÷ 30)% increase of the binding energy due to dynamical screening effects over and above static screening [56]. Moreover, deviations from static screening lead also to a narrowing of the Auger width when passing from the core hole to the core exciton [56], an effect which is a fingerprint of dynamical screening, since it cannot be obtained within the framework of a static theory.

* * *

The author is indebted to Prof. F. BASSANI for his continuous interest and support during the course of this work. Helpful discussions with C. CASTELLANI, R. DEL SOLE, L. PELITI, and G. WENDIN are gratefully acknowledged. The author is also indebted to C. ROMERO for the precious typing and help in preparing the manuscript.

## APPENDIX A

### A functional derivative identity.

Let $F[\Psi(x)]$ be a functional and let $\delta F[\Psi(x)]$ be its first variation when a small change $\delta\Psi(x)$ is made in the argument function $\Psi(x)$. The functional derivative $\delta F/\delta\Psi(x)$ is then defined as that function of $x$ for which

$$\delta F[\Psi(x)] = F[\Psi(x) + \delta\Psi(x)] - F[\Psi(x)] = \int \mathrm{d}y \frac{\delta F}{\delta\Psi(y)} \delta\Psi(y) , \tag{A.1}$$

to first order in $\delta\Psi$. This definition can be considered as a generalization of the ordinary (partial) derivatives of a function $F(\{x_i\})$ whereby the variables $\{x_i\}$ $(i = 1, \ldots, N)$ are specified at $N$ points of a lattice:

$$F(\{x_i + \delta x_i\}) - F(\{x_i\}) = \sum_{i=1}^{N} \frac{\delta F}{\delta x_i} \delta x_i . \tag{A.2}$$

This remark implies that the usual rules for differentiation can also be derived for functional derivatives. We consider some examples.

$$\text{(A.3)}\qquad \text{i)}\ \frac{\delta\Psi(x)}{\delta\Psi(y)} = \delta(x-y)\,.$$

$$\text{(A.4)}\qquad \text{ii)}\ \frac{\delta}{\delta\Psi(y)}F[\Psi(x)]\,G[\Psi(x)] = \frac{\delta F[\Psi(x)]}{\delta\Psi(y)}G[\Psi(x)] + F[\Psi(x)]\frac{\delta G[\Psi(x)]}{\delta\Psi(y)}\,.$$

$$\text{(A.5)}\qquad \text{iii)}\ \frac{\delta}{\delta\Psi(y)]}\frac{F[\Psi(x)]}{G[\Psi(x)]} = \frac{1}{G[\Psi(x)]^2}\left[\frac{\delta F[\Psi(x)]}{\delta\Psi(y)}G[\Psi(x)] - F[\Psi(x)]\frac{\delta G[\Psi(x)]}{\delta\Psi(y)}\right].$$

iv) Let $F[\Psi(\xi);\,x,\,y]$ be the inverse of $G[\Psi(\xi);\,x,\,y]$ in the sense that the following identity is satisfied:

$$\text{(A.6)}\qquad \int \mathrm{d}z F[\Psi(\xi);\,x,\,z]\,G[\Psi(\xi);\,z,\,y] = \delta(x-y)$$

for any $\Psi(\xi)$. Then

$$\text{(A.7)}\qquad \frac{\delta F[\Psi(\zeta);\,x,\,y]}{\delta\Psi(z)} = -\int \mathrm{d}\xi\,\mathrm{d}\eta\,F[\Psi(\zeta);\,x,\,\xi]\frac{\delta G[\Psi(\zeta);\,\xi,\,\eta]}{\delta\Psi(z)}F[\Psi(\zeta);\,\eta,\,y]\,.$$

v) Let $F[G[\Psi(x);\,y]]$. Then

$$\text{(A.8)}\qquad \frac{\delta F}{\delta\Psi(x)} = \int \mathrm{d}y\frac{\delta F}{\delta G(y)}\frac{\delta G(y)}{\delta\Psi(x)}\,,$$

which is referred to as the «chain rule».

We are now in a position to derive eq. (3.9) of the text. To this end, we recall that all the $U$-dependence in the generalized single-particle Green's function (2.9) is explicit in the $\hat{S}$ factor. Varying the potential $U$ by a small amount $\delta U$ and keeping only first-order terms then yields (cf. eq. (A.5)):

$$\text{(A.9)}\qquad \delta G_1(1,\,2) = -\frac{i}{\hbar}\frac{\langle N|T[\delta\hat{S}\hat{\Psi}(1)\,\hat{\Psi}^{\dagger}(2)]|N\rangle}{\langle N|T[\hat{S}]|N\rangle} - G_1(1,\,2)\frac{\langle N|T[\delta\hat{S}]|N\rangle}{\langle N|T[\hat{S}]|N\rangle}\,.$$

Since $\delta\hat{S}$ appears only within a time-ordered product wherein boson like operators, such as $\hat{\Psi}^{\dagger}(\mathbf{x},\,t^{+})\,\hat{\Psi}(\mathbf{x}',\,t)$, can be treated as though they commute, we can evaluate $\delta\hat{S}$ as follows:

$$\text{(A.10)}\qquad \delta\hat{S} = -\frac{i}{\hbar}\int_{-\infty}^{+\infty}\mathrm{d}t\int \mathrm{d}\mathbf{x}\mathrm{d}\mathbf{x}'\,\hat{\Psi}^{\dagger}(\mathbf{x},\,t^{+})\,\delta U(\mathbf{x},\,\mathbf{x}';\,t)\,\hat{\Psi}(\mathbf{x}',\,t)\,.$$

Entering eq. (A.10) into eq. (A.9) and recalling the definition (2.10) of the generalized two-particle Green's function result into

$$\text{(A.11)}\qquad \delta G_1(1,2)=\int_{-\infty}^{+\infty}\mathrm{d}t\int \mathrm{d}\boldsymbol{x}\,\mathrm{d}\boldsymbol{x}'\,\delta U(\boldsymbol{x},\boldsymbol{x}';t)\,[-G_2(1,\boldsymbol{x}'t;2,\boldsymbol{x}t^+)+ \\ +G_1(1,2)\,G_1(\boldsymbol{x}'t,\boldsymbol{x}t^+)]\,.$$

Comparison with eq. (A.1) eventually identifies the expression within brackets in eq. (A.11) with the functional derivative of $G_1(1, 2)$ with respect to $U(\boldsymbol{x}, \boldsymbol{x}'; t)$, namely,

$$\text{(A.12)}\qquad \frac{\delta G_1(1,2)}{\delta U(\boldsymbol{x},\boldsymbol{x}';t)}=-G_2(1,\boldsymbol{x}'t;2,\boldsymbol{x}t^+)+G_1(1,2)\,G_1(\boldsymbol{x}'t,\boldsymbol{x}t^+)\,.$$

For a local potential of the type (2.5) we can write instead

$$\text{(A.13)}\qquad \frac{\delta G_1(1,2)}{\delta U(3)}=-G_2(1,3;2,3^+)+G_1(1,2)\,G_1(3,3^+)\,.$$

The generalized single-particle Green's function can thus be considered as a generating functional for higher-order Green's functions, while the external potential $U$ acts as a source.

## APPENDIX B

### Dyson's equation.

In the absence of both the interaction among the electrons ($v$) and the external potential ($U$), the (zeroth-order) single-particle Green's function $G_1^{(0)}$ satisfies the equation

$$\text{(B.1)}\qquad \left[i\hbar\frac{\partial}{\partial t_1}-h(1)\right]G_1^{(0)}(1,2)=\left[-i\hbar\frac{\partial}{\partial t_2}-h(2)\right]G_1^{(0)}(1,2)=\delta(1,2)\,,$$

whereby the corresponding inverse Green's function is given by

$$\text{(B.2)}\qquad G_1^{(0)-1}(1,2)=\left[i\hbar\frac{\partial}{\partial t_1}-h(1)\right]\delta(1,2)=\left[-i\hbar\frac{\partial}{\partial t_2}-h(2)\right]\delta(1,2)\,.$$

The introduction of $G_1^{(0)-1}$ allows us to express eqs. (3.14) of the text as follows:

$$\text{(B.3}a\text{)}\qquad \int \mathrm{d}3\,[G_1^{(0)-1}(1,3)-U(1)\,\delta(1,3)-\Sigma(1,3)]\,G_1(3,2)=\delta(1,2)\,,$$

$$\text{(B.3}b\text{)}\qquad \int \mathrm{d}3\,G_1(1,3)[G_1^{(0)-1}(3,2)-U(2)\,\delta(3,2)-\overline{\Sigma}(3,2)]=\delta(1,2)\,.$$

Equations (B.3*a*) and (B.3*b*) identify the expressions within brackets as the left and right inverse of $G_1$, respectively. Demanding these two inverses to coincide leads thus to the identification

$$G_1^{-1}(1, 2) = G_1^{(0)-1}(1, 2) - U(1)\,\delta(1, 2) - \Sigma(1, 2) \tag{B.4}$$

and

$$\Sigma(1, 2) = \bar{\Sigma}(1, 2)\,. \tag{B.5}$$

The integral form of Dyson's equation (3.14) can readily be obtained by multiplying eq. (B.4) from the left by $G_1^{(0)}(3, 1)$ and from the right by $G_1(2, 4)$, and integrating over 1 and 2. The result acquires the familiar form

$$G_1(1, 2) = G_1^{(0)}(1, 2) + \int \mathrm{d}34\, G_1^{(0)}(1, 3)\,[U(3)\,\delta(3, 4) + \Sigma(3, 4)]\,G_1(4, 2)\,. \tag{B.6}$$

## APPENDIX C

### Reducible *vs.* irreducible parts of the correlation functions.

*a) Scalar and vector vertex functions.* Generalized Green's functions of the form (2.9) and (2.10) can also be defined when the interaction Hamiltonian (2.4) is replaced by, *e.g.*, the interaction Hamiltonian between a system of charged particles and the electromagnetic field:

$$\hat{H}'(t) = q\int \mathrm{d}\boldsymbol{x}\,\varphi(\boldsymbol{r}, t)\,\hat{\rho}(\boldsymbol{x}) - \frac{q}{c}\int \mathrm{d}\boldsymbol{x}\,\boldsymbol{A}(\boldsymbol{r}, t)\cdot\hat{\boldsymbol{j}}(\boldsymbol{x}) + \frac{q^2}{2mc^2}\int \mathrm{d}\boldsymbol{x}\,\boldsymbol{A}^2(\boldsymbol{r}, t)\,\hat{\rho}(\boldsymbol{x})\,. \tag{C.1}$$

Here $\varphi(\boldsymbol{r}, t)$ and $\boldsymbol{A}(\boldsymbol{r}, t)$ are the scalar and vector potentials of the electromagnetic field, respectively, $q$ is the charge of a particle in the system, and $\hat{\rho}(\boldsymbol{x})$ and $\hat{\boldsymbol{j}}(\boldsymbol{x})$ are the density and current operators

$$\hat{\rho}(\boldsymbol{x}) = \hat{\Psi}^{+}(\boldsymbol{x})\,\hat{\Psi}(\boldsymbol{x})\,, \tag{C.2}$$

$$\hat{\boldsymbol{j}}(\boldsymbol{x}) = \frac{\hbar}{2im}\,[\hat{\Psi}^{+}(\boldsymbol{x})\,\boldsymbol{\nabla}\hat{\Psi}(\boldsymbol{x}) - (\boldsymbol{\nabla}\hat{\Psi}^{+}(\boldsymbol{x}))\,\hat{\Psi}(\boldsymbol{x})]\,. \tag{C.3}$$

In what follows we shall omit the diamagnetic term of eq. (C.1) since its contribution vanishes in the limit $\boldsymbol{A}\to 0$ which will eventually be taken.

Following the procedure outlined in appendix A one can readily show that

$$\frac{\delta G_1(1, 2)}{\delta(q\varphi(3))} = L(1, 3; 2, 3^+)\,, \tag{C.4}$$

$$\frac{\delta G_1(1, 2)}{\delta\left(-\dfrac{q}{c}\boldsymbol{A}(3)\right)} = \frac{\hbar}{2im}\,[(\boldsymbol{\nabla}_3 - \boldsymbol{\nabla}_{3'})\,L(1, 3; 2, 3')]_{3'=3^+}\,. \tag{C.5}$$

It is convenient at this point to introduce the (reducible) scalar and vector vertex functions according to the definitions

$$\Gamma(1,\,2;\,3) \equiv -\frac{\delta G_1^{-1}(1,\,2)}{\delta(q\varphi(3))}, \tag{C.6}$$

$$\boldsymbol{\Gamma}(1,\,2;\,3) \equiv -\frac{\delta G_1^{-1}(1,\,2)}{\delta\left(-\dfrac{q}{c}\boldsymbol{A}(3)\right)}. \tag{C.7}$$

These functions can be related to the two-particle correlation function $L(1,\,3;\,2,\,3')$ by eqs. (C.4) and (C.5) and rule iv) of appendix A, to obtain

$$L(1,\,3;\,2,\,3^+) = \int \mathrm{d}45\, G_1(1,\,4)\, G_1(5,\,2)\, \Gamma(4,\,5;\,3)\,, \tag{C.8}$$

$$\frac{\hbar}{2im}[(\boldsymbol{\nabla}_3 - \boldsymbol{\nabla}_{3'})L(1,\,3;\,2,\,3')]_{3'=3^+} = \int \mathrm{d}45\, G_1(1,\,4)\, G_1(5,\,2)\, \boldsymbol{\Gamma}(4,\,5;\,3)\,. \tag{C.9}$$

Equations (C.8) and (C.9) could alternatively be considered as definitions for $\Gamma$ and $\boldsymbol{\Gamma}$ [16].

The integral equations satisfied by $\Gamma$ and $\boldsymbol{\Gamma}$ can be obtained by combining eqs. (C.8) and (C.9) with the Bethe-Salpeter equation (4.5) for $L$. The result is

$$\Gamma(1,\,2;\,3) = \delta(1,\,3)\,\delta(2,\,3) + \int \mathrm{d}4567 \frac{\delta\Sigma(1,\,2)}{\delta G_1(4,\,5)} G_1(4,\,6)\, G_1(7,\,5)\, \Gamma(6,\,7;\,3) \tag{C.10}$$

and

$$\boldsymbol{\Gamma}(1,\,2;\,3) = \frac{\hbar}{2im}[(\boldsymbol{\nabla}_3 - \boldsymbol{\nabla}_{3'})\,\delta(1,\,3')\,\delta(2,\,3)]_{3'=3} + \int \mathrm{d}4567 \frac{\delta\Sigma(1,\,2)}{\delta G_1(4,\,5)} G_1(4,\,6)\, G_1(7,\,5)\, \boldsymbol{\Gamma}(6,\,7;\,3)\,. \tag{C.11}$$

Equation (C.10) has to be compared with eq. (3.18) for the scalar irreducible vertex function $\tilde{\Gamma}$ whose kernel is $\delta M/\delta G_1$ instead of $\delta\Sigma/\delta G_1$. The difference between the two kernels is just the Coulomb term (cf. eq. (4.6))

$$\Xi_{\mathrm{C}}(3,\,5;\,4,\,6) = -i\hbar\,\delta(3,\,4)\,\delta(5,\,6)\,v(3,\,6) \tag{C.12}$$

with respect to which $\tilde{\Gamma}$ is defined to be irreducible. The irreducible counterpart of the vector vertex function can also be introduced through an equation of the form (C.9) (see below).

For a system which is homogeneous in space and time the integral equations (C.10) and (C.11) can be rewritten using the Fourier representations (D.13), once the spin variables have been eliminated by summing over $\xi_3$

$$\text{(C.13)}\qquad \Gamma(p;\, q) = 1 + \int \frac{\mathrm{d}p'}{(2\pi)^4}\, \Xi_s(p,\, p';\, q)\, G_1(p' + q/2)\, G_1(p' - q/2)\, \Gamma(p';\, q)\,,$$

$$\text{(C.14)}\qquad \boldsymbol{\Gamma}(p;\, q) = \frac{\hbar \boldsymbol{p}}{m} + \int \frac{\mathrm{d}p'}{(2\pi)^4}\, \Xi_s(p,\, p';\, q)\, G_1(p' + q/2)\, G_1(p' - q/2)\, \boldsymbol{\Gamma}(p';\, q)\,.$$

Notice how these equations involve only the effective interaction (D.8*a*) for the singlet channel since the four-momentum $q$ corresponds to a Coulomb line that carries no spin.

*b*) *The irreducible two-particle correlation function.* By breaking the effective two-particle interaction (4.4) as the sum of the Coulomb term (C.12) and of the remainder

$$\text{(C.15)}\qquad \Xi_{\mathrm{R}}(3,\, 5;\, 4,\, 6) = \frac{\delta M(3,\, 4)}{\delta G_1(6,\, 5)}$$

(cf. eq. (4.6)), one can introduce the *irreducible* part $\tilde{L}$ of the two-particle correlation function as the solution to the integral equation

$$\text{(C.16)}\qquad \tilde{L}(1,\, 2;\, 1',\, 2') =$$
$$= G_1(1,\, 2')\, G_1(2,\, 1') + \int \mathrm{d}3456\, G_1(1,\, 3)\, G_1(4,\, 1')\, \Xi_{\mathrm{R}}(3,\, 5;\, 4,\, 6)\, \tilde{L}(6,\, 2;\, 5,\, 2')$$

with kernel $\Xi_{\mathrm{R}}$. Once $\tilde{L}$ is known, the full two-particle correlation function $L$ can be obtained by solving the additional integral equation

$$\text{(C.17)}\qquad L(1,\, 2;\, 1',\, 2') =$$
$$= \tilde{L}(1,\, 2;\, 1',\, 2') + \int \mathrm{d}3456\, \tilde{L}(1,\, 4;\, 1',\, 3)\, \Xi_{\mathrm{C}}(3,\, 5;\, 4,\, 6)\, L(6,\, 2;\, 5,\, 2')\,.$$

The system of equations (C.16) and (C.17) is, in fact, equivalent to the original Bethe-Salpeter equation (4.5) for $L$.

Several quantities can be expressed in terms of $\tilde{L}$. We give some examples.

i) The irreducible polarizability (3.25) is given by

$$\text{(C.18)}\qquad \tilde{\chi}(1,\, 2) = -i\hbar \tilde{L}(1,\, 2;\, 1^+,\, 2^+)\,,$$

in analogy with eq. (4.13) for the full polarizability in terms of $L$.

ii) The irreducible scalar vertex function (3.17) can be obtained from

$$\text{(C.19)}\qquad \tilde{L}(1,\, 3;\, 2,\, 3^+) = \int \mathrm{d}45\, G_1(1,\, 4)\, G_1(5,\, 2)\, \tilde{\Gamma}(4,\, 5;\, 3)\,,$$

in analogy with eq. (C.8) for the full-scalar vertex function in terms of $L$.

iii) The irreducible many-particle $T$-matrix can be defined as

$$\tilde{L}(1, 2; 1', 2') - G_1(1, 2')G_1(2, 1') = = \int d3456\, G_1(1, 3)\, G_1(4, 1')\, \tilde{T}(3, 5; 4, 6)\, G_1(6, 2')\, G_1(2, 5), \tag{C.20}$$

in analogy with eqs. (4.9) and (4.12). Alternatively, $\tilde{T}$ can be obtained as the solution to the integral equation

$$\tilde{T}(1, 2; 1', 2') = = \Xi_R(1, 2; 1', 2') + \int d3456\, \Xi_R(1, 4; 1', 3)\, G_1(3, 6)\, G_1(5, 4)\, \tilde{T}(6, 2; 5, 2'), \tag{C.21}$$

which is the analogue of eq. (4.11) for the full $T$-matrix $T$. $T$ and $\tilde{T}$ can further be related through the identity

$$T(1, 2; 1', 2') = \tilde{T}(1, 2; 1', 2') - i\hbar \int d33'\, \tilde{\Gamma}(1, 1'; 3)\, W(3, 3')\, \tilde{\Gamma}(2, 2'; 3'). \tag{C.22}$$

Equation (C.22) implies, in particular, that for the triplet channel $T$ coincides with $\tilde{T}$, while for the singlet channel an additional contribution due to polarization is present (cf. also appendix D).

c) *Density-current and current-current correlation functions.* Together with the (time-ordered) density-density correlation function

$$\chi(1, 2) = -\frac{i}{\hbar} \langle N|T[\hat{\rho}'(1)\hat{\rho}'(2)]|N\rangle, \tag{C.23}$$

we can also consider the density-current and current-current correlation functions

$$\vec{\chi}(1, 2) = -\frac{i}{\hbar} \langle N|T[\hat{\rho}'(1)\hat{\boldsymbol{j}}'(2)]|N\rangle, \tag{C.24a}$$

$$\overleftarrow{\chi}(1, 2) = -\frac{i}{\hbar} \langle N|T[\hat{\boldsymbol{j}}'(1)\hat{\rho}'(2)]|N\rangle, \tag{C.24b}$$

$$\overleftrightarrow{\chi}(1, 2) = -\frac{i}{\hbar} \langle N|T[\hat{\boldsymbol{j}}'(1)\hat{\boldsymbol{j}}'(2)]|N\rangle, \tag{C.24c}$$

where

$$\hat{\rho}'(1) = \hat{\rho}(1) - \langle N|\hat{\rho}(1)|N\rangle, \tag{C.25a}$$

$$\hat{\boldsymbol{j}}'(1) = \hat{\boldsymbol{j}}(1) - \langle N|\hat{\boldsymbol{j}}(1)|N\rangle, \tag{C.25b}$$

are the density and current deviation operators, respectively. More general definitions of the type (3.22) may also be considered.

The correlation functions (C.23) and (C.24) can be expressed in terms of the (reducible) vertex functions as follows:

$$\text{(C.26}a\text{)}\qquad \chi(1,\,2) \equiv -i\hbar L(1,\,2;\,1^+,\,2^+) = -i\hbar\int \mathrm{d}45\, G_1(1,\,4)\, G_1(5,\,1)\, \Gamma(4,\,5;\,2)\,,$$

$$\text{(C.26}b\text{)}\qquad \vec{\chi}(1,\,2) \equiv -i\hbar\left[\frac{\hbar}{2im}(\boldsymbol{\nabla}_2 - \boldsymbol{\nabla}_{2'})\, L(1,\,2;\,1^+,\,2')\right]_{2'=2^+} =$$

$$= -i\hbar\int \mathrm{d}45\, G_1(1,\,4)\, G_1(5,\,1)\, \boldsymbol{\Gamma}(4,\,5;\,2)\,,$$

$$\text{(C.26}c\text{)}\qquad \overleftarrow{\chi}(1,\,2) \equiv -i\hbar\left[\frac{\hbar}{2im}(\boldsymbol{\nabla}_1 - \boldsymbol{\nabla}_{1'})\, L(1,\,2;\,1',\,2^+)\right]_{1'=1^+} = \vec{\chi}(2,\,1) =$$

$$= -i\hbar\int \mathrm{d}45\, G_1(2,\,4)\, G_1(5,\,2)\, \boldsymbol{\Gamma}(4,\,5;\,1)\,,$$

$$\text{(C.26}d\text{)}\qquad \overleftrightarrow{\chi}(1,\,2) \equiv -i\hbar\left[\frac{\hbar}{2im}(\boldsymbol{\nabla}_1 - \boldsymbol{\nabla}_{1'})\frac{\hbar}{2im}(\boldsymbol{\nabla}_2 - \boldsymbol{\nabla}_{2'})\, L(1,\,2;\,1',\,2')\right]_{\substack{1'=1^+\\ 2'=2^+}} =$$

$$= -i\hbar\left[\frac{\hbar}{2im}(\boldsymbol{\nabla}_1 - \boldsymbol{\nabla}_{1'})\int \mathrm{d}45\, G_1(1,\,4)\, G_1(5,\,1')\, \boldsymbol{\Gamma}(4,\,5;\,2)\right]_{1'=1^+} =$$

$$= -i\hbar\int \mathrm{d}4567\, \boldsymbol{\Gamma}_0(7,\,6;\,1)\, G_1(6,\,4)\, G_1(5,\,7)\, \boldsymbol{\Gamma}(4,\,5;\,3)\,,$$

where $\boldsymbol{\Gamma}_0$ is the noninteracting part of $\boldsymbol{\Gamma}$ (cf. eq. (C.11))

$$\text{(C.27)}\qquad \boldsymbol{\Gamma}_0(1,\,2;\,3) = \frac{\hbar}{2im}\left[(\boldsymbol{\nabla}_3 - \boldsymbol{\nabla}_{3'})\,\delta(1,\,3')\,\delta(2,\,3)\right]_{3'=3}.$$

Equation (C.26*a*) follows from eq. (C.8), while eqs. (C.26*b*) to (C.26*d*) follow from eq. (C.9). Notice also that the four equations (C.26) have a similar structure and could accordingly be expressed as a single tensor equation of rank 4.

The irreducible correlation functions associated with $\chi$, $\vec{\chi}$, and $\overleftrightarrow{\chi}$ can be defined in analogy with eqs. (C.26), whereby the two-particle correlation function $L$ is replaced by its irreducible part $\tilde{L}$. We have already seen, in fact, that the irreducible density-density correlation function can be expressed as (cf. eqs. (C.18) and (C.19))

$$\text{(C.28)}\qquad \tilde{\chi}(1,\,2) = -i\hbar\tilde{L}(1,\,2;\,1^+,\,2^+) = -i\hbar\int \mathrm{d}45\, G_1(1,\,4)\, G_1(5,\,1)\, \tilde{\Gamma}(4,\,5;\,2)\,.$$

We can similarly define

$$\text{(C.29}a\text{)}\qquad \vec{\tilde{\chi}}(1,\,2) \equiv -i\hbar\left[\frac{\hbar}{2im}(\boldsymbol{\nabla}_2 - \boldsymbol{\nabla}_{2'})\, \tilde{L}(1,\,2;\,1^+,\,2')\right]_{2'=2^+},$$

$$\text{(C.29}b\text{)}\qquad \tilde{\overleftarrow{\chi}}(1,\,2) \equiv -i\hbar\left[\frac{\hbar}{2im}(\boldsymbol{\nabla}_1 - \boldsymbol{\nabla}_{1'})\,\tilde{L}(1,\,2;\,1',\,2^+)\right]_{1'=1^+},$$

$$\text{(C.29}c\text{)}\qquad \tilde{\overleftrightarrow{\chi}}(1,\,2) \equiv -i\hbar\left[\frac{\hbar}{2im}(\boldsymbol{\nabla}_1 - \boldsymbol{\nabla}_{1'})\,\frac{\hbar}{2im}(\boldsymbol{\nabla}_2 - \boldsymbol{\nabla}_{2'})\,\tilde{L}(1,\,2;\,1',\,2')\right]_{\substack{1'=1^+\\ 2'=2^+}}.$$

Furthermore, in analogy with eq. (C.28), we can also introduce the irreducible vector vertex function $\tilde{\boldsymbol{\Gamma}}\,(1,\,2;\,3)$ defined as the solution to the integral equation obtained from eq. (C.11) by replacing the kernel $\delta\Sigma/\delta G_1$ with $\delta M/\delta G_1$. In terms of $\tilde{\boldsymbol{\Gamma}}$ we can then express

$$\text{(C.30}a\text{)}\qquad \tilde{\overrightarrow{\chi}}(1,\,2) = \tilde{\overleftarrow{\chi}}(2,\,1) = -i\hbar\int \mathrm{d}45\, G_1(1,\,4)\, G_1(5,\,1)\, \tilde{\boldsymbol{\Gamma}}(4,\,5;\,2)\,,$$

$$\text{(C.30}b\text{)}\qquad \tilde{\overleftrightarrow{\chi}}(1,\,2) = -i\hbar\int \mathrm{d}4567\, \boldsymbol{\Gamma}_0(7,\,6;\,1)\, G_1(6,\,4)\, G_1(5,\,7)\, \tilde{\boldsymbol{\Gamma}}(4,\,5;\,3)\,.$$

Once the irreducible correlation functions (C.28) and (C.29) have been determined, their reducible counterparts can be obtained from eq. (3.24) and from

$$\text{(C.31}a\text{)}\qquad \overrightarrow{\chi}(1,\,2) = \tilde{\overrightarrow{\chi}}(1,\,2) + \int \mathrm{d}34\, \tilde{\chi}(1,\,3)\, v(3,\,4)\, \overrightarrow{\chi}(4,\,2)\,,$$

$$\text{(C.31}b\text{)}\qquad \overleftrightarrow{\chi}(1,\,2) = \tilde{\overleftrightarrow{\chi}}(1,\,2) + \int \mathrm{d}34\, \tilde{\overleftarrow{\chi}}(1,\,3)\, v(3,\,4)\, \overrightarrow{\chi}(4,\,2)\,.$$

## APPENDIX D

### Elimination of the spin variables and transformation to the energy-momentum representation.

The value of the spin variable $\xi$ does not change along a single fermion line whenever the Hamiltonian is spin independent. This implies, in particular, that

$$\text{(D.1)}\qquad G_1(1,\,2) = \delta_{\xi_1\xi_2}\, G(x_1,\,x_2)\,,$$

$$\text{(D.2)}\qquad M(1,\,2) = \delta_{\xi_1\xi_2}\, M(x_1,\,x_2)\,,$$

$$\text{(D.3)}\qquad \int \mathrm{d}\xi_3\, \tilde{\Gamma}(1,\,2;\,3) = \delta_{\xi_1\xi_2}\, \tilde{\Gamma}(x_1,\,x_2;\,x_3)\,,$$

$$\text{(D.4)}\qquad \int \mathrm{d}\xi_1\, d\xi_2\, \chi(1,\,2) = \chi(x_1,\,x_2)\,,$$

$$\text{(D.5)}\qquad \int \mathrm{d}\xi_2\, \epsilon^{-1}(1,\,2) = \epsilon^{-1}(x_1,\,x_2)\,,$$

where we have introduced the notation $x \equiv (\boldsymbol{r}, t)$. These identities allow us to readily remove the spin variables from the set of coupled equations discussed in sect. 3. Elimination of the spin variables from the Bethe-Salpeter equation, on the other hand, requires to distinguish between the two alternative paths that can be followed by joining the vertices of the effective interaction $\Xi$. Specifically, we can set

$$\text{(D.6)} \qquad \Xi(3,\, 5;\, 4,\, 6) = \delta_{\xi_3\xi_4}\frac{1}{2}\Xi^{\uparrow}_{\uparrow}(x_3,\, x_5;\, x_4,\, x_6)\,\delta_{\xi_5\xi_6} + \delta_{\xi_3\xi_6}\Xi_{\uparrow\uparrow}(x_3,\, x_5;\, x_4,\, x_6)\,\delta_{\xi_4\xi_5}\,,$$

where $\Xi^{\uparrow}_{\uparrow}$ and $\Xi_{\uparrow\uparrow}$ correspond to pairing the fermion lines in the way shown in fig. 12*a*) (the factor 1/2 in front of $\Xi^{\uparrow}_{\uparrow}$ has been introduced for later convenience). For example, the Hartree-Fock approximation for the self-energy yields

$$\text{(D.7)} \qquad \Xi_{\text{HF}}(3,\, 5;\, 4,\, 6) = \delta_{\xi_3\xi_4}[-i\hbar\delta(x_3,\, x_4)\,v(x_3,\, x_6)\,\delta(x_5,\, x_6^+)]\,\delta_{\xi_5\xi_6} + \\ + \delta_{\xi_3\xi_6}[i\hbar\delta(x_3,\, x_6)\,v(x_3^+,\, x_4)\,\delta(x_4,\, x_5)]\,\delta_{\xi_4\xi_5}\,,$$

whereby the Hartree and the Fock terms correspond to a $\Xi^{\uparrow}_{\uparrow}$ and to a $\Xi_{\uparrow\uparrow}$ pairing, respectively (fig. 12*b*). Alternatively, we could introduce the effective interactions for the *singlet* and the *triplet* channels

$$\text{(D.8}a\text{)} \qquad \Xi_{\text{s}}(\{x_i\}) = \Xi_{\uparrow\uparrow}(\{x_i\}) + \Xi^{\uparrow}_{\uparrow}(\{x_i\})\,,$$

$$\text{(D.8}b\text{)} \qquad \Xi_{\text{t}}(\{x_i\}) = \Xi_{\uparrow\uparrow}(\{x_i\})\,,$$

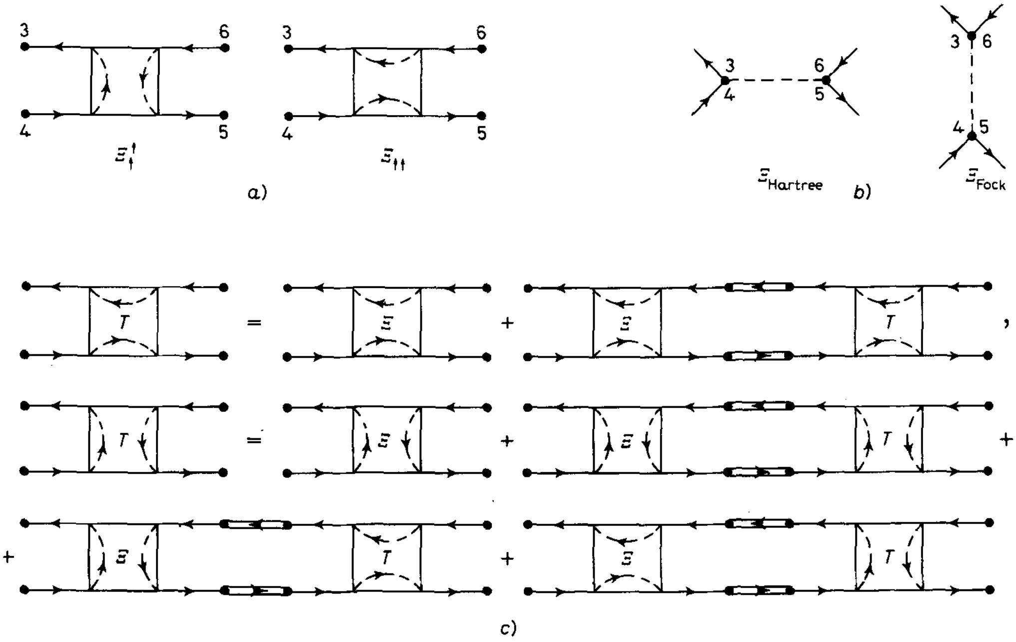

Fig. 12. – *a*) Alternative pairing of fermion lines in the effective interaction; *b*) lowest-order (Hartree and Fock) terms in the effective interaction; *c*) Bethe-Salpeter equation for $T_{\uparrow\uparrow}$ and $T^{\uparrow}_{\uparrow}$.

and express the spin dependence of the (total) effective interaction $\Xi$ in terms of the Pauli matrices as follows:

$$\text{(D.9)} \qquad \Xi(3,\,5;\,4,\,6) = \frac{1}{2}\delta_{\xi_3\xi_4}\delta_{\xi_5\xi_6}\Xi_{\mathrm{s}}(x_3,\,x_5;\,x_4,\,x_6) + \frac{1}{2}\boldsymbol{\sigma}_{\xi_3\xi_4}\cdot\boldsymbol{\sigma}_{\xi_5\xi_6}\Xi_{\mathrm{t}}(x_3,\,x_5;\,x_4,\,x_6)\,.$$

The $T$-matrix can similarly be decomposed. From the Bethe-Salpeter equation (4.11) one then finds that $T_{\uparrow\uparrow}$ is obtained by iterating $\Xi_{\uparrow\uparrow}$ only, while $T^{\uparrow}_{\uparrow}$ derives from both $\Xi^{\uparrow}_{\uparrow}$ and $\Xi_{\uparrow\uparrow}$ and couples also with $T_{\uparrow\uparrow}$ as shown graphically in fig. 12*c*). The coupled equations for $T^{\uparrow}_{\uparrow}$ and $T_{\uparrow\uparrow}$ can, however, be transformed by introducing the $T$-matrices $T_a$ $(a = s,\,t)$ for the singlet and triplet channels in analogy with eqs. (D.8), yielding two uncoupled equations for $T_{\mathrm{s}}$ and $T_{\mathrm{t}}$:

$$\text{(D.10)} \qquad T_a(x_1,\,x_2;\,x_{1'},\,x_{2'}) = \Xi_a(x_1,\,x_2;\,x_{1'},\,x_{2'}) + \\ + \int \mathrm{d}x_3\,\mathrm{d}x_4\,\mathrm{d}x_5\,\mathrm{d}x_6\,\Xi_a(x_1,\,x_4;\,x_{1'},\,x_3)\,G_1(x_3,\,x_6)\,G_1(x_5,\,x_4)\,T_a(x_6,\,x_2;\,x_5,\,x_{2'})\,.$$

The transformation to the energy-momentum representation can be done *after* the elimination of the spin variables has been performed. To this end, we adopt the following convention for the Fourier representation:

$$\text{(D.11)} \qquad f(x) = \int \frac{\mathrm{d}k}{(2\pi)^4}\exp[ik\cdot x]\,f(k)\,,$$

where $k \equiv (\boldsymbol{k},\,\omega)$, $\mathrm{d}k = \mathrm{d}\boldsymbol{k}\,\mathrm{d}\omega$, and $k\cdot x = \boldsymbol{k}\cdot\boldsymbol{r} - \omega t$. In particular, for any system which is translationally invariant in time and space we can write

$$\text{(D.12}a\text{)} \qquad M(x_1,\,x_2) = M(x_1 - x_2)\,,$$

$$\text{(D.12}b\text{)} \qquad \tilde{\Gamma}(x_1,\,x_2;\,x_3) = \tilde{\Gamma}(x_1 - x_3,\,x_2 - x_3)\,,$$

$$\text{(D.12}c\text{)} \qquad \Xi(x_3,\,x_5;\,x_4,\,x_6) = \Xi(x_3 - x_6,\,x_4 - x_6,\,x_5 - x_6)\,.$$

This implies the following Fourier representations:

$$\text{(D.13}a\text{)} \qquad M(x_1,\,x_2) = \int \frac{\mathrm{d}q}{(2\pi)^4}\exp[iq\cdot(x_1 - x_2)]\,M(q)\,,$$

$$\text{(D.13}b\text{)} \qquad \tilde{\Gamma}(x_1,\,x_2;\,x_3) = \int \frac{\mathrm{d}p}{(2\pi)^4}\frac{\mathrm{d}q}{(2\pi)^4}\exp[i(p + q/2)\cdot(x_1 - x_3)]\,\cdot \\ \cdot\exp[-i(p - q/2)\cdot(x_2 - x_3)]\,\tilde{\Gamma}(p;\,q)\,,$$

$$\text{(D.13}c\text{)} \qquad \Xi(x_3,\,x_5;\,x_4,\,x_6) = \int \frac{\mathrm{d}p}{(2\pi)^4}\frac{\mathrm{d}p'}{(2\pi)^4}\frac{\mathrm{d}q}{(2\pi)^4}\exp[i(p + q/2)\cdot x_3]\exp[i(p' - q/2)\cdot x_5]\,\cdot \\ \cdot\exp[-i(p - q/2)\cdot x_4]\,\exp[-i(p' + q/2)\cdot x_6]\,\Xi(p,\,p';\,q)\,,$$

which are shown graphically in fig. 13.

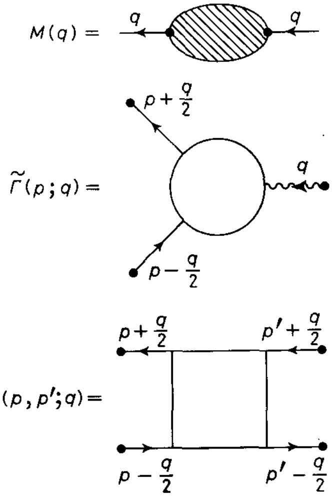

Fig. 13. – Structure of $M(q)$, $\tilde{\Gamma}(p;q)$, and $\Xi(p,p';q)$ from energy and momentum conservation.

Elimination of the spin variables for the two-particle correlation function proceeds as follows. The functions $L(x_1\sigma_1, x_2\sigma_2; x_{1'}\sigma_{1'}, x_{2'}\sigma_{2'})$ corresponding to the six possible arrangements of the spin projections $\{\sigma_i\}$ at the four external legs (cf. fig. 2*a*)) can be expressed as linear combinations of the singlet (s) and triplet (t) amplitudes

$$(\mathrm{D.14})\qquad L_{\mathrm{s,t}}(x_1, x_2; x_{1'}, x_{2'}) = L(x_1\uparrow, x_2\uparrow; x_{1'}\uparrow, x_{2'}\uparrow) \pm \pm L(x_1\uparrow, x_2\downarrow; x_{1'}\uparrow, x_{2'}\downarrow),$$

with the + (−) sign referring to singlet (triplet), provided the ground state $|N\rangle$ possesses overall spin rotational symmetry (*i.e.*, it is a spin singlet). In this case one may show that $L_\mathrm{s}$ and $L_\mathrm{t}$ satisfy two distinct Bethe-Salpeter equations with kernels $\Xi_\mathrm{s}$ and $\Xi_\mathrm{t}$, respectively.

## APPENDIX E

### The Thomas-Reiche-Kuhn sum rule.

In this appendix we show that a «$\Phi$-derivable» approximation preserves the information about the (ground state) expectation value of the equal-time density-current commutator, thereby fulfilling the so-called Thomas-Reiche-Kuhn sum rule. In fact, a combination of eqs. (7.9) and (7.10) yields

$$(\mathrm{E.1})\qquad \frac{\partial}{\partial t_1}\langle N|T[\hat{\rho}'(1)\hat{\Psi}(3)\hat{\Psi}^+(3')]|N\rangle + \nabla_1\cdot\langle N|T[\hat{\mathbf{j}}'(1)\hat{\Psi}(3)\hat{\Psi}^+(3')]|N\rangle = = (\delta(1,3') - \delta(1,3))\langle N|T[\hat{\Psi}(3)\hat{\Psi}^+(3')]|N\rangle\,;$$

applying then the operator $(\hbar/2im)(\nabla_3 - \nabla_{3'})$ to both sides of eq. (E.1) and setting $3' = 3^+$ leads eventually the equal-time density-current commutator in the form

$$\text{(E.2)} \qquad \langle N|[\hat{\rho}(\boldsymbol{x}), \hat{\boldsymbol{j}}(\boldsymbol{x}')]|N\rangle = \frac{i\hbar}{m}\langle N|\hat{\rho}(\boldsymbol{x}')|N\rangle\, \nabla'\delta(\boldsymbol{x}, \boldsymbol{x}')\,.$$

The connection between the Thomas-Reiche-Kuhn sum rule and the commutator (E.2) can now be readily established by expressing (in the absence of magnetic fields):

$$\text{(E.3)} \qquad \sum_s (E_s - E_0)|\rho_s(\boldsymbol{k})|^2 = \\ = \frac{1}{2V}\int \mathrm{d}\boldsymbol{x}\,\mathrm{d}\boldsymbol{x}'\, \exp[-i\boldsymbol{k}\cdot\boldsymbol{r}']\,\langle N|[[\hat{\rho}(\boldsymbol{x}'), \hat{H}], \hat{\rho}(\boldsymbol{x})]|N\rangle\, \exp[i\boldsymbol{k}\cdot\boldsymbol{r}] = \\ = \frac{i\hbar}{2V}\int \mathrm{d}\boldsymbol{x}\,\mathrm{d}\boldsymbol{x}'\, \exp[i\boldsymbol{k}\cdot(\boldsymbol{r}-\boldsymbol{r}')]\,\nabla'\cdot\langle N|[\hat{\rho}(\boldsymbol{x}), \hat{\boldsymbol{j}}(\boldsymbol{x}')]|N\rangle\,,$$

where $V$ is the volume occupied by the system, $E_s - E_0$ are the excitation energies of the system, and

$$\text{(E.4)} \qquad \rho_s(\boldsymbol{k}) = V^{-1/2}\int \mathrm{d}\boldsymbol{x}\, \exp[-i\boldsymbol{k}\cdot\boldsymbol{r}]\,\langle N|\hat{\rho}(\boldsymbol{x})|N, s\rangle$$

are the corresponding matrix elements of the fluctuation density operator of wave vector $\boldsymbol{k}$ between the ground state $|N\rangle$ and an excited state $|N, s\rangle$. Insertion of eq. (E.2) into eq. (E.3) gives finally

$$\text{(E.5)} \qquad \sum_s (E_s - E_0)|\rho_s(\boldsymbol{k})|^2 = \frac{\hbar^2 \boldsymbol{k}^2}{2m}\,\frac{1}{V}\int \mathrm{d}\boldsymbol{x}\langle N|\hat{\rho}(\boldsymbol{x})|N\rangle\,,$$

for any «$\Phi$-derivable» approximation. Since the integral on the right-hand side of eq. (E.5) is taken to give the total number $N$ of particles which are present in the volume $V$, eq. (E.5) reproduces the desired sum rule. In particular, taking $\boldsymbol{k} = (0, 0, k)$ with $k$ small, one can approximate

$$\text{(E.6)} \qquad \rho_s(\boldsymbol{k}) \simeq -ikV^{-1/2}q^{-1}\langle N|\hat{d}_z|N, s\rangle\,,$$

where $\hat{d}_z$ is the ($z$-component of the) dipole moment operator and $q$ is the charge of a particle. Equation (E.5) thus acquires the more familiar form [61]

$$\text{(E.7)} \qquad \sum_s (E_s - E_0)|\langle N|\hat{d}_z|N, s\rangle|^2 = \frac{\hbar^2 N}{2m}q^2\,.$$

Well-known examples of conserving approximations for which the sum rule (E.7) can be explicitly verified are the RPA and the RPAE approximations [62].

## APPENDIX F

### The Clausius-Mossotti relation.

The formalism presented in subsect. 8·4 provides a link between calculations based on the microscopic properties of the material and the macroscopic theory of the dielectric constant $\epsilon_M(\omega)$. One then expects to recapture from it the classical Clausius-Mossotti relation for the macroscopic dielectric constant

$$\epsilon_M(\omega)=\frac{1+\frac{8}{3}\pi\alpha(\omega)}{1-\frac{4}{3}\pi\alpha(\omega)} \tag{F.1}$$

in the limit of completely localized electrons, such that the electronic excitations are represented by the polarization of *point dipoles* at the (Bravais) lattice sites (that we take throughout of cubic symmetry). In eq. (F.1) $\alpha(\omega)$ is the site polarizability per unit volume that relates the polarization density (cf. eq. (8.8)) to the local electric field acting on the individual point dipoles [63]. The single function $\alpha(\omega)$ thus provides the eigenfrequencies of the longitudinal and transverse excitations in the long-wavelength limit by considering the zeros of the numerator and of the denominator in eq. (F.1), respectively [64].

In the limit of extreme localization, we may retain only the form factors (8.53) with $\boldsymbol{l}=0$ and approximate

$$A_c(\boldsymbol{q}+0)\simeq -i\boldsymbol{q}\cdot\boldsymbol{p}_c, \tag{F.2}$$

where $\boldsymbol{p}_c$ is the dipole matrix element

$$\boldsymbol{p}_c=\int \mathrm{d}\boldsymbol{r}\phi_\nu^*(\boldsymbol{r})\,\boldsymbol{r}\phi_\mu(\boldsymbol{r}) \tag{F.3}$$

between an occupied ($\nu$) and an unoccupied ($\mu$) local orbital. The net charge corresponding to this dipole excitation is thus zero. Notice that the integral in eq. (F.3) is limited in practice within the volume of the reference cell centred at $\boldsymbol{r}=0$. Combining eq. (F.2) with eqs. (8.26) and (8.59) yields for the macroscopic dielectric function

$$\epsilon_M(\omega)=1-\frac{4\pi e^2}{\Omega_0}\sum_{cc'}p_c^\beta\hat{S}_{cc'}(\boldsymbol{q}=0;\,\omega)\,p_{c'}^{\beta *}, \tag{F.4}$$

where $\beta$ denotes any Cartesian component of the vector (F.3). The proper screening matrix $\hat{S}$ given by eq. (8.60) can be considerably simplified in the limit of extreme localization, by expanding the Coulomb matrix elements of eq. (8.61) into multipoles. To leading order, we get the dipole-dipole interaction

$$\begin{aligned}\hat{V}^{\mathrm{C}}_{cc'}(\boldsymbol{q})-\frac{1}{2}V^{sx}_{cc'}(\boldsymbol{q})\simeq&-\frac{4\pi e^2}{\Omega_0}\hat{q}\cdot\boldsymbol{p}_c^*\boldsymbol{p}_c\cdot\hat{q}+\\&+e^2\sum_{\boldsymbol{m}}{}'\exp[-i\boldsymbol{q}\cdot\boldsymbol{m}]\,\frac{[(\boldsymbol{p}_c^*\cdot\boldsymbol{p}_{c'})|\boldsymbol{m}|^2-3(\boldsymbol{m}\cdot\boldsymbol{p}_c^*)(\boldsymbol{m}\cdot\boldsymbol{p}_{c'})]}{|\boldsymbol{m}|^5},\end{aligned} \tag{F.5}$$

where the prime on the summation means that the term $\boldsymbol{m}=0$ is omitted. In other words, we have assumed that the exchange Coulomb matrix (8.56) (and possible modifications to it due to electronic correlation effects beyond the TDSHF approximation considered in subsect. 8'4) removes the self-interaction term from the proper Coulomb matrix (8.61) [65]. Proviso of this self-polarization correction, albeit irrelevant if the electronic wave functions are extended throughout the crystal, becomes indeed essential when the wave functions are localized [66].

The right-hand side of eq. (F.5) can be evaluated by the Ewald's method. Taking advantage of the results given in sect. 30 and appendix VI of ref. [28], we split the dipolar sum into a term that absorbs all that is nonregular at $\boldsymbol{q}=0$ and a regular remainder. The nonregular term corresponds to the «macroscopic field» and cancels with the first term at the right-hand side of eq. (F.5), while the regular term corresponds to the so-called «inner field» and gives

$$\text{(F.6)} \qquad \hat{V}^{\mathrm{C}}_{cc'}(\boldsymbol{q}=0)-\frac{1}{2}V^{sx}_{cc'}(\boldsymbol{q}=0)\simeq-\frac{4\pi e^2}{3\Omega_0}\boldsymbol{p}^*_c\cdot\boldsymbol{p}_{c'}\,.$$

Insertion of eq. (F.6) into eq. (8.60) and of the result into eq. (F.4) requires us to sum the geometric series

$$\text{(F.7)} \qquad \frac{1}{\Omega_0}\sum_{cc'}p^\beta_c\hat{S}_{cc'}(\boldsymbol{q}=0;\,\omega)\,p^{\beta*}_{c'}=\frac{1}{\Omega_0}\sum_{cc'}p^\beta_c\bigg[(-i\hbar)N^0_{cc'}(\boldsymbol{q}=0;\,\omega)-$$

$$-\sum_{c''c'''}(-i\hbar)N^0_{c'c''}(\boldsymbol{q}=0;\,\omega)\frac{4\pi e^2}{3\Omega_0}\boldsymbol{p}^*_{c''}\cdot\boldsymbol{p}_{c'''}(-i\hbar)N^0_{c'''c'}(\boldsymbol{q}=0;\,\omega)+\dots\bigg]p^{\beta*}_{c'}=$$

$$=\frac{1}{\Omega_0}\sum_{cc'}p^\beta_c(-i\hbar)N^0_{cc'}(\boldsymbol{q}=0;\,\omega)\,p^{\beta*}_{c'}\cdot$$

$$\cdot\bigg[1-\frac{4\pi e^2}{3}\frac{1}{\Omega_0}\sum_{c''c'''}p^\beta_{c''}(-i\hbar)N^0_{c''c'''}(\boldsymbol{q}=0;\,\omega)\,p^{\beta*}_{c'''}+\dots\bigg]=\frac{\tilde{\chi}^0(\omega)}{1+\dfrac{4\pi e^2}{3}\tilde{\chi}^0(\omega)}\,,$$

where

$$\text{(F.8)} \qquad \tilde{\chi}^0(\omega)\equiv\frac{1}{\Omega_0}\sum_{cc'}p^\beta_c(-i\hbar)N^0_{cc'}(\boldsymbol{q}=0;\,\omega)\,p^{\beta*}_{c'}=\lim_{q\to0}\frac{1}{q^2}\tilde{\chi}^0(\boldsymbol{q}+0,\,\boldsymbol{q}+0;\,\omega)$$

is defined in terms of the polarizability for noninteracting particles (cf. eq. (8.58) with $N$ replaced by $N^0$). Combining eq. (F.7) with eq. (F.4) leads eventually to the Clausius-Mossotti relation (F.1), provided we identify $-e^2\tilde{\chi}^0(\omega)$ with the site polarizability per unit volume $\alpha(\omega)$, computed without regard to the dipole interactions [64]. To this end, it is sufficient to consider the polarization density at the reference cell produced by the (self-consistent) local electric field (whereby the self-polarization correction has been subtracted [66]) set up by a purely longitudinal perturbing electric field. We thus write

$$\text{(F.9)} \qquad \boldsymbol{P}(\boldsymbol{r}=0;\,\omega)=\frac{1}{\Omega_0}\int_{\Omega_0}\mathrm{d}\boldsymbol{r}\,\boldsymbol{r}\rho_{\mathrm{ind}}(\boldsymbol{r};\,\omega)=$$

$$= \frac{e^2}{\Omega_0} \int_{\Omega_0} \mathrm{d}\boldsymbol{r}\,\boldsymbol{r} \int_{\Omega} \mathrm{d}\boldsymbol{r}'\,\tilde{\chi}^0(\boldsymbol{r}, \boldsymbol{r}'; \omega)\,\varphi_{\mathrm{loc}}(\boldsymbol{r}'; \omega) =$$

$$= \frac{e^2}{\Omega_0} \int_{\Omega_0} \mathrm{d}\boldsymbol{r}\,\boldsymbol{r} \int_{\Omega} \mathrm{d}\boldsymbol{r}'\,\tilde{\chi}^0(\boldsymbol{r}, \boldsymbol{r}'; \omega)\,[\varphi_{\mathrm{loc}}(\boldsymbol{r}=0; \omega) - \boldsymbol{r}'\cdot\boldsymbol{E}_{\mathrm{loc}}(\boldsymbol{r}=0; \omega) + \ldots] =$$

$$= -\frac{e^2}{\Omega_0} \int_{\Omega_0} \mathrm{d}\boldsymbol{r}\,\mathrm{d}\boldsymbol{r}'\,\boldsymbol{r}\,\tilde{\chi}^0(\boldsymbol{r}, \boldsymbol{r}'; \omega)\,\boldsymbol{r}'\cdot\boldsymbol{E}_{\mathrm{loc}}(\boldsymbol{r}=0; \omega) + \ldots,$$

where use has been made of the short-range property of $\tilde{\chi}^0(\boldsymbol{r}, \boldsymbol{r}'; \omega)$ to confine both integration variables to the reference cell as well to neglect the spatial variation of the local electric field over the exent of the induced dipole, and of the cell neutrality condition [67]

$$\int_{\Omega_0} \mathrm{d}\boldsymbol{r}'\,\tilde{\chi}^0(\boldsymbol{r}, \boldsymbol{r}'; \omega) = 0 \tag{F.10}$$

that follows directly from the orthogonality of the pair of localized orbitals entering eq. (F.3). The condition (F.10) can further be exploited to identify

$$\frac{1}{\Omega_0} \int_{\Omega_0} \mathrm{d}\boldsymbol{r}\,\mathrm{d}\boldsymbol{r}'\,\boldsymbol{r}\,\tilde{\chi}^0(\boldsymbol{r}, \boldsymbol{r}'; \omega)\,\boldsymbol{r}' = \tilde{\chi}^0(\omega)\,\overleftrightarrow{1}, \tag{F.11}$$

thereby yielding the desired result

$$\boldsymbol{P}(\boldsymbol{r}=0; \omega) = -e^2\tilde{\chi}^0(\omega)\,\boldsymbol{E}_{\mathrm{loc}}(\boldsymbol{r}=0; \omega). \tag{F.12}$$

## APPENDIX G

### The particle-hole Green's function.

The two-particle Green's function

$$G_2(1, 2; 1', 2') = \left(-\frac{i}{\hbar}\right)^2 \langle N|T[\hat{\Psi}(1)\,\hat{\Psi}(2)\,\hat{\Psi}^\dagger(2')\,\hat{\Psi}^\dagger(1')]|N\rangle \tag{G.1}$$

can be expressed as the sum of the following six functions:

$$G_2^{\mathrm{I}}(1, 2; 1', 2') = \left(-\frac{i}{\hbar}\right)^2 \langle N|T[\hat{\Psi}(1)\,\hat{\Psi}^\dagger(1')]\,T[\hat{\Psi}(2)\,\hat{\Psi}^\dagger(2')]|N\rangle \cdot \cdot\,\theta\!\left(\tau - \frac{1}{2}|\tau_1| - \frac{1}{2}|\tau_2|\right), \tag{G.2$a$}$$

$$G_2^{\mathrm{II}}(1, 2; 1', 2') = \left(-\frac{i}{\hbar}\right)^2 \langle N|T[\hat{\Psi}(2)\,\hat{\Psi}^\dagger(2')]\,T[\hat{\Psi}(1)\,\hat{\Psi}^\dagger(1')]|N\rangle \cdot \cdot\,\theta\!\left(-\tau - \frac{1}{2}|\tau_1| - \frac{1}{2}|\tau_2|\right), \tag{G.2$b$}$$

$$\text{(G.2}c\text{)}\qquad G_2^{\rm III}(1,\,2;\,1',\,2') = -\left(-\frac{i}{\hbar}\right)^2 \langle N|T[\hat\Psi(2)\,\hat\Psi^\dagger(1')]\,T[\hat\Psi(1)\,\hat\Psi^\dagger(2')]|N\rangle\,\cdot$$
$$\cdot\,\theta\!\left(\frac{\tau_2}{2}-\frac{\tau_1}{2}-\frac{1}{2}\left|-\tau+\frac{\tau_1}{2}+\frac{\tau_2}{2}\right|-\frac{1}{2}\left|\tau+\frac{\tau_1}{2}+\frac{\tau_2}{2}\right|\right),$$

$$\text{(G.2}d\text{)}\qquad G_2^{\rm IV}(1,\,2;\,1',\,2') = -\left(-\frac{i}{\hbar}\right)^2 \langle N|T[\hat\Psi(1)\,\hat\Psi^\dagger(2')]\,T[\hat\Psi(2)\,\hat\Psi^\dagger(1')]|N\rangle\,\cdot$$
$$\cdot\,\theta\!\left(\frac{\tau_1}{2}-\frac{\tau_2}{2}-\frac{1}{2}\left|-\tau+\frac{\tau_1}{2}+\frac{\tau_2}{2}\right|-\frac{1}{2}\left|\tau+\frac{\tau_1}{2}+\frac{\tau_2}{2}\right|\right),$$

$$\text{(G2}e\text{)}\qquad G_2^{\rm V}(1,\,2;\,1',\,2') = \left(-\frac{i}{\hbar}\right)^2 \langle N|T[\hat\Psi(1)\,\hat\Psi(2)]\,T[\hat\Psi^\dagger(2')\,\hat\Psi^\dagger(1')]|N\rangle\,\cdot$$
$$\cdot\,\theta\!\left(\frac{\tau_1}{2}+\frac{\tau_2}{2}-\frac{1}{2}\left|\tau+\frac{\tau_1}{2}-\frac{\tau_2}{2}\right|-\frac{1}{2}\left|\tau-\frac{\tau_1}{2}+\frac{\tau_2}{2}\right|\right),$$

$$\text{(G.2}f\text{)}\qquad G_2^{\rm VI}(1,\,2;\,1',\,2') = \left(-\frac{i}{\hbar}\right)^2 \langle N|T[\hat\Psi^\dagger(2')\,\hat\Psi^\dagger(1')]\,T[\hat\Psi(1)\,\hat\Psi(2)]|N\rangle\,\cdot$$
$$\cdot\,\theta\!\left(-\frac{\tau_1}{2}-\frac{\tau_2}{2}-\frac{1}{2}\left|\tau+\frac{\tau_1}{2}-\frac{\tau_2}{2}\right|-\frac{1}{2}\left|\tau-\frac{\tau_1}{2}+\frac{\tau_2}{2}\right|\right).$$

Inserting a complete set of $N$-particle states (for functions I-IV), of $(N+2)$-particle states (for function V), and of $(N-2)$-particle states (for function VI) between the two time-ordered products in eqs. (G.2), and introducing the right- and left-hand particle-hole amplitudes

$$\text{(G.3}a\text{)}\qquad \chi_s^{\rm ph}(\boldsymbol{x}_i,\,\boldsymbol{x}_j;\,t_i-t_j) = \langle N|T[\hat\Psi(i)\,\hat\Psi^\dagger(j)]|\,N,\,s\rangle\,\exp[i(E_s-E_0)(t_i+t_j)/2\hbar]\,,$$

$$\text{(G.3}b\text{)}\qquad \tilde\chi_s^{\rm ph}(\boldsymbol{x}_i,\,\boldsymbol{x}_j;\,t_i-t_j) = \langle N,\,s|T[\hat\Psi(i)\,\hat\Psi^\dagger(j)]|N\rangle\,\exp[-i(E_s-E_0)(t_i+t_j)/2\hbar]\,,$$

the right- and left-hand particle-particle amplitudes

$$\text{(G.4}a\text{)}\qquad \chi_s^{\rm pp}(\boldsymbol{x}_i,\,\boldsymbol{x}_j;\,t_i-t_j) = \langle N|T[\hat\Psi(i)\,\hat\Psi(j)]|N+2,\,s\rangle\,\cdot$$
$$\cdot\exp[i(E_s(N+2)-E_0)(t_i+t_j)/2\hbar]\,,$$

$$\text{(G.4}b\text{)}\qquad \tilde\chi_s^{\rm pp}(\boldsymbol{x}_i,\,\boldsymbol{x}_j;\,t_i-t_j) = \langle N+2,\,s|T[\hat\Psi^\dagger(i)\,\hat\Psi^\dagger(j)]|N\rangle\,\cdot$$
$$\cdot\exp[-i(E_s(N+2)-E_0)(t_i+t_j)/2\hbar]\,,$$

and the right- and left-hand hole-hole amplitudes

$$\text{(G.5}a\text{)}\qquad \chi_s^{\rm hh}(\boldsymbol{x}_i,\,\boldsymbol{x}_j;\,t_i-t_j) = \langle N|T[\hat\Psi^\dagger(i)\,\hat\Psi^\dagger(j)]|N-2,\,s\rangle\,\cdot$$
$$\cdot\exp[i(E_s(N-2)-E_0)(t_i+t_j)/2\hbar]\,,$$

$$\text{(G.5}b\text{)}\qquad \tilde\chi_s^{\rm hh}(\boldsymbol{x}_i,\,\boldsymbol{x}_j;\,t_i-t_j) = \langle N-2,\,s|T[\hat\Psi(i)\,\hat\Psi(j)]|N\rangle\,\cdot$$
$$\cdot\exp[-i(E_s(N-2)-E_0)(t_i+t_j)/2\hbar]\,,$$

TABLE I. – *List of symbols needed in eq.* (G.6) *of the text to identify the six functions* (G.2).

| $\alpha$ | $\lambda(\alpha)$ | $M_\alpha$ | $t_\alpha$ | $\tau_\alpha$ | $T_\alpha$ | $f_s^\alpha(\tau_\alpha)$ | $g_s^\alpha(T_\alpha)$ |
|---|---|---|---|---|---|---|---|
| I | $+1$ | $N$ | $\tau$ | $\tau_1$ | $\tau_2$ | $\chi_s^{\text{ph}}(\boldsymbol{x}_1, \boldsymbol{x}_{1'}; \tau_\alpha)$ | $\tilde{\chi}_s^{\text{ph}}(\boldsymbol{x}_2, \boldsymbol{x}_{2'}; T_\alpha)$ |
| II | $+1$ | $N$ | $-\tau$ | $\tau_2$ | $\tau_1$ | $\chi_s^{\text{ph}}(\boldsymbol{x}_2, \boldsymbol{x}_{2'}; \tau_\alpha)$ | $\tilde{\chi}_s^{\text{ph}}(\boldsymbol{x}_1, \boldsymbol{x}_{1'}; T_\alpha)$ |
| III | $-1$ | $N$ | $-\frac{\tau_1}{2}+\frac{\tau_2}{2}$ | $-\tau+\frac{\tau_1}{2}+\frac{\tau_2}{2}$ | $\tau+\frac{\tau_1}{2}+\frac{\tau_2}{2}$ | $\chi_s^{\text{ph}}(\boldsymbol{x}_2, \boldsymbol{x}_{1'}; \tau_\alpha)$ | $\tilde{\chi}_s^{\text{ph}}(\boldsymbol{x}_1, \boldsymbol{x}_{2'}; T_\alpha)$ |
| IV | $-1$ | $N$ | $\frac{\tau_1}{2}-\frac{\tau_2}{2}$ | $\tau+\frac{\tau_1}{2}+\frac{\tau_2}{2}$ | $-\tau+\frac{\tau_1}{2}+\frac{\tau_2}{2}$ | $\chi_s^{\text{ph}}(\boldsymbol{x}_1, \boldsymbol{x}_{2'}; \tau_\alpha)$ | $\tilde{\chi}_s^{\text{ph}}(\boldsymbol{x}_2, \boldsymbol{x}_{1'}; T_\alpha)$ |
| V | $+1$ | $N+2$ | $\frac{\tau_1}{2}+\frac{\tau_2}{2}$ | $\tau+\frac{\tau_1}{2}-\frac{\tau_2}{2}$ | $-\tau+\frac{\tau_1}{2}-\frac{\tau_2}{2}$ | $\chi_s^{\text{pp}}(\boldsymbol{x}_1, \boldsymbol{x}_2; \tau_\alpha)$ | $\tilde{\chi}_s^{\text{pp}}(\boldsymbol{x}_{2'}, \boldsymbol{x}_{1'}; T_\alpha)$ |
| VI | $+1$ | $N-2$ | $-\frac{\tau_1}{2}-\frac{\tau_2}{2}$ | $-\tau+\frac{\tau_1}{2}-\frac{\tau_2}{2}$ | $\tau+\frac{\tau_1}{2}-\frac{\tau_2}{2}$ | $\chi_s^{\text{hh}}(\boldsymbol{x}_{2'}, \boldsymbol{x}_{1'}; \tau_\alpha)$ | $\tilde{\chi}_s^{\text{hh}}(\boldsymbol{x}_1, \boldsymbol{x}_2; T_\alpha)$ |

(where the collective index $s$ labels in each case the relevant set of states), we may rewrite the six functions (G.2) in the compact form

$$G_2^\alpha(1,\,2;\,1',\,2') = \left(-\frac{i}{\hbar}\right)^2 \lambda(\alpha)\,\theta\!\left(t_\alpha - \frac{1}{2}|\tau_\alpha| - \frac{1}{2}|T_\alpha|\right)\cdot \sum_s \exp\left[i(E_0 - E_s(M_\alpha))\,t_\alpha/\hbar\right] f_s^\alpha(\tau_\alpha)\,g_s^\alpha(T_\alpha) \tag{G.6}$$

($\alpha =$ I-VI). The entries needed in eq. (G.6) are listed in table I.

Notice that the excitation energies $E_s(M_\alpha) - E_0$ enter eq. (G.6) only through the exponential factor that has been explicitly displayed. Suitable Fourier transformation with respect to the variable $t_\alpha$ thus enables us to exhibit the poles of the spectrum $E_s(M_\alpha) - E_0$. In particular, to locate the $N$-particle excited states it is convenient to make use of the freedom in the choice of the time variables $t_2$ and $t_{2'}$ in the Bethe-Salpeter equation (4.5) by setting $t_{2'} = t_2 + \delta$ ($\delta \to 0^+$). With this choice and Fourier transforming the variable $t_2$ we may only retain the so-called particle-hole Green's function

$$G_2^{\mathrm{ph}}(1,\,2;\,1',\,2') = G_2^{\mathrm{I}}(1,\,2;\,1',\,2') + G_2^{\mathrm{II}}(1,\,2;\,1',\,2'), \tag{G.7}$$

since the functions III-VI are nonsingular at the frequencies of interest.

## APPENDIX H

### The Haken potential.

In this appendix we show how the often-quoted Haken potential, that contains corrective terms to the electron-hole attractive interaction $-e^2 r^{-1} \epsilon_0^{-1}$ in the effective-mass approximation, can be derived from the last term at the left-hand side of eq. (11.16). To this end, we adopt the approximation (11.24) for the dynamically screened exchange matrix elements and take the (time-ordered) inverse dielectric function of eq. (11.25) within the so-called plasmon-pole approximation (cf. sect. 25*b*) of ref. [5] and eq. (9.16) with a single mode)

$$\epsilon_{\mathrm{T}}^{-1}(\boldsymbol{q};\,\omega) = 1 + \left(\frac{\epsilon_0 - 1}{\epsilon_0}\right)\frac{\omega_0^2}{\omega^2 - (\omega(\boldsymbol{q}) - i\delta)^2}, \tag{H.1}$$

where $\omega_0 = \omega(\boldsymbol{q} = 0)$. Equation (H.1) enables us to perform the frequency integration in eq. (11.16) in a close form. Changing in addition the integration variables $\boldsymbol{k}_v$ and $\boldsymbol{k}_{v'}$ into $\boldsymbol{p} = \boldsymbol{k}_{v'} - \boldsymbol{k}_0$ and $\boldsymbol{q} = \boldsymbol{k}_v - \boldsymbol{k}_{v'}$, we obtain

$$\sum_{\sigma_{v'}\sigma_{c'}} \int \frac{\mathrm{d}\boldsymbol{k}_v}{(2\pi)^3} \exp\left[i(\boldsymbol{k}_v - \boldsymbol{k}_0)\cdot \boldsymbol{r}\right] \int \frac{\mathrm{d}\boldsymbol{k}_{v'}}{(2\pi)^3} A_s(\sigma_{v'},\,\sigma_{c'};\,\boldsymbol{k}_{v'})\,\mathcal{N}\,\Omega_0 \cdot \\ \cdot\, i \int_{-\infty}^{+\infty} \frac{\mathrm{d}\hbar\omega}{2\pi} \exp\left[-i\omega\delta\right] \langle \sigma_c \boldsymbol{k}_v,\, \sigma_{v'} \boldsymbol{k}_{v'} | W(\omega) | \sigma_{c'} \boldsymbol{k}_{v'},\, \sigma_v \boldsymbol{k}_v \rangle \,\cdot \tag{H.2}$$

$$\cdot\left(\frac{1}{E_s^{\mathrm{B}}+\dfrac{\hbar^2}{2m_c^*}(\boldsymbol{k}_{v'}-\boldsymbol{k}_0)^2+\dfrac{\hbar^2}{2m_v^*}(\boldsymbol{k}_v-\boldsymbol{k}_0)^2+\hbar\omega-i\delta}+\right.$$

$$\left.+\frac{1}{E_s^{\mathrm{B}}+\dfrac{\hbar^2}{2m_c^*}(\boldsymbol{k}_v-\boldsymbol{k}_0)^2+\dfrac{\hbar}{2m_v^*}(\boldsymbol{k}_{v'}-\boldsymbol{k}_0)^2-\hbar\omega-i\delta}\right)\simeq$$

$$\simeq\int\frac{\mathrm{d}\boldsymbol{q}}{(2\pi)^3}\exp[i\boldsymbol{q}\cdot\boldsymbol{r}]\int\frac{\mathrm{d}\boldsymbol{p}}{(2\pi)^3}\exp[i\boldsymbol{p}\cdot\boldsymbol{r}]A_s(\sigma_v,\,\sigma_c;\,\boldsymbol{p}+\boldsymbol{k}_0)\,v(\boldsymbol{q})\,\cdot$$

$$\cdot\left\{-1+\left(\frac{\epsilon_0-1}{\epsilon_0}\right)\frac{\hbar\omega_0^2}{2\omega(\boldsymbol{q})}\cdot\left[\frac{1}{\hbar\omega(\boldsymbol{q})+E_s^{\mathrm{B}}+\dfrac{\hbar^2\boldsymbol{p}^2}{2m_c^*}+\hbar^2\dfrac{(\boldsymbol{p}+\boldsymbol{q})^2}{2m_v^*}}+\right.\right.$$

$$\left.\left.+\frac{1}{\hbar\omega(\boldsymbol{q})+E_s^{\mathrm{B}}+\hbar^2\dfrac{(\boldsymbol{p}+\boldsymbol{q})^2}{2m_c^*}+\dfrac{\hbar^2\boldsymbol{p}^2}{2m_v^*}}\right]\right\}.$$

Equation (H.2) may be further simplified by neglecting i) the $\boldsymbol{p}$-dependence in the energy denominators owing to the localization of the coefficient $A_s$ about $\boldsymbol{p}=0$, ii) the $\boldsymbol{q}$-dependence of the dispersion relation $\omega(\boldsymbol{q})$ that we assume to be weak in comparison with the $\boldsymbol{q}$-dependence of the single-particle energy levels about the extrema, and iii) the excitonic binding energy $E_s^{\mathrm{B}}$ in comparison with the characteristic screening energy $\hbar\omega_0$. The result is the product of the envelope function $F_s(\sigma_v,\,\sigma_c;\,r)$ times the Haken potential (cf., *e.g.*, ref. [59], sect. 7*b*))

$$\text{(H.3)}\qquad v_{\mathrm{H}}(r)=-v(r)\left[\frac{1}{\epsilon_0}+\frac{(\epsilon_0-1)}{2\epsilon_0}\left(\exp[-r/r_{\mathrm{e}}]+\exp[-r/r_{\mathrm{h}}]\right)\right].$$

In eq. (H.3) $r_{\mathrm{e}}$ and $r_{\mathrm{h}}$ stand for the electron and hole polaron radii, respectively,

$$\text{(H.4)}\qquad r_{\mathrm{e}}=\left[\frac{\hbar}{2m_c^*\,\omega_0}\right]^{1/2},\qquad r_{\mathrm{h}}=\left[\frac{\hbar}{2m_v^*\,\omega_0}\right]^{1/2},$$

and the quantity within brackets defines an $r$-dependent effective inverse dielectric function that interpolates smoothly between the values $\epsilon_0^{-1}$ for $r\to\infty$ and 1 for $r=0$. It should be recalled, however, that the potential (H.3) is meaningful insofar as it describes the leading corrections for large $r$ to the electron-hole interaction in the effective-mass approximation.

## REFERENCES

[1] W. HANKE: in *Festkörperprobleme XIX, Advanced Solid State Physics* (Vieweg, 1979), p. 43.

[2] W. HANKE, H. J. MATTAUSCH, and G. STRINATI: in *Electron Correlations in Solids, Molecules, and Atoms*, edited by J. T. DEVREESE and F. BROSENS (Plenum Press, New York, N.Y., 1983), p. 289.

[3] W. HANKE, N. MESKINI, and H. WEILER: in *Electronic Structure, Dynamics and Quantum Structural Properties of Condensed Matter*, edited by J. T. DEVREESE and P. VAN CAMP (Plenum Press, New York, N.Y., 1985), p. 113.

[4] A. A. ABRIKOSOV, L. P. GORKOV, and I. E. DZYALOSHINSKI: *Methods of Quantum Field Theory in Statistical Physics* (Prentice-Hall, Englewood Cliff, N.J., 1963); A. L. FETTER and J. D. WALECKA: *Quantum Theory of Many-Particle Systems* (McGraw-Hill, New York, N.Y., 1971); G. RICKAYZEN: *Green's Functions and Condensed Matter* (Academic Press, London, 1980); G. D. MAHAN: *Many-Particle Physics* (Plenum Press, New York, N.Y., 1981).

[5] We follow closely the treatment due to L. HEDIN and S. LUNDQVIST: in *Solid State Physics*, edited by H. EHRENREICH, F. SEITZ, and D. TURNBULL (Academic Press, New York, N.Y., 1969), Vol. 23, p. 1, although our presentation differs from theirs in several technical details.

[6] L. P. KADANOFF and G. BAYM: *Quantum Statistical Mechanics* (Benjamin, Menlo Park, 1962).

[7] A term which ensures the charge neutrality of the system is assumed to be included in $V(r)$.

[8] See, *e.g.*, C. CSANAK, H. S. TAYLOR, and R. YARIS: *Adv. At. Mol. Phys.*, 7, 287 (1971).

[9] P. NOZIÈRES: *Theory of Interacting Fermi Systems* (Benjamin, New York, N.Y., 1964).

[10] L. J. SHAM and T. M. RICE: *Phys. Rev.*, **144**, 708 (1966).

[11] G. BAYM and L. P. KADANOFF: *Phys. Rev.*, **124**, 287 (1961).

[12] M. GELL-MANN and F. LOW: *Phys. Rev.*, 84, 350 (1951).

[13] Cf., *e.g.*, the second of references [4], sects. **13**, **32**, and **52**.

[14] G. BAYM: *Phys. Rev.*, 127, 1391 (1962).

[15] Equation (6.4) can also be interpreted physically as the continuity equation in the presence of the external field $U$ whenever the time dependence of $U$ is slow enough for the adiabatic approximation to hold, *i.e.* if the external field drives the system back to the ground state after it has exhausted its action.

[16] J. R. SCHRIEFFER: *Theory of Superconductivity* (Benjamin, New York, N.Y., 1964), Chap. 8.

[17] L. J. SHAM and W. KOHN: *Phys. Rev.*, **145**, 561 (1966).

[18] L. J. SHAM: *Phys. Rev.*, **150**, 720 (1966).

[19] G. STRINATI, H. J. MATTAUSCH, and W. HANKE: *Phys. Rev. B*, **25**, 2867 (1982).

[20] W. HEITLER: *The Quantum Theory of Radiation* (Clarendon, Oxford, 1954), subsect. **1˙6**; see also the last of references [4], subsect. **1˙5**.

[21] R. DEL SOLE and E. FIORINO: *Phys. Rev. B*, **29**, 4631 (1984).

[22] Cf., *e.g.*, J. D. JACKSON: *Classical Electrodynamics* (J. Wiley, New York, N.Y., 1962), subsect. **6˙5**.

[23] L. ROSENFELD: *Theory of Electrons* (North-Holland, Amsterdam, 1951), Chap. 2.

[24] H. EHRENREICH: in *The Optical Properties of Solids*, Varenna Course XXXIV, edited by J. TAUC (Academic Press, New York, N.Y., 1966), p. 106.

[25] V. Ambegaokar and W. Kohn: *Phys. Rev.*, 117, 423 (1960).

[26] Equations (8.23) generalize to a crystalline material eqs. (6-168) of ref. [9] which hold for a homogeneous system. The latter, however, hold for any value of the wave vector.

[27] Equation (8.24) generalizes to all orders of perturbation theory the result obtained in ref. [23] within the time-dependent-screened-Hartree-Fock approximation which will be discussed in subsect. 8·4.

[28] M. Born and K. Huang: *Dynamical Theory of Crystal Lattices* (Clarendon Press, Oxford, 1968), Appendix VI.

[29] F. Bassani and M. Altarelli: in *Handbook of Synchrotron Radiation*, edited by E. E. Koch (North-Holland, Amsterdam, 1983), p. 463.

[30] For a truly isotropic medium an equation similar to eq. (8.42) can be proved for *any* finite wave vector, since the transverse and the longitudinal components of a tensor that satisfies eq. (8.28) for any rotation $\mathscr{R}$ are completely decoupled (cf. ref. [9], subsect. 6·6).

[31] W. Hanke and L. J. Sham: *Phys. Rev. B*, 12, 4501 (1975).

[32] W. Hanke and L. J. Sham: *Phys. Rev. B*, 21, 4656 (1980).

[33] H. J. Mattausch, W. Hanke, and G. Strinati: *Phys. Rev. B*, 27, 3735 (1983)

[34] N. Meskini, H. J. Mattausch, and W. Hanke: *Solid State Commun.*, 48, 807 (1983).

[35] G. Wendin: *Phys. Lett. A*, 51, 291 (1975); M. Ya. Amusia, V. K. Ivanov, and L. V. Chernysheva: *Phys. Lett. A*, 59, 191 (1976); M. Ya. Amusia: *Appl. Opt.*, 19, 4042 (1980); Z. Crljen and G. Wendin: *Phys. Scr.*, 32, 359 (1985).

[36] L. Hedin: *Phys. Rev.*, 139, A 796 (1965).

[37] The approximation $\overline{\mathrm{RPA}}$ is equivalent to the independent-electron approximation of the ordinary band theory. Cf., *e.g.*, F. Bassani and G. Pastori Parravicini: *Electronic States and Optical Transitions in Solids* (Pergamon Press, Oxford, 1975), subsect. 5·1.

[38] Cf. ref. [39], subsect. 6·3.

[39] M. del Castillo-Mussot and L. J. Sham: *Phys. Rev. B*, 31, 2092 (1985).

[40] L. J. Sham and M. Schlüter: *Phys. Rev. Lett.*, 51, 1888 (1983); L. J. Sham: *Phys. Rev. B*, 32, 3876 (1985); L. J. Sham and M. Schlüter: *Phys. Rev. B*, 32, 3883 (1985); M. Lannoo, M. Schlüter, and L. J. Sham: *Phys. Rev. B*, 32, 3890 (1985).

[41] G. Strinati, H. J. Mattausch, and W. Hanke: *Phys. Rev. Lett.*, 45, 290 (1980). See also ref. [19].

[42] W. Hanke, Th. Gölzen, and H. J. Mattausch: *Solid State Commun.*, 51, 23 (1984).

[43] C. S. Wang and W. E. Pickett: *Phys. Rev. Lett.*, 51, 597 (1983).

[44] M. S. Hybertsen and S. G. Louie: *Phys. Rev. Lett.*, 55, 1418 (1985); M. S. Hybertsen and S. G. Louie: *Phys. Rev. B*, 32, 7005 (1985).

[45] V. M. Galitskii and A. B. Migdal: *Sov. Phys. JEPT*, 7, 96 (1958).

[46] Physically, the energy dependence of the self-energy is connected to the coupling of multiple electron-hole excitations with the primary one-particle excitation. Cf. G. Strinati: *Nuovo Cimento D*, 4, 397 (1984).

[47] A. J. Layzer: *Phys. Rev.*, 129, 897 (1963).

[48] Cf., *e.g.*, the second of references [4], sect. 10.

[49] A. Mauger and M. Lannoo: *Phys. Rev. B*, 15, 2324 (1977).

[50] For numerical convenience, in the rest of this section we shall use the Bohr radius as the unit of length and the rydberg as the unit of energy ($\hbar = 1$, $m = 1/2$, $e^2 = 2$ in these units).

[51] For a core hole whose wave function is well localized within a lattice cell, neglecting the energy dependence of the screened interaction leads to a polarization shift which is twice the correct value, *i.e.* it misses the adiabatic factor of 1/2. Physically, the difference is due to the so-called Coulomb hole term (cf. ref. [5]).

[52] Cf., *e.g.*, sect. **14** of the second of references [4].

[53] For a review on impurity levels see ref. [31] and S. T. PANTELIDES: *Rev. Mod. Phys.*, **50**, 797 (1978).

[54] H. J. MATTAUSCH, W. HANKE, and G. STRINATI: *Phys. Rev. B*, **26**, 2302 (1982).

[55] Cf., *e.g.*, ref. [39], Chap. 6.

[56] G. STRINATI: *Phys. Rev. Lett.*, **49**, 1519 (1982); G. STRINATI: *Phys. Rev. B*, **29**, 5718 (1984).

[57] M. ALTARELLI and F. BASSANI: *J. Phys. C*, **4**, L328 (1971).

[58] M. H. COHEN and F. KEFFER: *Phys. Rev.*, **99**, 1128 (1955).

[59] R. S. KNOX: *Theory of Excitons* (Academic Press, New York, N.Y., 1963), sect. 3*b*.

[60] Y. ONODERA and Y. TOYOZAWA: *J. Phys. Soc. Jpn.*, **22**, 833 (1967).

[61] H. A. BETHE and E. SALPETER: *Quantum Mechanics of One- and Two-Electron Atoms* (Springer-Verlag, Berlin, 1957), sect. **61**.

[62] D. J. THOULESS: *Nucl. Phys.*, **22**, 78 (1961); M. YA. AMUS'YA, N. A. CHEREPKOV, and L. V. CHERNYSHEVA: *Sov. Phys. JETP*, **33**, 90 (1971).

[63] Cf., *e.g.*, N. W. ASHCROFT and N. D. MERMIN: *Solid State Physics* (Saunders College, Philadelphia, Penn., 1976), Chapter 27.

[64] U. FANO: *Phys. Rev.*, **118**, 451 (1960).

[65] This point is discussed in detail by S. K. SINHA, R. P. GUPTA, and D. L. PRICE: *Phys. Rev. B*, **9**, 2564 (1974). Within the TDSHF approximation it has been estimated that the screened electron-hole interaction reduces to only about 1/2 of the self-interaction (cf. ref. [34]).

[66] Y. ONODERA: *Prog. Theor. Phys.*, **49**, 37 (1973).

[67] Quite generally, the condition

$$\int_{\Omega} \mathrm{d}\boldsymbol{r}'\,\tilde{\chi}(\boldsymbol{r}, \boldsymbol{r}'; \omega) = 0$$

holds at any finite $\omega$ for the full irreducible polarizability including all possible many-body effects. This condition, that follows from the counterpart of the Ward identity (7.11) for the irreducible vertex functions, can be extrapolated at $\omega = 0$ for a system which, like a crystalline insulator or semiconductor, has an energy gap in its spectrum. It can thus be taken as a quantum-mechanical characterization of the insulator itself (cf. W. BARDYSZEWSKI, R. DEL SOLE, J. KRUPSKI, and G. STRINATI: *Surf. Sci.*, **167**, 363 (1986)).

---

© by Società Italiana di Fisica
Proprietà letteraria riservata

Direttore responsabile: RENATO ANGELO RICCI

Questo periodico
è iscritto
all'Unione Stampa
Periodica Italiana

Questo fascicolo è stato realizzato in fotocomposizione dalla Monograf, Bologna
e stampato dalla tipografia Compositori, Bologna
nel mese di gennaio 1989